

Regulation of cellular metabolism in tumor infiltrating CD8<sup>+</sup> T  
cells and its role in their dysfunction

Lelisa Fikru Gemta  
Nejo, Ethiopia

A.S., Community College of Aurora, Colorado, 2004  
B.S., University of Colorado Denver, Colorado, 2006

A Dissertation presented to the Graduate Faculty of the  
University of Virginia in Candidacy for the Degree of Doctor of  
Philosophy

Experimental Pathology

University of Virginia  
May, 2019

## Abstract

Tumor infiltrating CD8<sup>+</sup> T cells (CD8<sup>+</sup> TIL) play pivotal role in fighting cancers. Their accumulation within tumors has been associated with better tumor control in mouse models of cancers and favorable clinical outcomes in human patients. However, it has been well-understood that these cells undergo progressive loss of function and often fail to eradicate tumor cells. While significant progress has been made in understanding and targeting the mechanisms underlying CD8<sup>+</sup> TIL dysfunction, the molecular details of the dysfunction remain to be fully elucidated. It has been widely appreciated that elevated glycolysis and oxidative phosphorylation (OXPHOS) are essential to support the generation and function of effector T cells. Here, we demonstrate the perturbation of energy metabolism as a biochemical basis of CD8<sup>+</sup> TIL dysfunction. We found that both glycolytic metabolism and OXPHOS were attenuated in melanoma CD8<sup>+</sup> TIL. Glycolysis was repressed by impaired activity of enolase 1, a key glycolytic enzyme responsible for the synthesis of phosphoenolpyruvate that is essential for the effector function of T cells. While this enzyme is highly expressed in CD8<sup>+</sup> TIL, its activity was post-translationally regulated by mechanism that involved immune checkpoint signals from PD-1, CTLA-4, and TIM-3. The details of this mechanism remain to be elucidated, and we have developed a robust reporter of enolase activity to aid future investigation in this area. We also found impaired enolase activity in the CD8<sup>+</sup> TIL that infiltrated human melanoma tumors and different types of murine tumor models. In addition to glycolysis, impaired enolase activity also limited the OXPHOS capability of CD8<sup>+</sup> TIL. This was at

least partly mediated by inability of glycolysis to produce sufficient pyruvate to feed into the mitochondrial metabolism. However, CD8<sup>+</sup> TIL also had low mitochondrial mass and membrane potential that may be a major contributor to the OXPHOS deficiency of these cells. Importantly, we demonstrated that bypassing the enolase inactivity through provision of metabolites produced downstream of it significantly improved the glycolytic metabolism, OXPHOS, and effector function of CD8<sup>+</sup> TIL. Furthermore, we showed that a combination of immune checkpoint blockade therapy that slowed tumor growth in mouse model generated CD8<sup>+</sup> TIL with stronger enolase activity that was essential for their function. Our studies demonstrated that metabolic dysfunction mediated by impaired enolase activity is a major contributor to the functional impairment of CD8<sup>+</sup> TIL, and that reactivating this enzyme may reinvigorate antitumor immunity.

## Acknowledgements

I would first like to thank my mentor Dr. Timothy Bullock, who went above and beyond what is expected of him as a mentor to support me as a person and to make sure that I make the most out of the opportunities that graduate school provides. He continually pushed my limits and encouraged me to do things that are important not only to fulfill the requirements of my training, but are also beneficial to my future career as a scientist. As a result of such mentorship, I have obtained four merit-based travel awards to present my research at national and international scientific conferences and produced a manuscript that has been accepted for publication in a prestigious journal. Dr. Bullock has always been there for me throughout my time at UVA. Whenever I requested extra meetings with him to obtain advice on personal and professional matters, his responses were usually “for you, I will make time.”

I would also thank Dr. Janet Cross, Dr. Victor Engelhard, Dr. David Kashatus, and Dr. Adam Goldfarb for serving on my thesis committee and for their extraordinary contribution to the development my project into the work presented in this dissertation. When I asked each of them to serve on my committee, my intention was to assemble a group of exceptional scientists who would give me the best guidance with my project. However, I never expected that they would be invested as much as they have been in my personal growth as a scientist. I truly appreciate all the time and effort they put into guiding, encouraging, and challenging me. Especially thank you to Dr. Janet

Cross for serving as chair of my thesis committee and for all the personal and professional supports she provided me to overcome the challenges I faced while in graduate school. I am also indebted to Dr. Kyle Hoehn, who was instrumental in the establishment of the project described in this work. Thanks to all the members of Bullock lab and Engelhard lab who taught me, encouraged me, and supported me throughout my time at UVA. This work was financially supported by Immunology Training Grant and CRCHD Diversity Supplements (R01CA166458-03S1).

Finally, I need to thank all the members of my family who have been supportive of my long professional journey. Thank you does not come close to expressing my deepest appreciation for my father Fikru Gemta, whose loss I am mourning as I am writing this dissertation, and my mother Mulunesh Abdissa. Their endless love, support, and guidance made me who I am as a person today. They always put my best interest before their own even when that required sacrificing a lot and working extra hard to meet my needs. Especially, I will never forget how hard they worked from dawn to dusk to put my siblings and me through school in a small town in Ethiopia. Lastly, thank you to my amazing wife Biftu without whose love, support, understanding, and dedication to my career, I simply could have never been able to make it through graduate school.

## Table of Contents

<b>Abstract.....</b>	<b>i</b>
<b>Acknowledgements.....</b>	<b>iii</b>
<b>Table of Contents.....</b>	<b>v</b>
<b>List of Figures.....</b>	<b>ix</b>
<b>Abbreviations .....</b>	<b>xi</b>
<b>Chapter One: General Introduction.....</b>	<b>1</b>
The importance of antitumor immunity.....	1
Dysfunctional state of TIL.....	2
The link between immunity and cellular metabolism .....	4
Glucose metabolism.....	7
Role of glycolytic metabolism in T cell.....	10
Metabolism of TIL .....	14
Immunopathological consequence of altered glucose metabolism in T cell.....	15
<b>THESIS RATIONALE.....</b>	<b>16</b>
<b>Chapter Two: Materials and Methods.....</b>	<b>19</b>
Tumor cell line, mice, and tumor injection.....	19
Human Samples .....	19
Checkpoint blockade treatment .....	20

Adoptive T cell transfer .....	21
Glucose uptake .....	23
Analysis of enolase activity in <i>in vitro</i> and ex vivo T cell samples.....	24
Enolase reporter, MitoTracker Green (MTG), and tetramethylrhodamine, ethyl ester (TMRE) staining.....	25
Metabolic assay .....	25
Metabolomics .....	26
Development of Enolase reporter .....	27
Enolase 1 post-translational modification analysis.....	27
RNA extraction, cDNA synthesis, and real-time qPCR .....	29
Statistical Analysis.....	30
<b>Chapter Three: Impaired enolase 1 glycolytic activity restrains effector functions of tumor infiltrating CD8+ T cells.....</b>	<b>31</b>
ABSTRACT.....	31
INTRODUCTION.....	32
RESULTS.....	35
Glucose metabolism by CD8+ TIL is distinct from that of either quiescent or effector CD8+ T cells .....	35
CD8+ TIL express glucose transporter Glut1 and efficiently take up glucose.....	40
CD8+ TIL possess low levels of phosphoenolpyruvate .....	45

Overcoming PEP deficiency rescues CD8+ TIL metabolic and functional activity .....	49
Immune checkpoint blockade therapy recruits enolase-active CD8+ TIL into tumors.....	54
Human melanoma CD8+ TIL have low enolase activity.....	58
DISCUSSION.....	59
<b>Chapter Four: Advancing the understanding of enolase impairment in CD8+ TIL: studies in different cancer types, investigation of its molecular basis, and development of a reporter for Enolase activity.....</b>	<b>65</b>
INTRODUCTION.....	65
RESULTS.....	67
A. Interrogation of glycolysis in CD8+ TIL in cancers other than melanoma.....	67
B. Establishing a mechanistic basis for the loss of enolase enzymatic activity .....	73
C. The development of a chemical probe that allows a robust enolase expression/activity analysis.....	80
DISCUSSION.....	84
<b>Chapter Five: Analysis of mitochondria metabolism in CD8+ TIL .....</b>	<b>88</b>
INTRODUCTION.....	88
RESULTS.....	91
Effector CD8+ T cells induce mitochondrial metabolism in addition to glycolysis .....	91
Nutrient availability is not the major limiting factor in CD8+ TIL mitochondrial metabolism .....	94

The mitochondrial content and function of CD8+ TIL are consistent with their low OXPHOS capability.....	98
DISCUSSION.....	104
<b>Chapter 6: Conclusions and Future Directions .....</b>	<b>107</b>
Metabolic activity of CD8+ TIL .....	107
Role of competition for glucose and cell-intrinsic mechanism in controlling the metabolic activity of CD8+ TIL.....	109
Failure to induce glycolysis versus loss of glycolytic activity in CD8+ TIL .....	111
Mechanism of enolase impairment .....	113
Immune checkpoint signals and impaired enolase activity .....	117
Validation and usage of enolase reporter .....	120
Potential fates of glycolytic intermediate in CD8+ TIL with impaired enolase activity .....	123
Mechanism of pyruvate rescue of cytokine production in CD8+ TIL.....	126
Pyruvate availability and mitochondrial alterations as mediators of OXPHOS deficiency in CD8+ TIL .....	127
Contribution of this work to the understanding of CD8+ TIL metabolism .....	132
Translational/clinical relevance of manipulation of enolase activity in T cells.....	136
<b>References.....</b>	<b>139</b>

## List of Figures

Figure 1: B16cOVA infiltrating CD8+ TIL exhibit phenotypic and functional markers of exhaustion.....	37
Figure 2: CD8+ TIL are metabolically less active than acute effector CD8+ T cells, but more active than quiescent CD8+ T cells. ....	39
Figure 3: CD8+ TIL express high levels of glucose transporters.....	42
Figure 4: Glucose uptake is not limited in CD8+ TIL. ....	43
Figure 5: Glycolysis-regulating signaling molecules are expressed and active in CD8+ TIL.....	44
Figure 6: Weak enolase activity restrains glucose metabolism in glycolysis in CD8+ TIL. ....	47
Figure 7: The abundance of glycolytic enzymes and metabolites suggest that PEP deficiency of CD8+ TIL is driven by lack of strong enolase activity. ....	48
Figure 8: Bypassing enolase restores metabolic function and effector activity in CD8+ TIL. ....	51
Figure 9: Inhibition of the enolase activity in T cells limits cytokine production. ....	53
Figure 10: Checkpoint molecule blockade supports CD8+ TIL enolase function. ....	56
Figure 11: Enolase activity contributes to the effector function of CPI-treated CD8+ TIL. ....	57
Figure 12: Human melanoma TIL have low functional and enolase activity. ....	59
Figure 13: mTORC1 may be active in the CD8+ TIL that infiltrate the LLC and 4T1 tumors. ....	68
Figure 14: LLC and 4T1 CD8+ TIL take up 2-NBDG although not as efficiently as splenic CD8+ T cells. ....	70
Figure 15: CD8+ TIL in human melanoma and NSCLC tumors express similar amount of enolase 1. ....	72
Figure 16: Enolase is post-translationally regulated in the CD8+ TIL that infiltrated MC38 tumors.....	73

Figure 17: In vitro restimulation of CD8+ TIL modestly increases Glut1 expression, but not glucose uptake. ....	76
Figure 18: Tumor cells do not prevent induction of glucose uptake potential in Teff during in vitro coculture.....	77
Figure 19: Mg <sup>2+</sup> availability may not be limiting the activity of enolase in CD8+ TIL. ....	78
Figure 20: Differential post-translational modifications of enolase 1 in acute Teff and CD8+ TIL.....	80
Figure 21: Development and analysis of enolase reporter.....	82
Figure 22: Murine and human CD8+TIL weakly stained with the enolase reporter.....	84
Figure 23: Activation of CD8 T cells induces both glycolysis and OXPHOS.....	93
Figure 24: OXPHOS contributes to CD8+ TIL function. ....	93
Figure 25: The availability of glucose or glutamine may not be the major limiting factor in CD8+ TIL mitochondrial metabolism. ....	97
Figure 26: CD8+ TIL do not exhibit fatty acid deficiency.....	98
Figure 27: CD8+ TIL have low mitochondria mass and function, which are constituent with their limited OXPHOS capability.....	102
Figure 28: CD8+ TIL have low TCA cycle active compared to acute Teff. ....	103
Figure 29: Mitochondrial dysfunction may not be associated with the age of CD8+ TIL. ....	103
Figure 30: Human melanoma CD8+TIL have similar level membrane potential as quiescent antigen-experience CD8 T cells in healthy donors PBMC. ....	104
Figure 31: Model of CD8+ TIL metabolic and effector function restraint by impaired enolase activity.....	108

## Abbreviations

ACC1	Acetyl-coenzyme A (CoA) Carboxylase 1
ANOVA	Analysis of Variance
APC	Antigen Presenting Cell
ATP	Adenosine Triphosphate
CPi	Checkpoint Inhibitor
CTLA-4	Cytotoxic T lymphocyte antigen 4
CPT1a	Carnitine palmitoyl- transferase 1a
DC	Dendritic Cell
ECAR	Extracellular Acidification Rate
ETC	Electron Transport Chain
FACS	Fluorescent-activated Cell Sorting
FMO	Fluorescence Minus One
4E-BP1	Initiation factor 4E (eIF4E)-binding Protein-1
GMFI	Geometric Mean Fluorescence Intensity
Glut	Glucose Transporter
GzB	Granzyme B

HIF1 $\alpha$	Hypoxia Inducible Factor 1 alpha
IL-2	Interleukin-2
IFN $\gamma$	Interferon gamma
KO	Knock-out
LLC	Lewis lung carcinoma
MHC	Major Histocompatibility Complex
MDSC	Myeloid Derived Suppressor Cell
MTG	MitoTracker Green
mTORC1	Mammalian Target of Rapamycin Complex 1
NaF	Sodium Fluoride
NSCLC	Non-small Cell Lung Cancer
OCR	Oxygen Consumption Rate
OVA	Ovalbumin
OXPHOS	Oxidative Phosphorylation
PBMC	Peripheral Blood Mononuclear Cell
PEP	Phosphoenolpyruvate
PD-1	Programmed cell death 1

PDK1	3-phosphoinositide-dependent protein kinase 1
Poly I:C	Polyinosinic:polycytidylic acid
PPP	Pentose Phosphate Pathway
qPCR	Quantitative Polymerase Chain Reaction
TCR	T Cell Receptor
TDLN	Tumor Draining Lymph node
TCA	Tricarboxylic Acid
Teff	Effector T cell
TIL	Tumor Infiltrating Lymphocyte
TIM-3	T-cell Immunoglobulin, Mucin- 3
TME	Tumor Microenvironment
TMRE	Tetra-methylrhodamine ester
TNF $\alpha$	Tumor necrosis factor alpha
Treg	Regulatory T cell
2-NBDG	2-[N-(7-nitrobenz-2-oxa-1,3-diazol-4-yl) amino]-2-deoxy-D- glucose
s.c.	Subcutaneous
i.v.	Intravenous

## Chapter One: General Introduction

### The importance of antitumor immunity

The immune system plays a pivotal role in preventing cancer both by eradicating newly arising tumors (immunosurveillance) and by keeping tumor masses in a dormant (equilibrium) state. The increased susceptibility of immunodeficient patients(1, 2) and IFN $\gamma$  deficient or Rag2 $^{-/-}$  mice (3, 4) to cancer have provided the strongest evidence for cancer immunosurveillance. The ability of the immune system to keep tumors in a dormant state was demonstrated by the fact that the depletion of CD4 $^{+}$  T cells, CD8 $^{+}$  T cells, or IFN $\gamma$  led to outgrowth of tumors in carcinogen treated mice that were originally keeping the tumors in check(5). Nevertheless, tumors escape the immune system by creating immunosuppressive environments and/or by developing resistance to the immune response(6).

Although tumor escape can be a sign of a failure in immune system-mediated control, it is not “game over” for antitumor immunity. This is highlighted by the positive correlation between the accumulation of CD8 $^{+}$  TIL in the escaped tumors and favorable clinical outcomes. This correlation has been demonstrated in many types of cancers including melanoma(7, 8), ovarian cancer(9, 10), colorectal cancer(11, 12), and breast cancer(13). Therefore, mechanisms that can enhance CD8 $^{+}$  T cell-mediated immune

responses to tumors have been intensively investigated. Vaccine-based induction of endogenous CD8+ T cells response and CD8+ T cell adoptive therapy are two important examples of such works(6, 13). These studies have resulted in significant improvement in anti-tumor immunity and in extended the lives of some cancer patients. However, the success of both approaches is limited to only small fraction of cancer patients (6, 13). Therefore, identifying mechanisms by which TIL anti-tumor activity can be improved is still of great interest to the field of tumor immunology.

### **Dysfunctional state of TIL**

Cancer patients and tumor-bearing mice can mount an immune response to their tumors. Activation of T cell responses to cancer begins with the acquisition and processing of tumor-derived proteins by antigen presenting cells (APC)(14). The APC then migrate to the tumor draining lymph nodes where they present the tumor antigens to T cells and activate them(14). Some of the responding cells can infiltrate the tumors, but they commonly fail to eradicate the tumor cells or to stop the progression of disease. Their failure has been largely attributed to progressive loss of function or exhaustion(6), which is characterized by expression of high levels of inhibitory molecules such as PD-1, CTLA-4, TIM-3 and LAG-3 and by reduced proliferation and effector cytokine production capability(15, 16). The tumor microenvironment (TME) is thought to be the major mediator of TIL dysfunctional(6, 13). Ahmadzadeh *et al*

provided a strong direct evidence that linked TME to exhaustion of human TIL by comparing TIL with CD8+ T cells from the blood and normal tissues of cancer patients(16). They found a marked increase in phenotypic (especially PD-1 and CTLA-4) and functional markers of T cell exhaustion in TIL compared to tumor specific CD8+ T cells in the blood(16).

Several cell-intrinsic and cell-extrinsic immunosuppressive mechanisms have been implicated the inhibition of antitumor immunity in the TME. Among the chief cell-extrinsic mechanisms are suppressive factors like IL-10, TGF $\beta$ , indoleamine 2,3-dioxygenase (IDO), arginase, and more(17, 18); inhibitory cells such as regulatory T cells (Treg) and myeloid derived suppressor cells (MDSC)(17, 18); non-physiologic environment characterized by increased acidity and hypoxia(19, 20); and metabolic restriction via deprivation of critical nutrients(21, 22). The cell-intrinsic mechanism of TIL regulation includes sustained, elevated expression of inhibitory checkpoint molecules mentioned above(15, 16), loss of nutrient uptake potential(21, 22) and alteration of mitochondrial biogenesis and function(23, 24).

Finding Approaches by which TIL exhaustion can be prevented or reversed is currently an area of active investigation. Blocking the immune checkpoint molecules is one of such strategies that resulted in significant improvement in anti-cancer immunity and earned FDA approvals for the treatment of several cancer types. PD-1 blockade has

been shown to reverse T cell exhaustion although its effectiveness decreases as the level of PD-1 expressed by the T cells increases, which reflects the higher dysfunctional state found in cells expressing the highest levels of PD1 (25). Anti-PD1 and anti-CTLA-4 combinatorial therapy has also been shown to reverse the exhaustion of HCV-specific CD8+ T cells in vitro(26). These antibodies (in combination and singly) have resulted in durable response in some patients in clinical trials for cancer therapy(6, 13, 27, 28). While this is very encouraging, the proportion of the patients that respond to these therapies is generally low(29–31), and the molecular details of how the blockade reverses the dysfunctional state TIL is still not well understood.

### **The link between immunity and cellular metabolism**

The functional status of the immune cells is tightly linked to their metabolic state. Much like normal cells, quiescent T cells acquire low amount of nutrients from their environment and metabolize them in order to produce ATP that is needed to support their homeostatic cellular activities(32, 33). The activation of T cells accelerates several complex cellular processes including biomolecular synthesis, migration, and proliferation, which are biosynthetically and bioenergetically costly activities(34, 35). To meet the metabolic demands created by these activities, activated T cells strongly induce the rate at which they take up and metabolize glucose(36). While this strikingly high capacity to consume glucose was first observed over half a century ago in both immune and tumor cells by Otto Warburg (37), the strong link between cellular

metabolism and immunology has only recently obtained a wide appreciation. Failing to induce glucose metabolism impairs T cells growth, activation, and function even in the presence of other nutrients(38–43), indicating the critical role of glucose in these cells, as discussed in more detail below.

Activation of T cells via strong T cell receptor (TCR) signal or a combination of TCR and costimulatory (specifically CD28) signals is required for optimal induction and maintenance of glycolytic metabolism(40, 44). Studies have elucidated the mechanism by which T cells coordinate their immunological and metabolic activities. TCR- and CD28-mediated signals rapidly upregulate the expression of the transcription factor c-Myc, which drives the transcription of multiple genes involved in glucose metabolism and the initial induction of glycolytic metabolism(35, 36, 45). TCR and CD28 can also activate phosphatidylinositol 3-kinase (PI3K), which facilitates the activation of Akt by serine/threonine kinase phosphoinositol-dependent protein kinase 1 (PDK1) and enable Akt to activate its downstream target mTORC1(33, 36, 46). Akt has been reported to promote glycolytic induction by supporting the translocation of glucose transporters to the cell surface(40), inducing the expression of the glycolytic enzyme lactate dehydrogenase alpha (LDH $\alpha$ )(47), and mediating the rapid increase in glycolysis observed in during the reactivation of effector memory T cells(48). mTORC1 has also be shown to promote glucose uptake and glycolysis in a PI3K-and Akt-independent manner in effector CD8+ T cells (49, 50). Once it is induced, glycolytic metabolism is sustained in

activated CD8+ T cells by TCR- and IL-2-mediated PDK1-mTORC1-HIF1a signaling pathway(47, 49–51). Taken together, studies have demonstrated that the signaling pathway downstream of TCR and cytokine signals drive the induction and the maintenance glycolytic metabolism, which is critical for the immunological activities of CD8+ T cells as will be discussed later this chapter.

Whether CD8+ TIL can activate the signaling pathway described above and induce and maintain glycolytic metabolism is currently unknown. It is established that the tumor-associated dendritic cells (TADC) that are expected to prime the CD8+ T cells in the tumor draining lymph nodes are poor antigen presenting cells and express low level of CD28 ligands (CD80/86)(52–54). In addition, CD8+ T cells express a high level of inhibitory receptor CTLA-4(16), which has high affinity for CD80/86 and thus may outcompete CD28 for the ligands. The ligation of CTLA-4 can inhibit both TCR and CD28 signaling(55, 56), and hence can profoundly impair metabolic induction and maintenance. PD-1, which is expressed at high levels on TIL, has likewise been reported to inhibit both TCR and CD28 signaling(57). Most of the TADC in the tumor and tumor draining lymph nodes express PD-1 ligands (PD-L1) at high levels(58). PD-L1/PD-L2 are also expressed by many types of tumors including melanoma(59), which can continually interact with TIL. Furthermore, CD8+ TIL may have limited access to glucose and IL-2 as they have to compete with tumor cells for glucose(21) and with Treg for IL-2(60, 61). Considering the presence of all these elements that can impede the pro-glycolytic

signaling in CD8<sup>+</sup> TIL, these cells may not be able to maintain glycolytic metabolism in the TME.

### **Glucose metabolism**

Glucose is a well-documented essential nutrient for the growth, survival, and function of both murine and human T cells(38–42). Consequently, upon activation T cells sharply upregulate the expression of Glut1, the major glucose transport in lymphocytes, and take up high amount of glucose(36, 40). The induction Glut1 expression and its maintenance on the cell surface requires external signals from either TCR or cytokines such as IL-2, IL-4, or IL-7 (38, 39). In resting T cells, IL-7 has also been reported to drive the expression of Hexokinase 2, a metabolic enzyme that catalyzes the phosphorylation of glucose, which is important for its retention inside the cell(62). Once they take up glucose, T cells generally consume it during glycolysis to produce 2 molecules of pyruvate, 2 ATP, and 2 nicotinamide adenine dinucleotide (NADH) molecules per glucose molecule(63). Pyruvate has two major metabolic fates; it either is converted into lactate by lactate dehydrogenase (LDH) in the cytoplasm or enters the mitochondria where it further metabolized in the tricarboxylic acid (TCA) cycle(64) (Fig. i). The fermentation of glucose to lactate in T cells is referred to as aerobic glycolysis, which is analogous to the Warburg effect in the cancer cells(65). The term ‘aerobic’ in aerobic glycolysis does not mean that oxygen is involved in this metabolic process, but used only

to emphasize the fact that the process occurs in the presence of plenty of oxygen that can support OXPHOS(65) as opposed to anaerobic glycolysis that occurs under hypoxia that limits OXPHOS(66). During the conversion of pyruvate to lactate, NADH produced by GAPDH activity in glycolysis is oxidized to NAD<sup>+</sup>, which in turn promotes glycolysis by serving as an essential cofactor for GAPDH(63, 67) (Fig. i). Therefore, one of the major advantages of the reduction of pyruvate to lactate during aerobic glycolysis is thought to be supporting the high glycolytic rate of effector T cells via rapid NAD<sup>+</sup> recycling(67–70).

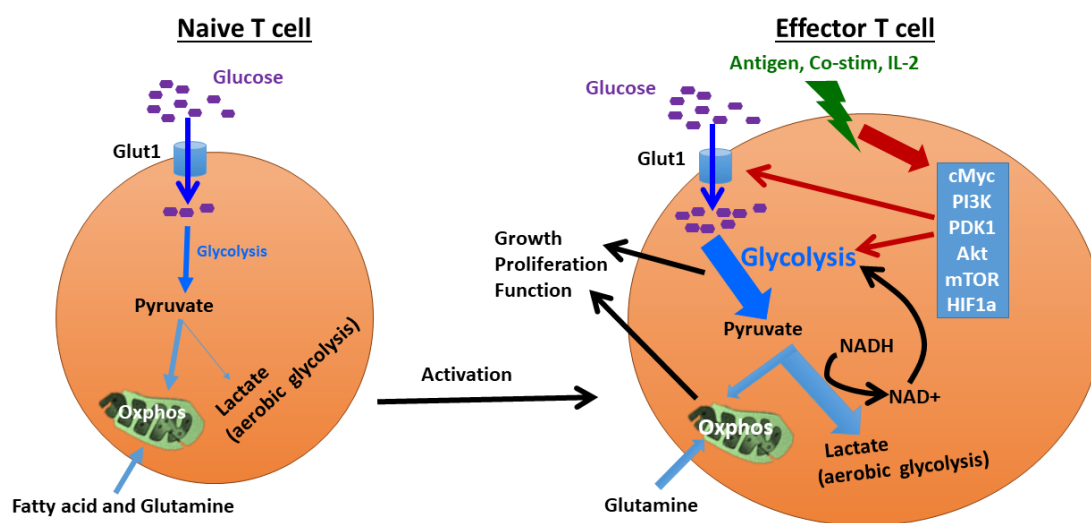


**Figure i. Activation of T cells induces cellular metabolism to support growth, proliferation, and effector function.**

Naive T cells generally take up low amounts of nutrients and consume them during mitochondrial metabolism to meet their relatively low metabolic demands. Activation of these cells via TCR and co-stimulatory signals upregulates the expression of a transcription factor cMyc, which strongly induces (represented by weight of arrows) glucose uptake and glycolysis. Priming of T cells also activates the PI3K-Akt-mTOR-HIF1 $\alpha$  signaling pathway that in combination with IL-2 sustains the elevated glycolytic activity. Effector T cells convert most of the glucose-derived pyruvate into lactate, and in the process regenerate NAD<sup>+</sup> that serves as a cofactor for GAPDH and supports the heightened glycolytic activity in these cells. Effector T cells also have higher OXPHOS capability (glutamine and glucose oxidation) relative to naive T cells although the induction of OXPHOS upon activation of T cells is not as

high as the increase observed in glycolysis. Both of these metabolic programs are important for the generation and function of effector T cells.

While effector T cells convert the majority of their glycolysis-derived pyruvate into lactate, quiescent T cells use most of these metabolites to fuel the mitochondrial TCA cycle(36, 71) (Fig. i). Hence, as T cells become activated, they undergo a phenomenon known as metabolic reprogramming or switching, which is to say they go from predominantly depending on mitochondrial metabolism to mainly relying on glycolytic metabolism(35, 48, 69). It worth noting here that the term metabolic switch does not mean completely abandoning mitochondrial metabolism and engaging glycolytic metabolism. In fact, it is now widely recognized that T cell activation also induces mitochondrial metabolism, although the proportional increase in mitochondrial metabolism is lower than the increase observed in glycolytic metabolism(72–74). The consumption of pyruvate in the mitochondrial TCA cycle results in the production of multiple TCA intermediary metabolites and additional high energy molecules (NADH and flavin adenine dinucleotide (FADH<sub>2</sub>)), which donate electrons to the mitochondrial electron transport chain (ETC)(69, 75). The flow of electron through the ETC pumps protons out of the mitochondrial matrix into the intermembrane space establishing an electrochemical gradient with an accumulation of negative charge on inside and positive charge and protons on the outside of the inner mitochondrial membrane(38). The mitochondria under such polarized state are considered functional as they have the

membrane potential ( $\Delta\Psi_m$ ) necessary to drive protons back into their matrix through ATP synthase, a process that results in the production of ATP (76).

### **Role of glycolytic metabolism in T cell**

There is a tight link between the functional state of effector T cells and their glycolytic activity that reaches beyond the capacity to produce ATP to meet the bioenergetic demands of these cells. In fact glycolysis is an inefficient way of producing ATP compared to OXPHOS, which can produce up to 18 time more ATP per glucose molecule(63). Effector T cells can compensate for the ATP inefficiency of glycolytic metabolism by increasing the amount glucose they take up and the rate of glycolytic flux (40, 77, 78). In addition to being an ATP source, glucose is the major source of metabolites required for generation of cellular building blocks(66, 70). It is generally thought that actively dividing cells such as activated T cells trade the ATP production efficiency of OXPHOS for the biosynthetic efficiency of glycolysis(36, 66, 70). Hence, one of the advantages of relying on glycolytic metabolism is that it allows effector T cells to produce metabolic intermediates that are important for anabolic processes such as the synthesis of amino acids, fatty acids, and nucleotides that are necessary for proliferation(36, 66, 70). Specific examples of glycolytic-mediated anabolic processes includes the utilization of Glucose-6-Phosphate for nucleotide synthesis(63, 79), glyceraldehyde-3-phosphate and dihydroxyacetone phosphate for lipid synthesis, 3-PG

for serine and nucleotide production(65, 80, 81), and pyruvate for alanine generation(65) (Fig. ii). These metabolites are also substrates for the downstream reactions in glucose metabolism(70). Therefore, glycolysis-biased metabolic induction enables effector T cells to increase the production of these metabolites in order to simultaneously support their biosynthetic and metabolic demands(35, 64, 66).

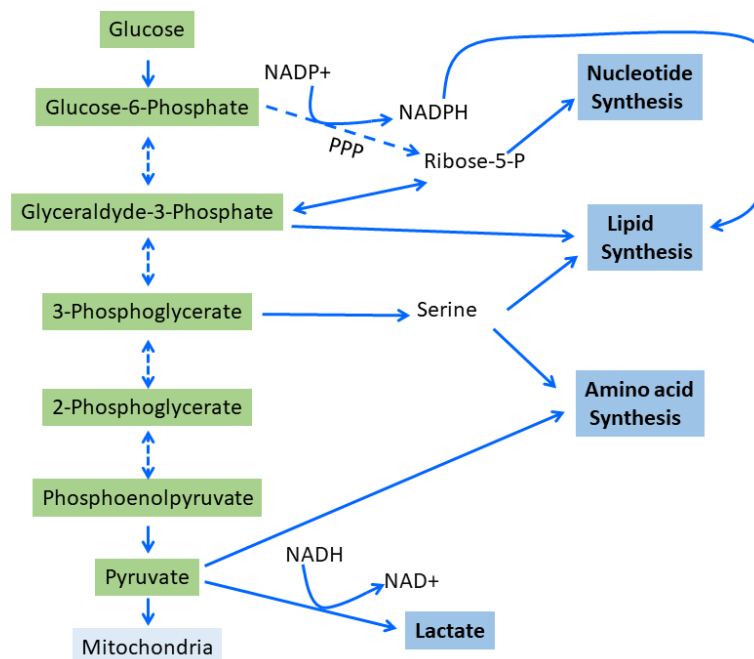


**Figure ii. Glycolytic metabolism is an important source of biosynthetic precursors.**

This schematic shows that several glycolytic intermediates can be used for the synthesis of cellular building blocks such as nucleotides, lipids, and amino acids. Some of the molecules can also be converted back to upstream metabolites that are biosynthetic precursors, as in the case of 2-phosphoglycerate and 3-phosphoglycerate interconversion. PPP, Pentose phosphate pathway

Another essential role of elevated glycolytic metabolism in activated T cells is supporting their effector functions. Activating T cells under conditions that inhibit glycolysis, or in

the absence of glucose, severely impairs cytokine production by murine(78, 82) and human(42) T cells, indicating the critical role of this metabolic program for effector function of T cells. Furthermore, promoting the glycolytic metabolism in vivo via HIF1a stabilization has recently been shown to enhance effector function of CD8+ T cells(83).

Studies have started to elucidate the mechanism by which the glycolytic activity of effector T cells enhances their immunological activities. Chang et al. showed that the engagement of this metabolic program prevents the glycolytic enzyme GAPDH from binding to the 3'-UTR of IFN $\gamma$  and IL-2 mRNA and inhibiting translation of these transcripts in activated CD4+ T cells(84). The authors concluded that GAPDH takes on its secondary role (regulating cytokine mRNA translation) when it is not involved in glycolysis. Multiple studies have previously reported the negative regulation of cytokine mRNA translation by GAPDH (85, 86). Hence, it is possible that glycolytic metabolism promotes effector cytokine production by effector CD8+ T cells, as in the CD4+ T cells, by preventing GAPDH-mediated inhibition. The glycolytic metabolism has also been reported to promote effector function (IFN $\gamma$  production) of T cells via epigenetic modulation(67). This was linked to the ability of glycolytic metabolism to increase the cytoplasmic pool of acetyl-coenzyme A (Acetyl-CoA), which served as substrates for histone acetylation and promoted IFN $\gamma$  expression(67). Another mechanism by which glycolytic metabolism influences T cell effector function is through production of metabolites that can promote TCR downstream signaling(22). A recent study has shown

that the glycolytic intermediate phosphoenolpyruvate (PEP) promotes the effector function of T cells by regulation of TCR-induced  $\text{Ca}^{2+}$ -NFAT1 signaling(22).

Glycolytic metabolism is important not only for the induction of effector function, but also for its maintenance in activated T cells including under immunologically and metabolically challenging conditions such as in chronic viral infection. This has recently been demonstrated by using a mouse model in which glycolytic metabolism was constitutively activated via stabilization of HIF1 $\alpha$ , a key component of the signaling pathway known to promote maintenance of glycolysis, through a conditional deletion of Von Hippel-Lindau (Vhl) in T cells (83, 87). Upon adoptive transfer, the CD8+ T cells in this mouse model were effective at controlling persistent viral infection, slowing melanoma tumors, and extending the survival of tumor-bearing mice, demonstrating that augmenting glycolytic metabolism can make T cells resistant to the immunosuppressive activity of these chronic diseases. Another recent study has shown that elevated glycolytic metabolism can maintain effector activity in CD8+ T cells by making these cells more refractory to metabolic inhibition(88) and by giving them an alternative way of meeting their energy demands under conditions that suppress OXPHOS, such as hypoxia(89). In contrast to the long held thought that enforcing glycolysis may promote effector function at the expense of memory formation, constitutive glycolysis did not prevent the development of functional memory T cells (87, 90). Interestingly, the quick responsiveness of the effector memory CD8+ T cells

has been linked to their capacity to rapidly induce glycolytic metabolism upon antigen exposure(48). Taken together, there are various mechanisms by which an optimally induced glycolytic metabolism can support the generation and maintenance of functional effector T cells.

### **Metabolism of TIL**

Studies have begun to identify a link between T cell exhaustion and metabolic alteration. *In vitro* coculture studies of T cells and tumor cells have shown that the tumor cells limit T cells' access to glucose(84). Effector T cells possess metabolic plasticity, which allows them to utilize other nutrients and metabolic programs when glucose is not available(82, 87). A great example of such metabolic flexibility of T cells is their ability to increase glutaminolysis, the consumption of glutamine, to fuel the TCA cycle that drives OXPHOS, when they are deprived of glucose(82). However, TIL may not be able to engage glutaminolysis as they express high level of PD-1, which has been shown to repress glutamine metabolism in *in vitro* effector T cells(74). Furthermore, immune checkpoint molecules such as PD-1 and CTLA-4 that are highly expressed on CD8+ TIL have been shown to inhibit both the glycolytic and oxidative metabolism in T cells during *in vitro* studies(74). Immune checkpoint signals have also recently been shown to establish metabolic dysfunction even prior to T cell exhaustion in the chronic viral infection model(91), indicating that metabolic dysfunction may be a mediator of T

cells exhaustion. Collectively, these observations suggest that CD8+ TIL may have metabolic alterations that underlie their dysfunction.

### **Immunopathological consequence of altered glucose metabolism in T cell**

Alteration of the glycolytic metabolism in the T cells can have profound immunological consequences. Its hyperactivation leads to immunopathology(72, 92) while its inactivation results in lack of effector function(78, 84). The potential for glycolytic metabolism to empower the immune system to the level it can lead to immunopathology was demonstrated in Glut1 transgenic mice where constitutive expression of Glut1 in T cells resulted in the development of lymphadenopathy and other inflammatory disorders(43). Constitutive glycolysis in CD8+ T cells has also been shown to result in lethal lung tissue damage following chronic LCMV infection(83). Elevated glycolytic activity in CD4+ T cells has also been reported to promote lupus in a mouse model and in human patients (72, 92). Other the other hand, inhibiting the metabolic activities of these cells was sufficient to significantly reduce the disease phenotype in a mouse model(72). Failing to engage glycolytic metabolism can be immunosuppressive as shown by the deficits in effector function of the T cells that are activated in the absence of glucose(78, 82) or in the presence of glycolysis inhibitor(84). Moreover, attenuated glycolytic activity has been associated with T cell anergy(93) and

exhaustion<sup>(91)</sup>. Hence, it is critical to understand whether the CD8+ TIL have alteration in glucose metabolism that could contribute to their exhaustion.

## **THESIS RATIONALE**

It is now widely recognized that the tumor infiltrating CD8+ T cells (CD8+ TIL) play a significant role in fighting against transformed cells. As such, the accumulation of these cells in tumors positively correlates with favorable clinical outcome for most cancer patients. However, these T cells usually lose functional activity and fail to eradicate tumors or prevent disease progression. Interventions such as the inhibition of immune checkpoint molecules that aim to prevent or reverse the dysfunction of these cells have significantly improved cancer immunotherapy. While this has brought great excitement and been proven to work in different cancer types, only small proportion of patients respond to the treatment. Furthermore, the therapy is very expensive. Hence, finding more approaches that can improve the function of CD8+ TIL is still of great interest.

Recent studies have demonstrated that the functional and activation state of T cells is strongly tied to their metabolic activity. Glucose metabolism has been shown to be especially critical for the activation, growth, and function T cells. T cell activation accelerates the metabolism of this critical nutrient by strongly inducing a metabolic program known as glycolysis, which converts it to essential biosynthetic precursors. The

elevated glycolytic activity of these cells allows them to meet the increase in the bioenergetic and biosynthetic demands, which are created by the robust growth, proliferation, and function that ensues immunological activation. Consistent with this, enforcing glycolytic metabolism in T cells has been shown to drive the development of immunopathology including localized tissue damage, lymphadenopathy and other inflammatory disorder in mouse model. It has also been shown to promote autoimmune disease like lupus and to promote tumor control in mouse model and human patients. Inhibition of glycolytic metabolism, on the other hand, strongly suppresses the effector activity of CD8<sup>+</sup> T cells. It has also been associated with T cell anergy and been shown to mediate T cell exhaustion in chronic viral infection. We hypothesized that the limited function in TIL could be dictated by their inability to utilize glycolysis.

My work aimed at investigating the regulation of glucose metabolism as a molecular and biochemical basis of the dysfunction of CD8<sup>+</sup> TIL. CD8<sup>+</sup> TIL have many characteristics that may suggest lack of strong glycolytic activity including diminished effector activities that are known to rely on this metabolic program. These cells also express high level of inhibitory receptors that have been reported to disrupt glycolytic metabolism and they also reside in an environment that has limited availability of glucose and cytokines that are important to maintain glycolysis. Therefore, we tested whether CD8<sup>+</sup> TIL have a glycolytic deficiency that is consistent with a reduction in metabolic support of effector activity. We also investigated cell-intrinsic and cell-extrinsic mechanisms of regulation of

glycolytic metabolism in CD8+ TIL including potential regulation by immune checkpoint signals. Furthermore, we investigated whether mitochondrial metabolism is disrupted in CD8+ TIL.

This study has produced several key findings that contribute to our understanding of the basis of the dysfunction of CD8+ TIL and opens up a new avenue for developing interventions that can improve the metabolic and functional activities of these cells. First, these cells have attenuated metabolic activity that may not be sufficient to support their effector function. Second, the lack of strong glycolytic activity is mediated by post-translational regulation of the activity of a key glycolytic enzyme, enolase. Third, we demonstrated that interventions which can improve enolase activity in CD8+ TIL may have strong translational relevance by showing that the CD8+ TIL that are recruited by immune checkpoint blockade therapy have stronger enolase activity, and further that human melanoma TIL exhibit diminished enolase activity.

## Chapter Two: Materials and Methods

### Tumor cell line, mice, and tumor injection

Ovalbumin-expressing B16 melanoma cell line (B16cOVA) was previously generated in our laboratory<sup>(94)</sup> and was maintained in RPMI1640 (ThermoFisher) supplemented with 5% FBS (Gemini Bio) in the presence of selection agent (blastocidin, Invitrogen). Tumors were generated by subcutaneously injection of  $4 \times 10^5$  B16cOVA cells, MC38 cells (a kind gift from Dr. Victor Engelhard, University of Virginia), or LLC cells (also a kind gift from Dr. Victor Engelhard) into shoulders or flanks of male C57BL/6 mice purchased from National Cancer Institute or ACC1 knockout mice that were obtained by crossing ACC1<sup>fl/fl</sup> mice (a kind gift from Dr. Kyle Hoehn, University of Virginia) with Granzyme-Cre mice in our laboratory.  $1 \times 10^4$  4T1 cells were injected into mammary fat pad of female BALB/c mice purchased from Charles River Laboratories (tumors were generated with help of Kristen Balogh in Dr. Janet Cross Laboratory, University of Virginia). Tumors were allowed to develop for 2-3 weeks before harvesting for analysis. Tumor size was monitored ever one to two days by measuring two perpendicular diameters with calipers, and tumor area was expressed as the product of the two perpendicular diameters of tumors. Mice were sacrificed when tumors reached 16 mm in any one dimension. All mice were treated in accordance to procedures established by the University of Virginia Animal Care and Use Committee protocol #3292.

### Human Samples

Metastatic melanoma samples were collected with informed consent under protocol UVA-IRB# 10598. Excised tumors were processed by the UVA Biorepository and Tissue Procurement Facility (BTRF) Core using a protocol of an initial non-enzymatic disaggregation followed by sequential incubations in a mixture of DNase/collagenase/hyaluronidase (95). Non-digested and digested fractions were stored in the liquid nitrogen. Anonymous male and female healthy donor PBMC were generated from Buffy Coats purchased from Research Blood Components. PBMC were isolated from the Buffy coat by density gradient centrifugation using Ficoll–Hypaque plus (VWR). PBMC were cultured with 10 IU/ml IL-2 alone or in combination with anti-CD3 (1 µg/ml plate bound) and anti-CD28 (1 µg/ml in solution), as indicated in the Figure legends. The activity of enolase in the lysates of the human Teff and TIL was assessed after FACS sorting the *in vitro* stimulated healthy donor PBMC and the *ex vivo* human melanoma TIL (non-digested tumor fractions) for live, CD8+ or CD4+ T cells that are CD3+CD45RO+ and CD137+ or CD137-. All sorts were performed under BSL-2 conditions using Becton Dickinson Influx cell sorter by the UVA Flow Cytometry Core.

### **Checkpoint blockade treatment**

Tumor-bearing mice received no treatment, i.p. injection of 300 µg of control IgG (Equitech-Bio, Inc.) or a combination of 100 µg i.p. of each of anti-PD1 (RMP1-14), anti-TIM3 (RMP3-23) (both from Dr Hideo Yagita, Juntendo University), and anti-CTLA4 (9H10, BioXcell) with or without 2 µg/ml FTY-720 (SML0700, Sigma) on days 8, 11, and 14 post-tumor injection. The FTY-720 treatment was continuously provided through the

drinking water starting on day 8 post-tumor injection. Tumor-bearing mice were treated with 250  $\mu\text{g}$  of each of antibodies in the monotherapy studies.

### **Adoptive T cell transfer**

OT-I T cells were *in vitro* stimulated with plate-bound anti-CD3 and soluble anti-CD28 (both at 5  $\mu\text{g}/\text{ml}$ ) and transferred (2 million cells/mouse i.v.) into day 5 B16cOVA tumor-bearing mice. Tumor size was measured every three days by caliper. Mice were euthanized when tumor size reached 2000 $\text{mm}^3$ .

### **T cell preparation, staining, and flow cytometric analysis**

Splenocytes were isolated from the spleens of naive mice or mice that were immunized with combination of 500  $\mu\text{g}$  Ovalbumin (Sigma), 75  $\mu\text{g}$  poly I:C (Invitrogen), and 100  $\mu\text{g}$  anti-CD40 (clone FGK45, provided by Dr. Stephen Schoenberger, La Jolla Institute) by mechanical homogenization followed by either density gradient separation with Lympholyte-M (Cedarlane) or RBC lysis (Affymetrix). For mouse TIL isolation, intact tumors were excised from mice and subjected to mechanical homogenization and density gradient separation as above. Samples were then stained with Live/Dead Aqua (Invitrogen), OVA<sub>257</sub>-dextramer (Immudex) and fluorescent conjugate antibody specific to surface proteins (CD8, CD44). Following surface staining, samples were fixed/permeabilized with 4% paraformaldehyde/0.1% Tween 20 in 1x PBS or Cytofix/Cytoperm (BD) when stained with antibodies specific to intracellular proteins such as phosphorylated 3-Phosphoinositide-dependent protein kinase 1 (p-PDK1,

Ser244, Santa Cruz), p-mTORC1 (Ser2448, cell Signaling Technology), p-S6 (Ser235/236, Cell Signaling Technology), p4E-BP1 (Thr37/46, cell signaling), HIF1 $\alpha$  (IC1935P, R&D system), PKM2 (D78A4, cell Signaling Technology), Glut1 (EPR3915, Abcam), enolase 1 (EPR10863(B), Abcam), IFN $\gamma$  (XMG1.2, ThermoFisher), TNF $\alpha$  (MP6-XT22, Biolegend), CPT1a (ab171449, Abcam), and secondary goat anti-rabbit FITC (ab6009, Abcam). Foxp3 fixation/permeabilization buffer and nuclear staining protocol (ThermoFisher) was used to stain for HIF1 $\alpha$  (241812, E&D systems) and Ki67 (SolA15, ThermoFisher).

T Cells were *in vitro* stimulated with 1 or 5  $\mu$ g/ml anti-CD3 (specified in figure legends) or 10  $\mu$ g/ml OVA<sub>257</sub> peptide-pulsed CD45-mismatched splenocytes for 4 hours prior to cytokine staining or for 1hr prior to pS6 and p4E-BP1 staining. For PEP or pyruvate functional rescue experiments, cells were treated with DMSO, 1  $\mu$ g/ml PEP (Sigma), or 1mM pyruvate (ThermoFisher) for 10 minutes on ice in glucose-free XF minimal media (Agilent). 0.005% saponin (Sigma) was added to partially permeabilized cells to allow PEP entry into the cells as previously described(96). Cells were then washed with 1x PBS and incubated at 37°C in CO<sub>2</sub>-free incubator in the XF minimal media for 10 minutes to let the cells rest prior to proceeding to 4hr stimulation and cytokine staining. In the experiment involving analysis of cytokine production after acute inhibition of enolase activity, cells were *in vitro* stimulated with 1  $\mu$ g/ml anti-CD3 and 10 IU/ml IL-2 for 24 hours in the presence of vehicle control (water) or 2mM sodium fluoride (NaF). Brefeldin A (BFA) was added only for the last 4 hours of the cell culture to enhance cytokine staining. For assessment of cytokine production after pyruvate treatment and

OXPPOS inhibition, FACS-sorted CD8<sup>+</sup> TIL were cultured overnight in the media containing 2 mM pyruvate, and then stimulated with 1 µg/ml anti-CD3 for 4 hours in the presence of DMOS vehicle or 1 µM oligomycin (O4876, Sigma).

Flow cytometric analysis of the stained cells was conducted by using FACS Canto II (BD Scientific) or Cytoflex (Beckman Coulter) cytometers. Data were analyzed using FlowJo software (Versions 7 to 10, TreeStar). To identify the T cells population of interest, we gated on live cells, lymphocytes, singlets, and CD8<sup>+</sup> cells followed by CD44-low and dextramer-negative for naive T cells; CD44-high and dextramer-positive for Teff and TIL unless differently stated in the Figure legend, as in the case of some *in vitro* restimulation experiments where total CD44<sup>hi</sup> Teff and TIL were taken due to the impact of TCR stimulation on dextramer staining. For T cell sorting, single cell suspensions of spleens or tumors were initially enriched for CD8<sup>+</sup> T cells by MACS magnetic bead separation (Miltenyi Biotec), then stained with OVA<sub>257</sub>-dextramer and antibody against surface antigens as above and placed in 4,6-diamidino-2-phenylindole (DAPI, Sigma) containing media sorted by using Influx cell sorter (Becton Dickenson) applying stringent gating criterion to achieve >99% purity.

### **Glucose uptake**

Splenocytes and TIL samples were prepared as described above and subjected to live/dead staining in 1x PBS at 4 °C for 20 minutes followed by OVA<sub>257</sub>-dextramer staining in 5% FBS at 4 °C for 30min. Cells were then incubated at 37°C and 5% CO<sub>2</sub> for

1hr in glucose-free DMEM media (ThermoFisher) containing antibodies specific to surface proteins for cell identification. Cells were then washed with the glucose-free DMEM media, further incubated under the above culture condition for 15 minutes in DMEM media with or without 100  $\mu$ M 2-NBDG (ThermoFisher), and then washed in 1x PBS and immediately analyzed by flow cytometry while keeping samples on ice(97).

### **Analysis of enolase activity in *in vitro* and *ex vivo* T cell samples**

Cell lysates were prepared according to the enolase activity kit protocol (Sigma) from FACS-sorted CD8+ T cells and CD8+ TIL directly *ex vivo*. Alternatively, T cells were cultured *in vitro* for 4 days with either IL-2 alone (10 IU/ml) or with 5  $\mu$ g/ml plate-bound anti-CD3, 2  $\mu$ g/ml soluble anti-CD28, and 10 IU/ml IL-2. The lysates were then stored at -80 °C until fluorometric direct enolase activity (PEP formation) assay was conducted according to the manufacturer's instructions. Fluorescent intensity was read at  $\lambda_{\text{ex}} = 535/\lambda_{\text{em}} = 587$  nm for 45-60 minutes at 3minutes interval by using Spectramax M5 plate reader (Molecular Devices) set to kinetic reading. In the experiments involving the inhibition of enolase activity, CD8+ T cells from the spleens of the mice immunized with 500  $\mu$ g Ovalbumin, 75  $\mu$ g poly I:C, and 100  $\mu$ g anti-CD40 (FGK45) were restimulated with 1  $\mu$ g/ml plate-bound anti-CD3, 2  $\mu$ g/ml soluble anti-CD28, and 10 IU/ml IL-2 in the presence of 2 mM NaF or vehicle control (water). Alternative, the lysates prepared from *in vitro* CD8+ Teff generated as above without the inhibition of enolase activity were treated with 2  $\mu$ M NaF or vehicle control for 5 minutes prior to reading enolase activity. For assays involving MgSO4 treatment, Teff or TIL samples were cells were either

cultured in IL-2 (10 IU/ml or stimulated with 5 µg/ml plate-bound anti-CD3, 2 µg/ml soluble anti-CD28, and 10 IU/ml IL-2 in the presence or absence of 5 mM MgSO<sub>4</sub> for three days.

### **Enolase reporter, MitoTracker Green (MTG), and tetramethylrhodamine, ethyl ester (TMRE) staining**

Splenocytes and TIL samples were subjected to Live/Dead staining in 1× PBS at 4°C for 20 minutes followed by OVA<sub>257</sub>-dextramer staining in 50 µL of 5% FBS at room temperature for 10 min. Antibody specific to surface proteins were diluted (at 2x of the final concentration) in 50 µL 5% FBS and directly added to the cells being stained with OVA<sub>257</sub>-dextramer, and samples were further incubated for 20 minutes at 4°C. Cells were washed three times with 1xPBS, and then incubate at 37°C for 20 minutes in T cell media containing enolase reporter at the concentration indicated in the figure legends. For MTG and TMRE staining, murine and human T cell samples were stained with Aqua Live/Dead dye and antibodies specific to surface proteins as above, and then incubated at 37°C for 20 minutes with 50 nM MTG (M-7514, ThermoFisher) or 100 nM TMRE (ab113852, Abcam) diluted in T cells media. All samples were washed with 1xPBS twice and immediately analyzed by flow cytometry while keeping them on ice in 0.2% FBS in 1xPBS.

### **Metabolic assay**

Naïve and effector CD8<sup>+</sup> T cells and CD8<sup>+</sup> TIL were FACS sorted as described above, washed with 1xPBS, and seeded ( $2 \times 10^5$  cells/well) in XFp cell culture miniplate in XF minimal media (Agilent) supplemented with 10 mM glucose (Sigma), 2 mM glutamine (Invitrogen), and 2 mM or no sodium pyruvate (ThermoFisher). ECAR and OCR were measured by extracellular flux analysis using XFp (Agilent) in the response to 1  $\mu$ M oligomycin, 1  $\mu$ M fluoro-carbonyl cyanide phenylhydrazone (FCCP), and 0.5  $\mu$ M rotenone/antimycin (all from Sigma except antimycin, MP Biochemical). Radiotracer assays were conducted to measure glycolytic flux based on  $^3\text{H-H}_2\text{O}$  released from [3- $^3\text{H}$ ]-glucose, glucose and glutamine oxidation based on  $^{14}\text{CO}_2$  liberation from D-[ $^{14}\text{C}$  (U)]-glucose or from L[ $^{14}\text{C}$ (U)]-glutamic acid in the TCA cycle, and incorporation of carbon derived from these nutrients into fatty acid via quantification of  $^{14}\text{C}$ -lipid as previously described(98). Intracellular ATP levels of FACS-sorted naïve CD8<sup>+</sup> T cells, Teff, and CD8<sup>+</sup> TIL was determined by using luciferase-based ATP Bioluminescence Assay Kit HS II (Cat# 11699709001, Roche). Cell lysates were prepared and processed for ATP measurement according to the assay kit protocol. The ATP-dependent light emitted during the luciferase reaction was measured by luminometer (Zylux Femtomaster FB15, Zylux).

### **Metabolomics**

FACS-sorted naïve, effector and tumor-infiltrating CD8<sup>+</sup> T cells were washed in RPMI plus 10% FBS, resuspended in pre-chilled 80% methanol/water on dry ice and transferred to -80 °C freezer for 15 minutes to disrupted cells membrane and quench enzymatic activities. Samples were then vortexed while being kept cold and spun down

at 16,000rcf in table top centrifuge to extract the metabolites. Supernatants were harvested and dried by SpeedVac. Samples were then processed and subjected to LC-MS analysis in the Locasale lab at Duke University as previously described(99)

### **Development of Enolase reporter**

In a dram vial, ENOblock (S7443, Selleckchem; 5.0 mg, 0.0079mmol, 1 equivalent) was dissolved in 100 $\mu$ L of anhydrous DMF. In a separate vial, 5-TAMRA NHS ester (8.4 mg, 0.0158mg, 2.2 equivalents) was dissolved in 100 $\mu$ L and transferred to the reaction vial. Diisopropylethyamine (1.1 equivalent) was added to the reaction, and the reaction was stirred at room temperature overnight. Reaction was concentrated on roto-evaporator and purified by reverse-phase HPLC. Purity of product was determined by HPLC on Shimadzu Prominence series HPLC instrument with UV detection at 254 nm. Mobile phases A and B were composed of H<sub>2</sub>O and CH<sub>3</sub>CN, respectively. Using a constant flow rate of 1.0mL/min, mobile phase was as follows 0-5 min, 30% B, 5-17.5 minutes 30-55% B, 17.5-20 min, 100% B and was determined to be >95% pure. Conjugations and HPLC analysis were performed by the Hsu lab, Department of Chemistry, University of Virginia.

### **Enolase 1 post-translational modification analysis**

FACS-sorted melanoma CD8<sup>+</sup> TIL and *in vitro* generated d2 CD8 Teff were washed with PBS, pelleted by centrifugation, and frozen down at -80 °C. Cell pellets thawed and lysed by treating with lysis buffer (50 mM Tris HCl, pH 7.4, with 150 mM NaCl, 1 mM EDTA,

and 1% TRITON X-100) for 1 hour at 4 degrees while rocking. The resulting lysates were pre-cleared by treating them with 20  $\mu$ L protein A magnetic beads (73778, Cell Signaling Technology) per 500  $\mu$ L of lysate while rocking at room temperature for 20 minutes. The lysate was separated from the beads on a magnetic rack and treated with 4  $\mu$ L of Enolase 1 antibody (ab155102, Abcam:) per 200  $\mu$ L of 1 mg/mL lysate overnight at 4 degrees with rocking. The lysate antibody mix was treated with 20  $\mu$ L of pre-washed magnetic beads and rocked for 20 minutes at room temperature. The lysate was separated from the antibody bound beads and washed 5 times (500  $\mu$ L lysis buffer and mix by inversion). The antibody bead complex was washed with urea pre-wash buffer (50 mM Tris pH 8.5, 1 mM EGTA, 75 mM KCl) then eluted using 100  $\mu$ L of urea elution buffer (8 M Urea, 20 mM Tris pH 7.5, and 100 mM NaCl). The antibody bead complex with the urea buffer was incubated with rocking for 30 minutes and the eluate was separated using the magnetic rack. This was repeated 3 times. The resulting eluate was prepared for mass spectrometry using the filter-aided sample preparation (FASP) protocol as described by others(100) and mass spectrometry was conducted as previously described(100, 101). The resulting mass spectrometry files were searched using byonic search software(102) and the resulting peptide matches were included if the ppm error was between -5 and 5 and the cleavage of peptide was specific. The modified spectra count was normalized to the unmodified spectra count using and the figures were generated using a custom R programming script. The domain annotations

were taken from pfam and blast alignments(103). Procedures were performed in the Hsu lab, University of Virginia.

### RNA extraction, cDNA synthesis, and real-time qPCR

Total RNA was extracted from FACS-sorted naive CD8+ T cells, effector CD8+ T cells, and CD8+ TIL with RNeasy plus Kit (QIAGEN), and then reverse transcribed into cDNA using iScript cDNA Synthesis Kit (Bio- Rad). SYBR Green-based real-time qPCR analysis was performed using CFX96 Detection System (Bio-Rad). All samples were run in biological triplicates and normalized to ribosomal protein S18 (Rps18). Fold change in gene expression level was determined by  $\Delta\Delta C_t$  method comparing the expression level of each sample to that of naive CD8+ T cells. The sequences of the primers are as follows:

Gene	Forward primers	Reverse primers
<i>RPS18</i>	5'-ATGCGGC GGC GTTATTCC-3'	5'-GCTATCAATCGTTCAATCCTGTCC-3'
<i>S</i>		
<i>Glut1</i>	5'-CAGTTCGGCTATAAACTGGTG-3,	5'-GCCCCGACAGAGAAGATG-3'
<i>mGlut3</i>	TAAACCAGCTGGGCATCGTTGTTG	AATGATGGTTAAGCCAAGGAGCCC
<i>Hk2</i>	5'-TGATCGCCTGCTTATTCACGG-3'	5'-AACCGCCTAGAAATCTCCAGA-3'
<i>Pfkm</i>	5'-GGAAAGGAAGACAGAGTGGGAGGC-3'	5'-CAGATCGACCTCAACAGTGGGATTC-3'

<i>Pfkb</i>	5'-GGTACAGATTCAGCCCTGCACC-3'	5'-GTCGGCACCGCAAGTCAAGG-3'
<i>GAPD</i> <i>H</i>	GTCGGTGTGAACGGATTTG	5'-TAGACTCCACGACATACTCAGCA- 3'
<i>Pgm3</i>	5'- CCCAGCATCTCGATCATATCATGTTTCG- 3'	5'-GTCCTGCTCCTCCGCACTGG-3'
<i>Eno1</i>	5'-GGAAAGGAAGACAGAGTGGGAGGC- 3'	5'- CAGATCGACCTCAACAGTGGGATTC- 3'
<i>Ldha</i>	5'-CATTGTCAAGTACAGTCCACACT-3'	5'-TTCCAATTA- CTCGGTTTTTGGGA- 3'
<i>Ldhb</i>	5'-GGACAAGTGGGTATGGCATGTG-3'	5'-CCGTCACCACCACAATCTTAGA-3'
<i>MCT4</i>	5'-TCACGGGTTTCTCCTACGC-3'	5'-GCCAAAGC- GGTTCACACAC-3'

### Statistical Analysis

All data are presented as mean  $\pm$  SEM. Statistical significances were determined by unpaired student's *t*-test when comparing two groups and by one-way ANOVA or two-way ANOVA, followed by Tukey's Multiple Comparison Test when comparing more than two groups. GraphPad Prism versions 7 to 8 was used to perform the statistics.

## **Chapter Three: Impaired enolase 1 glycolytic activity restrains effector functions of tumor infiltrating CD8+ T cells**

Lelisa F. Gemta, Peter J. Siska, Marin E. Nelson, Xia Gao, Xiaojing Liu, Jason W. Locasale, Hideo Yagita, Craig L. Slingluff Jr, Kyle L. Hoehn, Jeffrey C. Rathmell, & Timothy N.J. Bullock.

Modified from publication in Science Immunology (2019).

### **ABSTRACT**

In the context of solid tumors, there is a positive correlation between the accumulation of cytotoxic CD8+ tumor infiltrating lymphocytes (TIL) and favorable clinical outcomes. However, CD8+ TIL often exhibit a state of functional exhaustion limiting their activity, and the underlying molecular basis of this dysfunction is not fully understood. Here, we show that TILs found in human and murine CD8<sup>+</sup> melanomas are metabolically compromised with deficits in both glycolytic and oxidative metabolism. While several studies have shown that tumors can outcompete T cells for glucose, thus limiting T cell metabolic activity, we report that a down-regulation of the activity of enolase 1, a critical enzyme in the glycolytic pathway, represses glycolytic activity in CD8+ TIL. Provision of pyruvate, a downstream product of enolase 1, bypasses this inactivity and promotes both glycolysis and oxidative phosphorylation resulting in improved effector function of CD8+ TIL. We found high expression of both enolase 1 mRNA and protein in CD8+ TIL,

indicating that the enzymatic activity of enolase 1 is regulated post-translationally.

These studies provide a critical insight into the biochemical basis of CD8+ TIL dysfunction.

## **INTRODUCTION**

Although the prognostic value of CD8+ tumor infiltrating lymphocytes (CD8+ TIL) in cancer has been reported in various types of cancers(10, 104, 105), the progressive loss of proliferative and effector function (exhaustion) of these cells(15, 16) is a major factor in diminishing anti-tumor immunity. The tumor microenvironment (TME) can promote TIL exhaustion via multiple cellular and molecular mechanisms, among which the expression of checkpoint inhibitory molecules, such as PD-L1, have proven clinically tractable. Blocking the inhibitory signals that TIL receive promotes the activation, expansion, and effector activity of TIL(106, 107). Several studies have defined nodes of transcriptional and enzymatic activity that are regulated by checkpoint molecules (108–110), but the underlying biochemical mechanism by which these inhibitors mediate the exhaustion of TIL is still poorly understood. Previous studies showed that the inhibitory checkpoint signals(21) and the TME(20, 96, 111) alter metabolic activity of TIL.

There is a strong link between activation-induced proliferation and effector function of T cells and their metabolic activity(64, 78, 84). In CD8+ T cells, glucose metabolism is induced initially by TCR signaling upregulating c-Myc expression(112, 113) and is

sustained by mTORC1-HIF1 $\alpha$  pathway with support from cytokines in a PDK1 dependent manner(50, 114). These signals promote glucose uptake and utilization(40, 44, 77, 115). T cell activation induces both glycolytic metabolism and mitochondrial oxidative phosphorylation (OXPHOS), with a more substantial increase occurring in glycolysis(84, 88). Glycolytic metabolism is essential for rapidly dividing cells such as activated T cells, which are thought to trade the ATP production efficiency of OXPHOS for the faster biosynthetic precursor- and ATP-production rate of glycolysis in order to rapidly produce macromolecules and energy(36, 66, 70). Notably, T cells that are activated in the absence of glucose(78) or under conditions that prevent them from engaging glycolysis(84) have deficits in their effector function, indicating that glycolytic metabolism contributes to more than the production of essential building blocks. Moreover, T cells with impaired functional activity, such as anergic T cells(93) and exhausted T cells in chronic viral infection(116), are known to have attenuated glycolytic and/or oxidative metabolism. Thus, limited metabolism constrains T cell function.

Recent studies have begun to discern that TIL dysfunction is associated with disrupted glucose metabolism. Competition between tumor cells and CD8<sup>+</sup> TIL for the limited amount of glucose in the TME results in attenuated glycolytic metabolism and effector function in CD8<sup>+</sup> TIL (21, 96). Further, CD8<sup>+</sup> TIL have also been reported to undergo progressive loss of mitochondrial biogenesis and function, in both murine and human settings (23, 111), limiting ATP production. Notably, enhancing the capacity of *in vitro*

activated T cells to produce the glycolytic intermediate, and pyruvate precursor, phosphoenolpyruvate (PEP) increases their anti-tumor activity after adoptive transfer into tumor-bearing mice(96). These studies imply that glucose deprivation prevents T cells from generating the critical glycolytic intermediates that are necessary for T cell function. However, in *ex vivo* studies, dysfunctional TIL retained their low metabolic and functional activities in the presence of supra-physiological level of glucose (21), suggesting the existence of T cell-intrinsic restraint on glycolysis that remains to be elucidated.

To identify the intrinsic regulator in CD8+ TIL glucose metabolism, here we examined the metabolic activity of CD8+ TIL, quiescent CD8+ T cells, and proliferative effector CD8+ T cells (Teff). We found that CD8+ TIL exhibit a post-translational regulation of the critical glycolytic enzyme, enolase 1 (also known as alpha enolase), leading to a deficit in PEP and its downstream metabolite pyruvate. Bypassing enolase 1 by providing of these metabolites partially restored multiple facets of the CD8+ TIL metabolism and effector function. We documented that a combination therapy consisting of CTLA-4, PD-1 and TIM-3 blocking antibodies increased the presence of enolase-active CD8+ TIL in the tumors. We propose that checkpoint blockade can promote the recruitment of CD8+ TIL with higher metabolic activity and thus effector function.

## RESULTS

### **Glucose metabolism by CD8+ TIL is distinct from that of either quiescent or effector CD8+ T cells**

CD8+ TIL that infiltrate B16cOVA melanoma tumors exhibit phenotypic and functional markers of exhaustion (Fig. 1) in agreement with our previous report of the progressive loss of functional effector CD8+ T cells from the melanoma microenvironment(117).

Given the importance of increased cellular metabolism for the proliferation and effector functions of T cells(64, 78, 84, 118), we hypothesized that CD8+ TIL are metabolically inactive. To test this, we compared the *ex vivo* metabolic activity of antigen-experienced CD8+ TIL (day 12-15 after tumor implantation) and OVA-specific acute effector CD8+ T cells (Teff, 5 days after vaccination with combination of ovalbumin,  $\alpha$ CD40, poly I:C), the latter of which are proliferative and have multiple effector activities. We used naive CD8+ T cells and late (d12) OVA-specific effector CD8+ T cells, whose initial exposure to cognate antigen was synchronized to the time of tumor inoculation, as controls for metabolic quiescence and to control for potential age-related downregulation of metabolic activity. A real-time metabolic assay via extracellular flux (Seahorse) analysis of FACS-sorted CD8+ T cell populations (sorted based on CD44 expression and MHC-dextramer as described in more detail in the Methods) identified that CD8+ TIL had significantly lower ECAR (extracellular acidification rate), a measure of glycolytic metabolism, than acute Teff (Fig. 2A). ECAR measures media acidification as a result of the production of protons from the conversion of pyruvate (the end product of

glycolysis) to lactate. These assays were performed in the presence of the physiological concentration of glucose (10 mM) reported in mouse blood and spleen(96) to eliminate glucose availability as a potential limitation on glycolysis. To confirm the attenuated glycolytic metabolism observed in CD8+ TIL, we took advantage of radiotracer assays in which the consumption of radioactive glucose ([3-<sup>3</sup>H]-glucose) in glycolysis leads to the liberation of tritiated water (<sup>3</sup>H-H<sub>2</sub>O)(98). CD8+ TIL produced 5-6-fold less <sup>3</sup>H-H<sub>2</sub>O than acute Teff (Fig. 2B), confirming the low glycolytic activity of CD8+ TIL. However, CD8+ TIL were glycolytically more active than naive CD8+ T cells (Fig. 2B) (which were metabolically quiescent (64)) and late Teff (Fig. 2C).

We next investigated if CD8+ TIL have low glycolytic metabolism as a result of preferential reliance on OXPHOS. OXPHOS was determined by quantifying the amount of oxygen consumption from the media (oxygen consumption rate; OCR). We found that CD8+ TIL had a lower OCR than acute Teff (Fig. 2D) both under basal conditions and in response to an un-coupler of mitochondrial OXPHOS (FCCP) that allows the determination of maximum OCR. As with ECAR, the OCR of CD8+ TIL was higher than that of the naive CD8+ T cells and late Teff (Fig. 2E). In agreement with the real-time metabolic analysis, an ATP-dependent luciferase assay showed that CD8+ TIL had significantly higher intracellular ATP levels than naive CD8+ T cells, but conversely significantly lower levels than acute Teff (Fig. 2F).

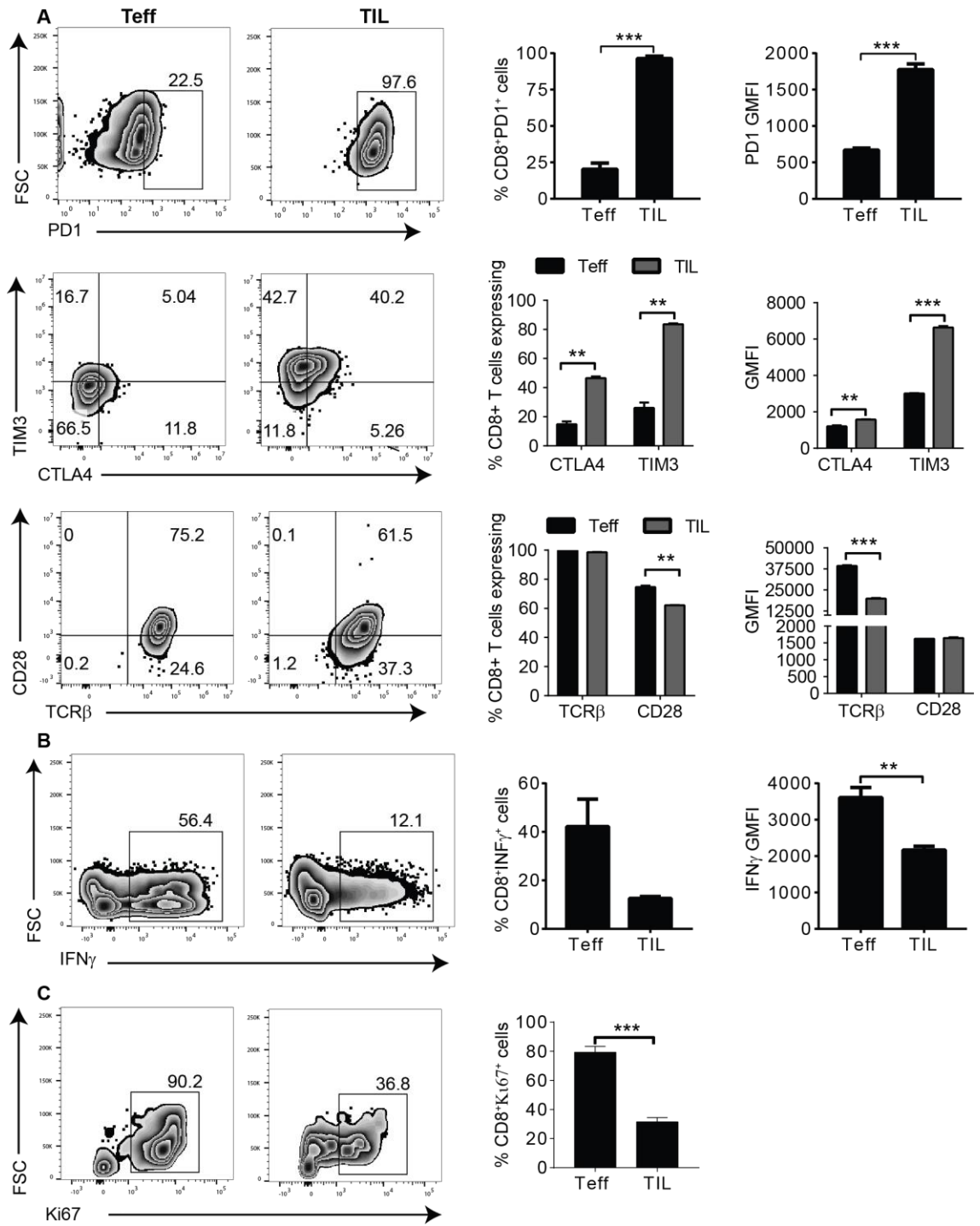


**Figure 1: B16cOVA infiltrating CD8<sup>+</sup> TIL exhibit phenotypic and functional markers of exhaustion.**

Flow cytometric analysis indicating differential expression of PD-1, CTLA-4, and TIM-3 (A), IFN $\gamma$  (B), and proliferation (Ki67 expression) (C) by OVA<sub>257</sub>-specific CD8<sup>+</sup>CD44<sup>hi</sup> T cells responding to vaccination (combination of OVA protein, poly I:C, and anti-CD40) or B16cOVA tumors. Numbers in dot plots show the frequency of expression in representative mice, while bar charts show data from all biological replicates in the experiment. Bar charts show the frequency of expression (middle charts) or the Geometric mean fluorescent intensity (GMFI, right charts) of PD-1 on PD-1<sup>+</sup> cells, CTLA-4 on CTLA-4<sup>+</sup>, TIM-3 on TIM-3<sup>+</sup>, or IFN $\gamma$  on IFN $\gamma$ <sup>+</sup> cells (B). IFN $\gamma$  staining was done after cells were *in vitro* stimulated with peptide-pulsed (10  $\mu$ g/ml OVA<sub>257</sub>) antigen presenting cells for 4hr. Data in A are representative of three to four independent experiments with n=2-3 mice per group. Data in B and C are on samples pooled from n = 5 mice per group. All data show mean  $\pm$  SEM, and were analyzed by unpaired student's *t*-test. \**p* <0.05, \*\**p*<0.01, \*\*\**p*<0.001.

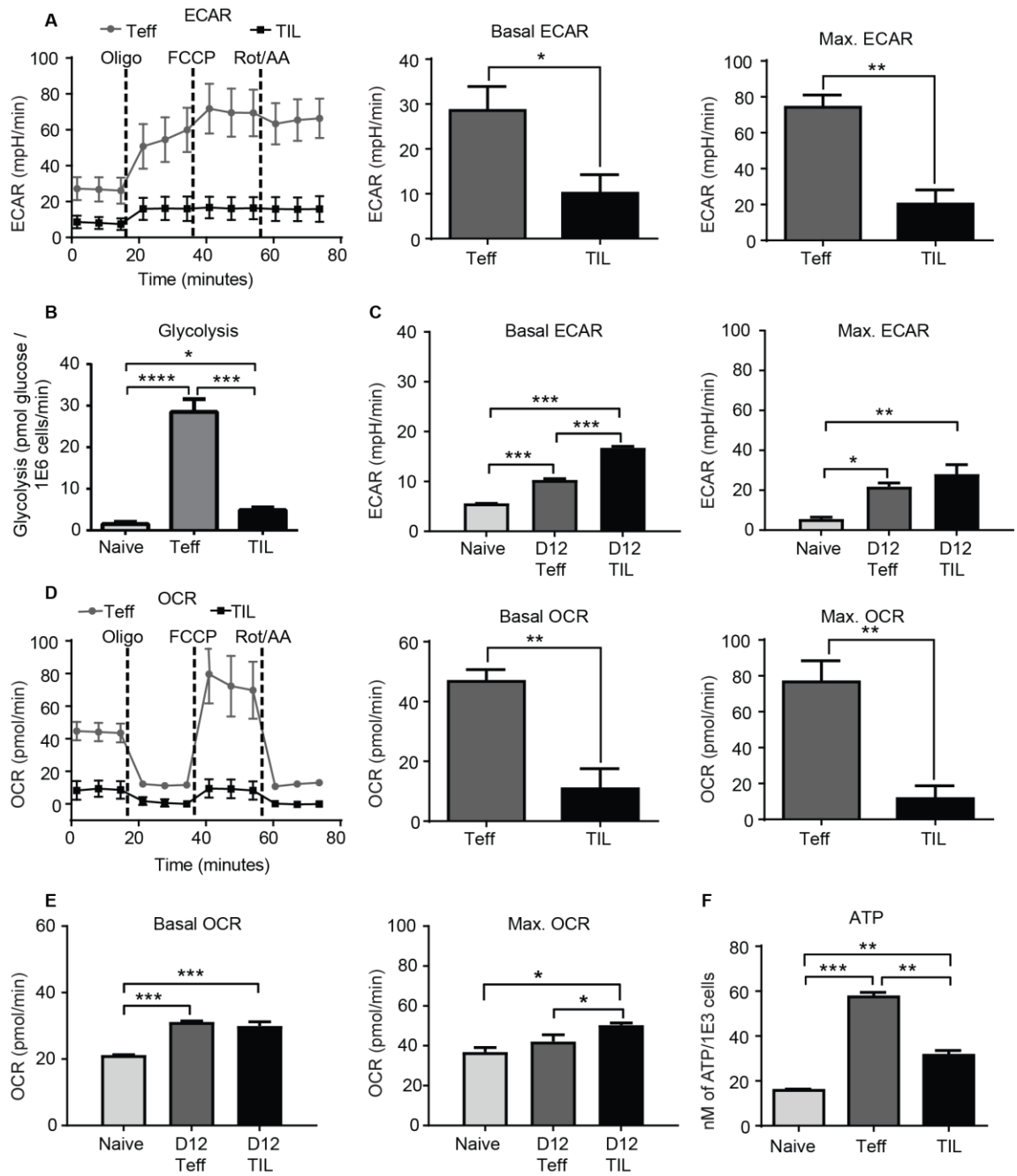


**Figure 2: CD8+ TIL are metabolically less active than acute effector CD8+ T cells, but more active than quiescent CD8+ T cells.**

(A-F) Naive and antigen-specific effector (day 5 and day 12) CD8+ T cells were FACS sorted from the spleens of C57Bl/6 mice immunized with OVA protein, poly I:C, and anti-CD40, while antigen-experienced CD8+ TIL were FACS sorted from B16cOVA melanoma tumors that developed subcutaneously in C57Bl/6 mice for 12-15 days. (A-C) *Ex vivo* T cell glycolytic metabolism as measured by the extracellular acidification rate (ECAR) (A and C) or the amount tritiated water ( $^3\text{H}_2\text{O}$ ) released from [ $3\text{-}^3\text{H}$ ]-glucose during glycolysis (B). The basal ECAR was

measured in unmanipulated cells while the maximum ECAR was quantified after exposing cells to a mitochondrial ATP synthase inhibitor (1  $\mu$ M oligomycin) during the extracellular flux assay. (D-E) Oxidative metabolism (OXPHOS) of the cells in A and C as quantified by oxygen consumption rate (OCR). Basal OCR from sorted cells in the steady state while maximum OCR are cells in response to exposure to an uncoupler of mitochondrial OXPHOS (1  $\mu$ M FCCP). (F) Intracellular ATP levels in sorted *ex vivo* naive CD8<sup>+</sup> T cells, day 5 (d5) Teff, and d14 CD8<sup>+</sup> TIL as measured by luciferase-based ATP determination kit. Data in A, C, D, and E are representative of at least three independent experiments where samples were sorted from  $n = 3-5$  mice per group then pooled in each experiment. Data used to generate graph in B were compiled from two independent experiments where the indicated sorted T cell samples were pooled from  $n = 5 - 9$  mice per group. Data in F are representative of three independent experiments with samples pooled from  $n=3-5$  mice per group in each experiment. Data in A and D show mean  $\pm$  SEM, and analyzed by unpaired Student's *t*-test. Data in B, C, E and F show mean  $\pm$  SEM, and analyzed by one-way ANOVA, followed by Tukey's Multiple Comparison Test. \* $p < 0.05$ , \*\* $p < 0.01$ , \*\*\* $p < 0.001$ .

### **CD8<sup>+</sup> TIL express glucose transporter Glut1 and efficiently take up glucose**

A potential cause of low metabolic activity in CD8<sup>+</sup> TIL could be low glucose availability in the tumor microenvironment(21, 96). However, in the described *ex vivo* extracellular flux assay system we used pure CD8<sup>+</sup> TIL and physiological level of glucose (10 times the amount reported in tumor microenvironments), arguing against competition being the sole limiting factor for CD8<sup>+</sup> TIL metabolism(21, 96). An alternative possibility is that CD8<sup>+</sup> TIL fail to take up glucose due to compromised expression of transporters.

However, qPCR analysis of the mRNA levels of *Glut1* (the major glucose transporter used by T cells(119)) and *Glut3* showed higher expressions of these transcripts in CD8<sup>+</sup> TIL than in naive T cells or Teff (Fig. 3A). Flow cytometric analysis of glucose transporter 1 (*Glut1*) protein also identified that the proportion of CD8<sup>+</sup> TIL that expressed *Glut1* protein was higher than naive CD8<sup>+</sup> T cells (75%), and similar to Teff (99%, Fig. 4A). On a per cell basis, CD8<sup>+</sup> TIL expressed the highest amount of *Glut1* (GMFI= 1075) compared

to naive CD8<sup>+</sup> T cells and acute Teff (GMFI= 255 and 820, respectively, Fig. 4A). The expression level of Glut1 protein on CD8<sup>+</sup> TIL is also higher than late Teff (Fig. 3B). Consistent with the high level of Glut1 expression, we found that CD8<sup>+</sup> TIL were more effective than late Teff and as effective as acute Teff at taking up glucose, as quantified by the uptake of fluorescent glucose analogue 2-NBDG (97) (Fig. 4B). Furthermore, adoptive transfer of *in vitro* activated Glut1 over-expressing OT-1 (2e6 cells/mouse, activated *in vitro* for 3d with anti-CD3 and anti-CD28) into B16cOVA tumor-bearing mice did not improve tumor control (Fig. 4C). Collectively, these data argue that glucose uptake is not the limiting factor that drives CD8<sup>+</sup> TIL glycolytic deficiency.

The sustained expression of Glut1 and glycolytic machinery in CD8 T cells is promoted by contributions of signals from PDK1, mTORC1, and HIF1 $\alpha$  (75, 114, 120) (Fig. 5A). To determine whether CD8<sup>+</sup> TIL had defects in these signaling components that could affect their glycolytic activity, we performed single cell flow cytometric analysis of phospho-PDK1 (p-PDK1) and phospho-mTORC1 (p-mTORC1) and HIF1 $\alpha$ . Note that PDK1 was detected using an antibody specific for the autophosphorylation site (S244) and thus reflects PDK1 expression levels rather than any differences in intrinsic activity. We found that these signaling components were activated to a similar level in CD8<sup>+</sup> TIL and acute Teff. Expression of p-PDK1, p-mTORC1, and HIF1 $\alpha$  were considerably higher in CD8<sup>+</sup> TIL than late Teff, indicating that CD8<sup>+</sup> TIL retain the ability to respond to stimuli that can promote the transport and metabolism of glucose (Fig. 5B-D). Given the

importance of mTORC1 activity in glycolysis, we further investigated its activity by measuring the levels of p-4E-BP1 and pS6, downstream targets of mTORC1. We found no substantial difference in the activity of mTORC1 between acute Teff and CD8+ TIL (Fig. 5E). Taken together, these data suggest that the glycolytic deficiency of CD8+ TIL is driven by a cell-intrinsic mechanism that is downstream of glucose uptake and is independent of the canonical signaling pathways that promote glycolysis.

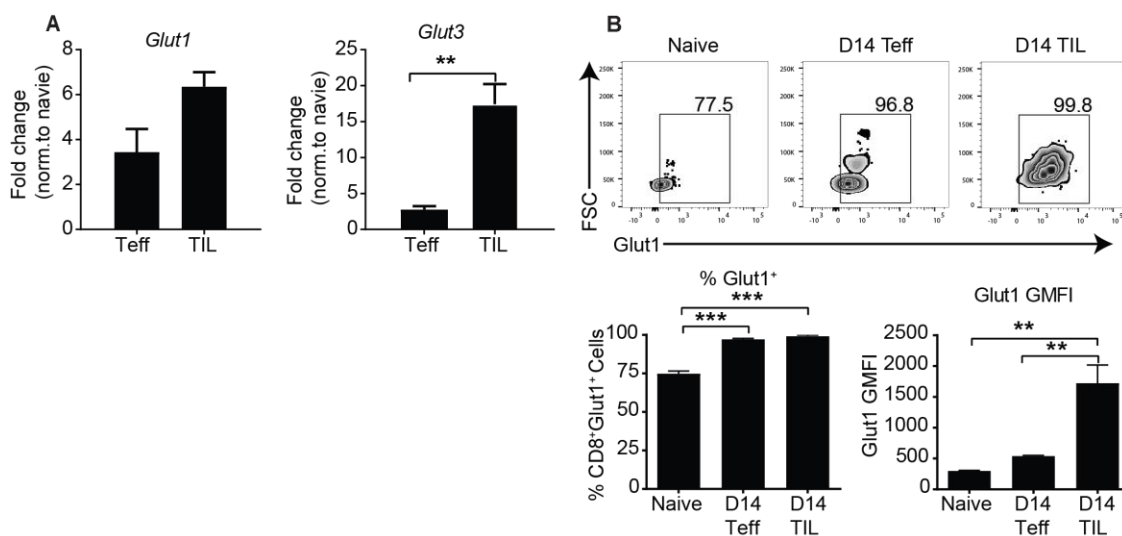


**Figure 3: CD8+ TIL express high levels of glucose transporters.**

Samples of T cells were prepared as in Figure 1 for all the panels. (A) Real-time quantitative PCR (qPCR) analysis of Glut1 and Glut3 mRNA level of FACS-sorted ex vivo d5 CD8+ Teff and d14 CD8+ TIL. (B) The frequency of Glut1-expressing cells (top left and bottom right) within the OVA-specific CD8+CD44<sup>hi</sup> population and the GMFI of Glut1 on Glut1<sup>+</sup> (bottom right) d14 CD8+ Teff and d14 CD8+ TIL. Data in A are representative of two independent experiments with samples pooled from  $n = 3-5$  mice per group. Data in B are representative of three independent experiments with  $n = 3$  mice per group in each experiment. Data show mean  $\pm$  SEM, and analyzed by unpaired student's  $t$ -test (A) or one-way ANOVA, followed by Tukey's Multiple Comparison Test (B). \* $p < 0.05$ , \*\* $p < 0.01$ , \*\*\* $p < 0.001$ .

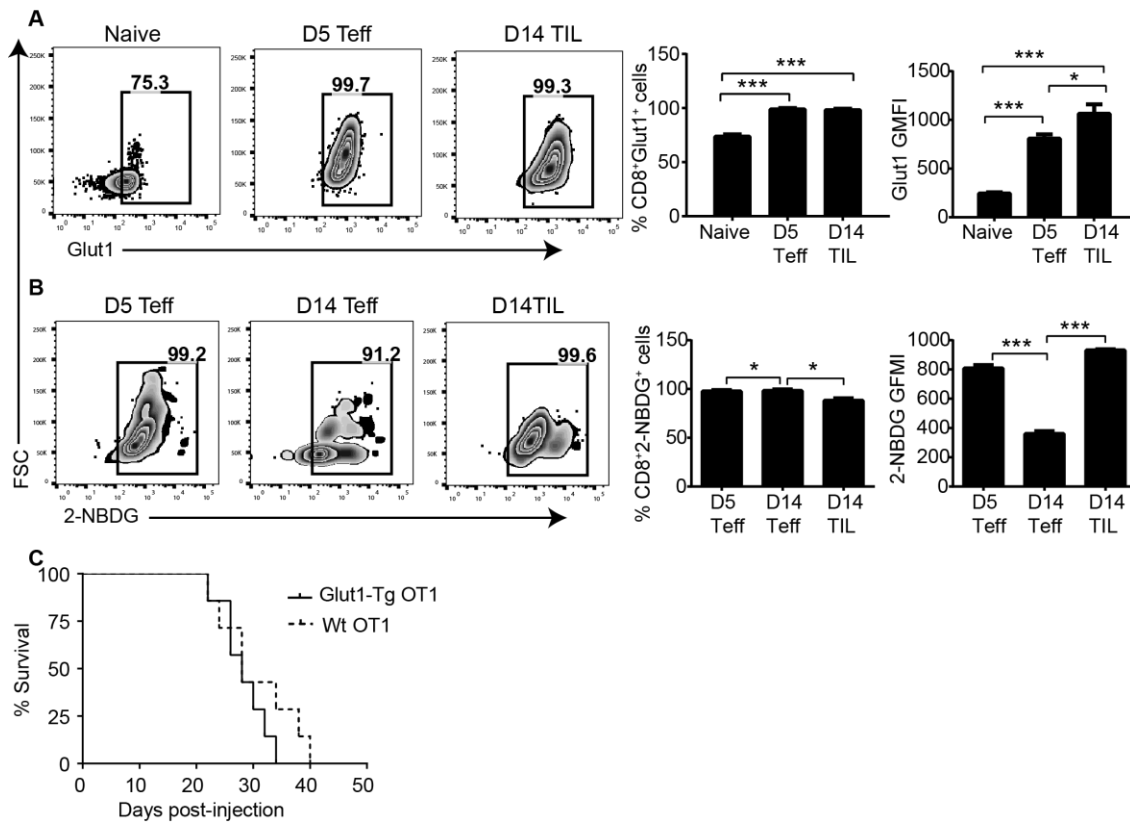


**Figure 4: Glucose uptake is not limited in CD8+ TIL.**

(A) Flow cytometric analysis of glucose transporter 1 (Glut1) protein expression by *ex vivo* naive CD8<sup>+</sup> T cell, d5 Teff, and d14 CD8<sup>+</sup> TIL generated as in Figure 1. The numbers within representative dot plots describe the frequency of cells expressing Glut-1 for individual samples. Bar charts show the overall frequency (middle chart) and intensity of Glut1 expression (GMFI, right chart), of Glut1<sup>+</sup> cells in CD8<sup>+</sup>CD44<sup>lo</sup> naive CD8<sup>+</sup> T cells and OVA-specific CD8<sup>+</sup>CD44<sup>hi</sup> for d5 Teff and CD8<sup>+</sup> TIL. (B) Glucose uptake potential of *ex vivo* d5 and d14 Teff and d14 CD8<sup>+</sup> TIL as measured by flow cytometry after pulsing cells with the fluorescent glucose analog, 2-NBDG. The frequency (middle chart) of 2-NBDG<sup>+</sup> cells and amount of uptake (right chart) within the OVA-specific CD8<sup>+</sup>CD44<sup>hi</sup> cell population are shown. (C) Survival of B16cOVA tumor bearing mice was assessed after adoptive transfer of *in vitro* activated non-transgenic or Glut1 transgenic OT-I T cells five days after s.c. tumor injection. Data in A and B are representative of three to five independent experiments, with at least two mice per group in each experiment. Data in C are from n = 7 mice per group, and the experiment was repeated twice. Data show mean ± SEM: one-way ANOVA, followed by Tukey's Multiple Comparison Test. \*p < 0.05, \*\*p < 0.01, \*\*\*p < 0.001.

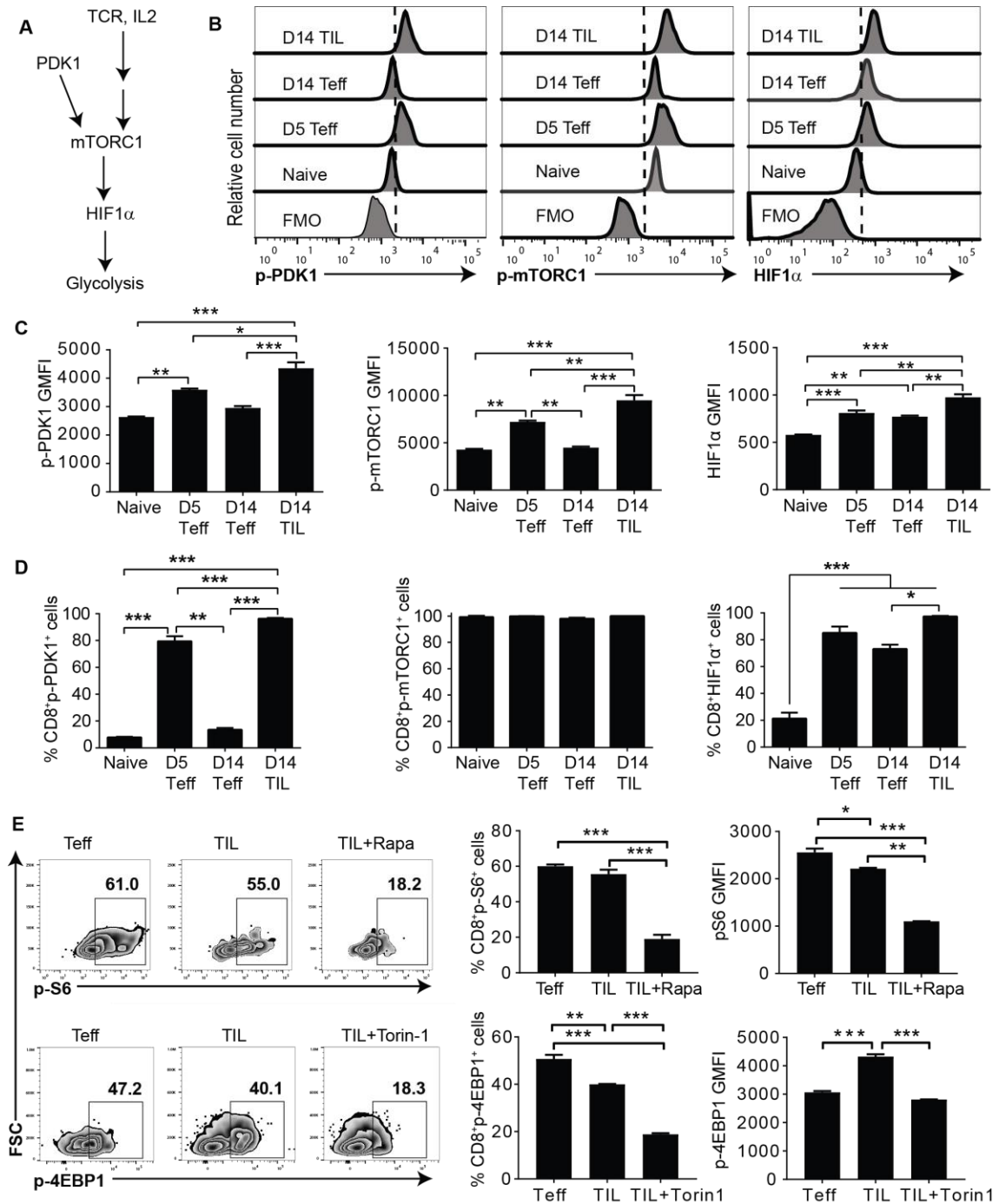


**Figure 5: Glycolysis-regulating signaling molecules are expressed and active in CD8<sup>+</sup> TIL.**

(A) The signaling pathway downstream of TCR and cytokine signals that are known to promote the glucose uptake and glycolysis. (B-D) Flow cytometric analysis of phosphorylated PDK1 (p-PDK1, Ser244), p-mTORC1 (Ser2448), and HIF1 $\alpha$  expression in naive CD8<sup>+</sup> T cells and OVA-specific d5 Teff, d14 Teff, and d14 CD8<sup>+</sup> TIL that were prepared as in Fig. 2. (C) GMFI of pPDK1, p-mTORC1, and HIF1 $\alpha$  in the CD8<sup>+</sup>CD44<sup>lo</sup> naive or OVA-specific CD8<sup>+</sup>CD44<sup>hi</sup> Teff and TIL

expressing the protein of interest. (D) The frequency of p-PDK1+, p-mTORC1+, or HIF1 $\alpha$ + cells within naive CD8+CD44<sup>lo</sup> and OVA-specific CD8+CD44<sup>hi</sup> Teff and TIL. (E) Phosphoflow cytometric analysis of mTORC1 activity via determination of the phosphorylated downstream targets (S6 and 4E-BP1) after 1hr *in vitro* stimulation of acute Teff and CD8+ TIL with 5  $\mu$ g/ml anti-CD3. The CD8+ TIL *in vitro* stimulation was also conducted in the presence of 250  $\mu$ M rapamycin to inhibit pS6 or 250  $\mu$ M Torin-1 to inhibit p4E-BP1 for staining negative control. Data in B-D are representative of three to five independent experiments, with at least two mice per group in each experiment. Data in E are from samples pooled from n = 5-6 mice per group, and the experiment was repeated twice. Data show mean  $\pm$  SEM: one-way ANOVA, followed by Tukey's Multiple Comparison Test. \*p <0.05, \*\*p<0.01, \*\*\*p<0.001.

### **CD8+ TIL possess low levels of phosphoenolpyruvate**

To determine whether a defect lying within the glycolytic pathway and downstream of glucose uptake is responsible for the low metabolic activity of CD8+ TIL, we performed a metabolomics analysis (an unbiased assessment of the relative cellular metabolite composition(99)). We identified a significant (~10-fold) reduction in the steady state level of phosphoenolpyruvate (PEP) in CD8+ TIL compared to acute Teff (Fig. 6A). The relative abundance of the glycolytic metabolites upstream of PEP was similar (Fig. 6A and Fig. 7A), implying that the PEP production step of glycolysis is the point at which glycolysis is disrupted in CD8+ TIL. Furthermore, low levels of pyruvate were found in CD8+ TIL, arguing that excessive PEP to pyruvate conversion does not account for the low levels of PEP (Fig. 6A). Therefore, we hypothesized that PEP deficiency in CD8+ TIL is mediated by reduced expression or activity of enolase 1, the enzyme that is responsible for PEP production in glycolysis. Surprisingly, qPCR and western blot analysis of enolase 1 in FACS-purified CD8+ T cell populations demonstrated that the mRNA and protein levels of enolase 1 were similar between acute Teff and CD8+ TIL (Fig 6B). Intracellular

flow cytometric analysis confirmed that equivalent proportions of Teff and TIL express enolase 1, and that the level of enolase 1 expression in acute Teff and CD8+ TIL were similar (Fig 6C). We also found that the mRNA levels of many glycolytic enzymes were equivalent between acute Teff and CD8+ TIL (Fig. 7, B and D). However, significantly higher amounts of the mRNAs of glycolytic enzymes were observed in CD8+ TIL than in age-matched d14 Teff (Fig. 7, C and D), confirming the notion that CD8+ TIL are not metabolically quiescent as shown in Fig. 2C and E. Together, these data demonstrate that the glycolytic metabolism of CD8+ TIL is altered at the level of PEP production by factors other than the availability of the precursor metabolites or the enzymes responsible for production of PEP.

To understand whether the enolase 1 protein in CD8+ TIL has compromised enzymatic activity that could result in PEP deficiency, we directly assessed the function of enolase in lysates prepared from FACS-sorted CD8+ T cell populations. We found a striking deficit in enolase activity in CD8+ TIL compared to acute Teff (Fig. 6E, left). Furthermore, enolase activity did not increase in FACS-sorted CD8+ TIL following a strong *in vitro* T cell stimulation achieved by cross-linking TCR with anti-CD3 in the presence of anti-CD28. In contrast, *in vitro* T cell stimulation resulted in a marked upregulation of the enolase activity in FACS-sorted acute Teff assessed in parallel (Fig. 6E, right). Taken together, these data support the hypothesis that CD8+ TIL glycolytic metabolism is restrained by

enolase activity rather than enolase expression, implying that enolase function is regulated at the post-translational level in CD8+ TILs.

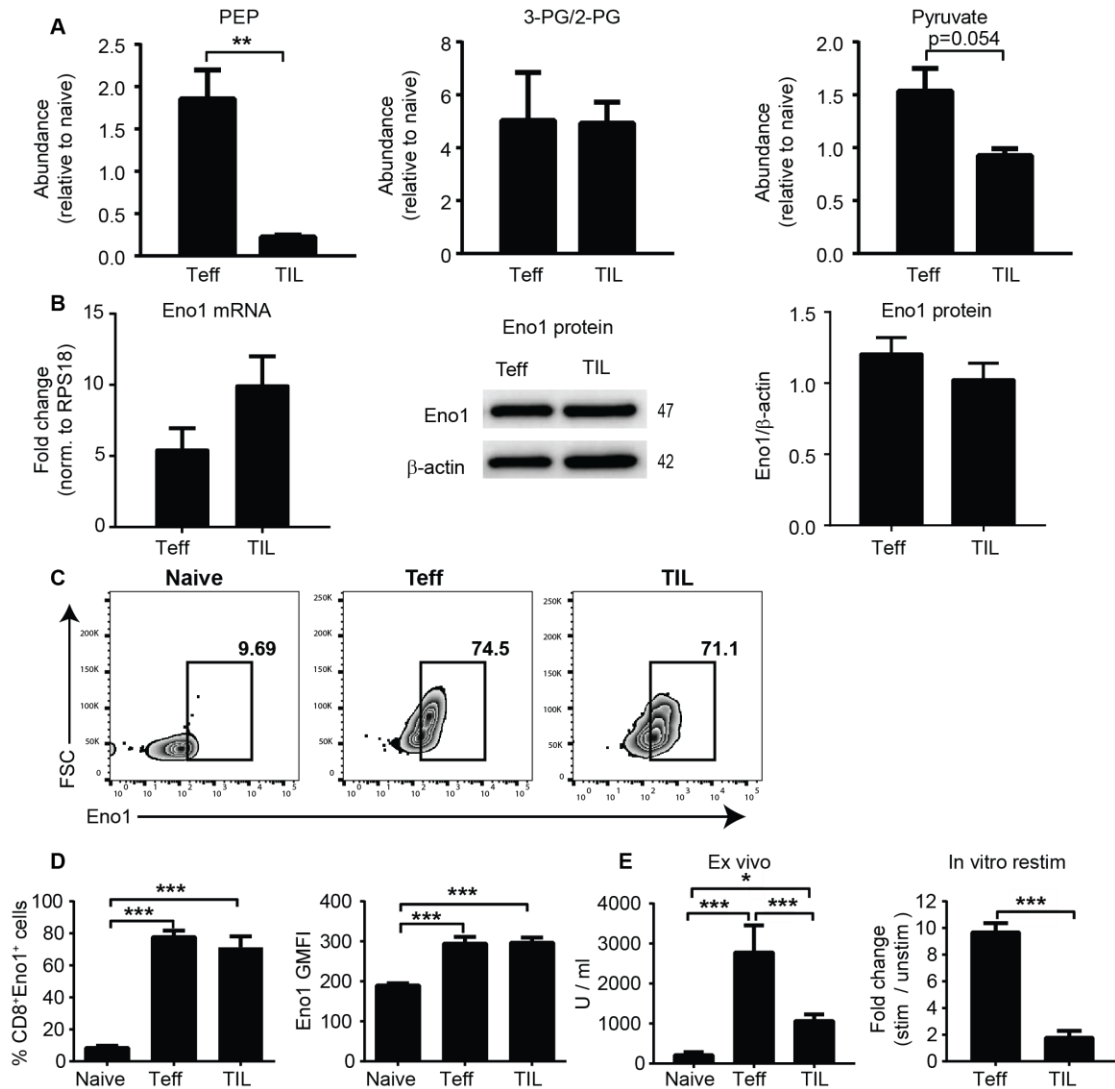


**Figure 6: Weak enolase activity restrains glucose metabolism in glycolysis in CD8+ TIL.**

(A) Metabolomic analysis of the relative metabolite composition of d5 Teff and d14 CD8+ TIL normalized to that of naive CD8+ T cells. Metabolites were extracted from similar samples to that described in Figure 1 and subjected to mass spectrometric analysis. PEP, phosphoenolpyruvate; 3-PG/2-PG, 3-phosphoglycerate and 2-phosphoglycerate. (B) The expression of enolase 1 transcripts in d5 Teff and d14 CD8+ TIL was measured by qPCR and protein by western blot (numbers indicate molecular weight). (C-D) Flow cytometric analysis of enolase 1 protein expression in naive CD8 T cells, d5 Teff, and d14 CD8+ TIL. The frequencies of

cells that express enolase 1 within naive CD8+CD44<sup>lo</sup> and OVA-specific CD8+CD44<sup>hi</sup> Teff or CD8+ TIL are indicated. GMFI is derived from enolase 1-expressing cells. (E) Fluorescence-based spectrophotometric analysis of enolase activity (PEP formation) measured in lysates prepared from FACS-sorted naive CD8+ T cells, acute Teff, and CD8+ TIL either directly *ex vivo* (left) or after *in vitro* stimulation with anti-CD3 and anti-CD28 for 4 days (right). Data are on samples pooled from n = 5-9 mice per group (A), representative from two independent experiments with samples pooled from at least six mice per group (B), and are representative of three independent experiments with at least three mice per group (C-D). Data in E is combined from multiple independent experiments with T cells pooled from 2-3 mice per group. Data show mean  $\pm$  SEM, and analyzed by unpaired student's *t*-test (A, B and E, right) or one-way ANOVA, followed by Tukey's Multiple Comparison Test (D and E, left). \**p* < 0.05, \*\**p* < 0.01, \*\*\**p* < 0.001

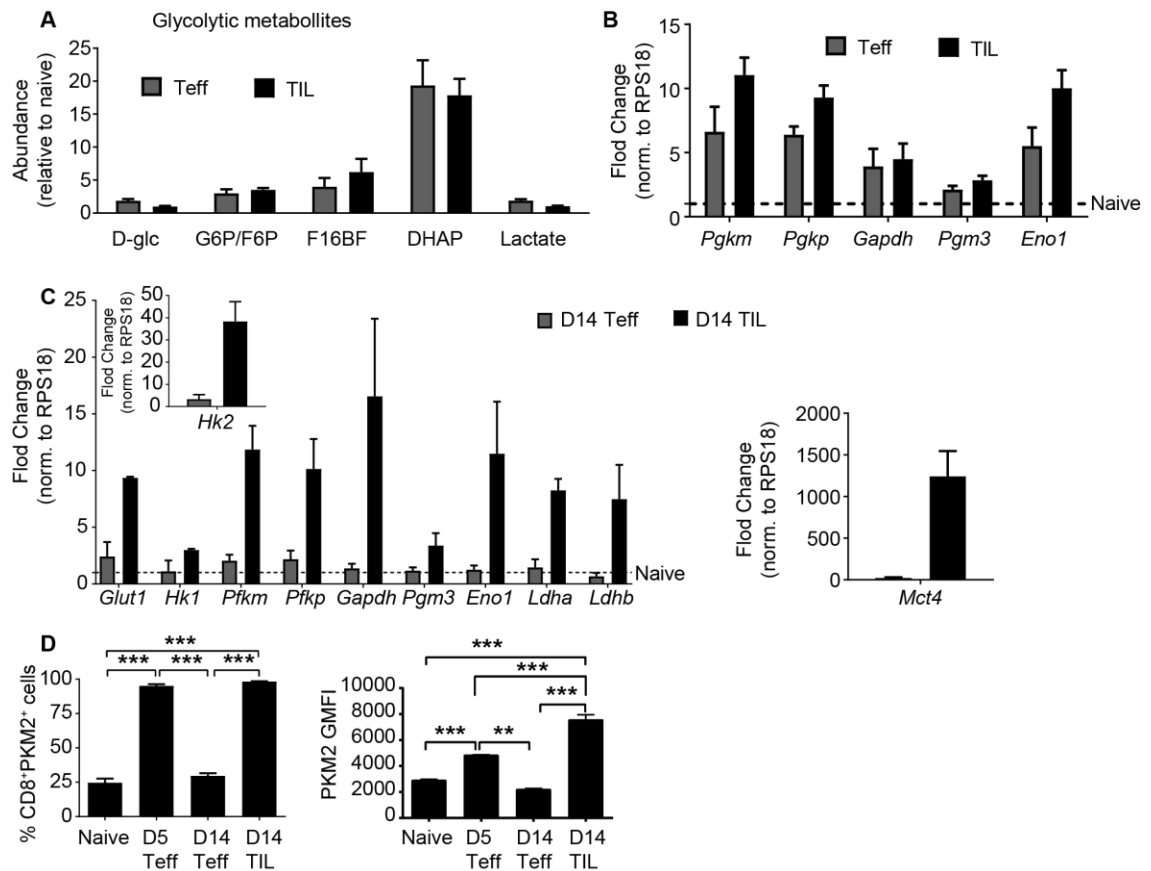


**Figure 7: The abundance of glycolytic enzymes and metabolites suggest that PEP deficiency of CD8+ TIL is driven by lack of strong enolase activity.**

(A) Metabolomic analysis of relative abundance of glycolytic intermediates in FACS sorted *ex vivo* d5 Teff and d14 CD8+ TIL normalized to that of naive CD8+ T cells. Samples were processed as in Fig. 4. D-glc, D-glucose; G6P, glucose 6-phosphate; F6P, fructose 6-phosphate; F16BF, fructose 1,6-bisphosphate; DHAP, dihydroxyacetone phosphate. (B-C) qPCR analysis of the amounts of glycolytic enzymes transcripts expressed by d5 Teff, 14 Teff and CD8+ TIL. Dash line

indicates the level of expression in naive CD8+ T cells, which was adjusted to 1 to determine the fold change in the other cell types. (D) Flow cytometric analysis of PKM2 protein expression level. Data are on samples pooled from n= 5-9 mice per group (A) or representative of two to three independent experiments (B-D), and are presented as mean  $\pm$  SEM. Statistical analysis was done by one-way ANOVA, followed by Tukey's Multiple Comparison Test. \*p <0.05, \*\*p<0.01, \*\*\*p<0.001.

### **Overcoming PEP deficiency rescues CD8+ TIL metabolic and functional activity**

During glycolysis, PEP serves as a substrate for synthesis of pyruvate, which can promote both glycolysis via generation of NAD<sup>+</sup> in a metabolic program known as aerobic glycolysis (the Warburg effect) and also fuels OXPHOS through the mitochondrial tricarboxylic acid (TCA) cycle(70). Given the low glycolytic and OXPHOS metabolism despite high glucose uptake that we observed in CD8+ TIL, we speculated that providing exogenous pyruvate (bypassing glycolysis, or more specifically overcoming the PEP shortage) should rescue CD8+ TIL aerobic glycolysis and OXPHOS. Indeed, exogenous pyruvate provided during metabolic flux analysis of FACS-sorted, ex vivo CD8+ TIL significantly increased the CD8+ TIL basal ECAR, yet had no impact on acute Teff basal ECAR (Fig. 8, A and B, Basal ECAR). The lack of effect on exogenous pyruvate on acute Teff presumably occurs because these cells produce sufficient pyruvate. Notably, provision of pyruvate also substantially increased the maximal ECAR achieved by CD8+ TIL (measurement of ECAR in the presence of oligomycin, which inhibits OXPHOS and forces cells to be dependent upon glycolysis for ATP production, Fig. 8, A and B, Max. ECAR). Interestingly, exogenous pyruvate also enhanced both the basal and maximal OXPHOS in CD8+ TIL as well as acute CD8+ Teff (Fig. 8, A and B, Basal OCR and Max.

OCR), suggesting that glycolytic or pyruvate deficiency could be limiting the OXPHOS capability of CD8+ TIL. Importantly, during a 4hr *in vitro* stimulation, the addition of pyruvate resulted in a significant increase in the frequency of CD8+ TIL that produced IFN $\gamma$  and TNF $\alpha$  (Fig. 8C). Similar results were observed when we provided exogenous PEP to the CD8+ TIL during the short-term *in vitro* cultures (Fig. 8D), suggesting that PEP shortage impairs CD8+ TIL function by limiting pyruvate availability. Together, these data indicate that low enolase activity impairs the metabolic and contributes to the lowered functional activity observed in CD8+ TIL.

To further interrogate the contribution of enolase activity to CD8+ T cell function, we investigated cytokine production after treating Teff and CD8+ TIL with sodium fluoride (NaF), a well-studied enolase inhibitor(121, 122). Consistent with the reported inhibitor effect of NaF on enolase activity in other cells types, NaF strongly inhibited enolase activity in Teff when added to cell culture during acute *in vitro* stimulation (Fig. 9A, cells). Furthermore, NaF completely inhibited enolase activity (Fig. 9A, lysate) when added to the lysates of untreated Teff 5 min prior to assay, suggesting that the reduction in enolase activity as a result of the NaF treatment of cell culture was due to the direct effect of NaF on enolase. Notably, NaF substantially reduced cytokine production from Teff after *in vitro* culture with peptide-pulsed antigen presenting cells (Fig. 9, B and C), further supporting the importance of enolase activity to the effector function of T cells. Importantly, NaF also significantly reduced the remaining cytokine

production from CD8+ TIL (Fig. 9, B and C and Fig 8C), indicating that although it is relatively weak, the activity of enolase in CD8+ TIL plays a significant role in supporting the residual effector function observed in these cells. Taken together, these results indicate that deficiency in enolase activity limits the effector function of CD8+ TIL.

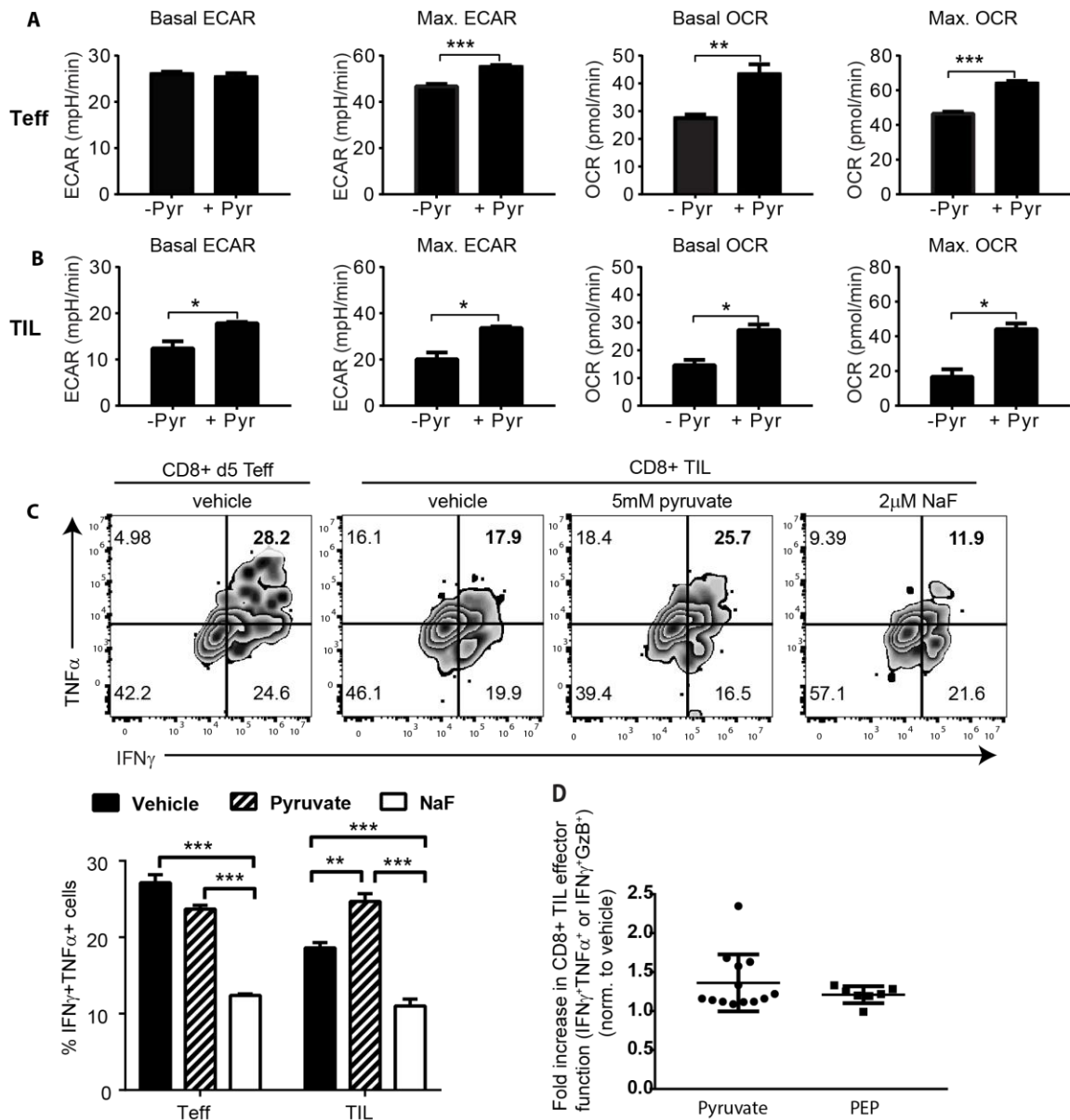


**Figure 8: Bypassing enolase restores metabolic function and effector activity in CD8+ TIL.**

(A and B) ECAR and OCR by FACS-sorted d5 Teff and d12 CD8+ TIL as measured by Seahorse in pyruvate-free or 2mM pyruvate-containing XF minimal media. Basal ECAR and basal OCR were measured without any manipulation while maximum ECAR and maximum OCR were determined after oligomycin or FCCP exposure, respectively. (C-E) Intracellular flow cytometric analysis of IFN $\gamma$  and TNF $\alpha$  production from Teff and CD8+ TIL treated for 4 hours with vehicle, 5mM pyruvate, or 2 $\mu$ M NaF during in vitro culture and stimulation with OVA257-pulsed antigen presenting cells. (D) Fold increase in the proportion of CD8+ T cell expressing cytokines after culturing with 5mM pyruvate or 1  $\mu$ g/ml PEP (after partial permeabilization) for 4 hours. Data are representative of two to three independent experiments and show mean  $\pm$  SEM. Statistical analyses were done by unpaired student's t-test (A, B and D), and two-way ANOVA, followed by Tukey's Multiple Comparison Test C. \* $p < 0.05$ , \*\* $p < 0.01$ , \*\*\* $p < 0.001$ .

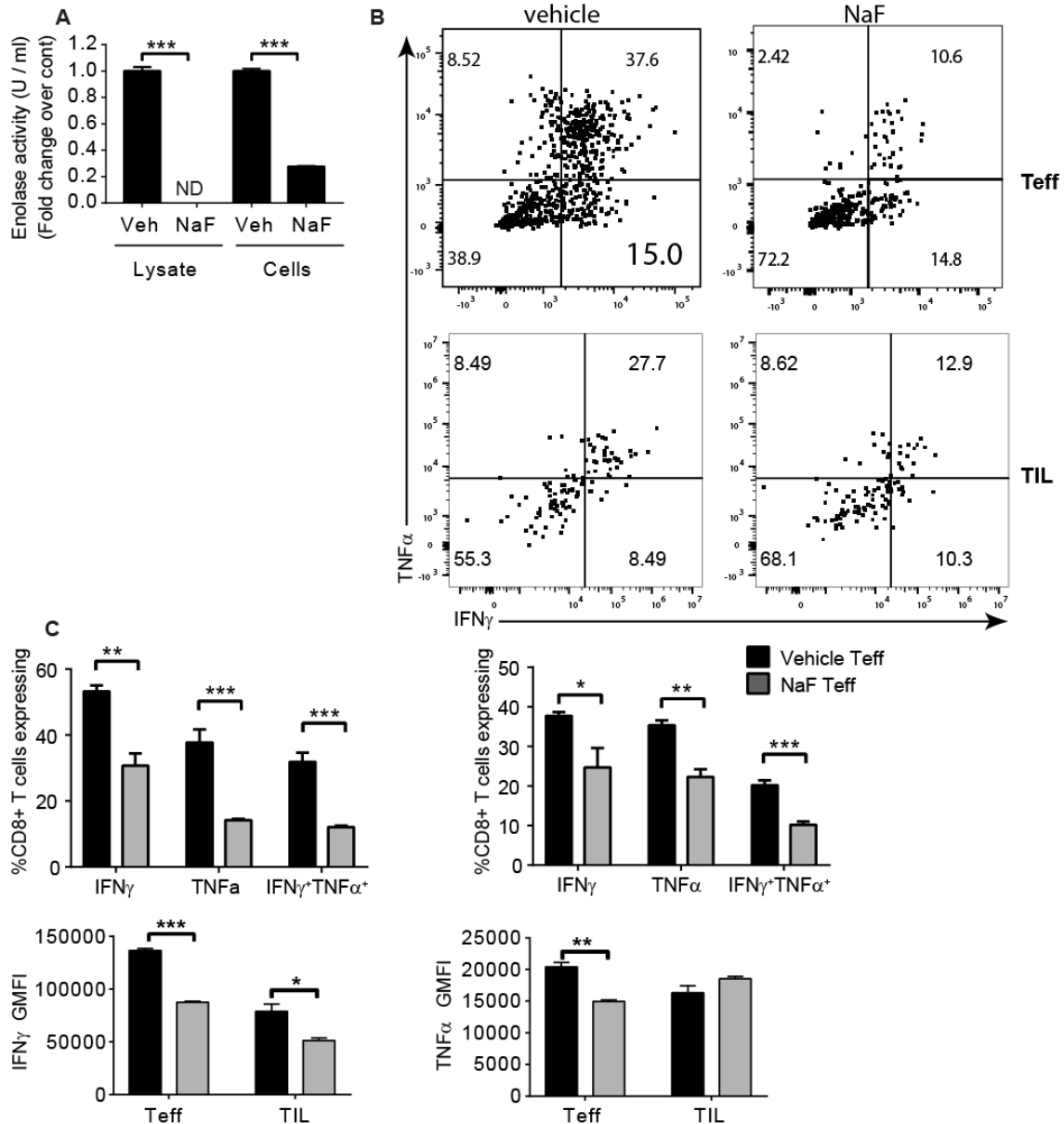


**Figure 9: Inhibition of the enolase activity in T cells limits cytokine production.**

(A) Fluorescent-based spectrophotometric direct enolase activity measurement in the lysates prepared from *in vitro* generated CD8+ Teff and then treated with vehicle (water) or 2  $\mu$ M sodium fluoride (NaF) starting 5 min prior to the initiation of the spectrophotometric reading (A, lysate) or harvested from CD8+ Teff which were treated with vehicle or 2 mM NaF for 24 hours during *in vitro* stimulation (A, cells). ND, not detected. (B-C) Flow cytometric analysis of TNF $\alpha$  and IFN $\gamma$  production from *in vivo* generated acute Teff and CD8+ TIL that were re-stimulated *in vitro* with 1  $\mu$ g/ml anti-CD3 and 10 IU/ml IL-2 for 24 hours in the presence vehicle or 2 mM NaF. Brefeldin A (BFA) was added only for the last 4 hours of the cell culture to enhance cytokine staining. (B) Representative dot plots of acute Teff and TIL, derived from independent experiments (thus differences in quadrant regions). (C) Summary of either the frequency (top

graphs) or the GMFI (bottom graphs) of cytokine production within CD8<sup>+</sup> CD44<sup>hi</sup> OVA<sub>257</sub>-specific T cells. Data are combined from two independent experiments (A) or are representative of three independent experiments with at least three mice per group (B-C), and show mean  $\pm$  SEM. Statistical analyses were done by unpaired student's t-test. \*p <0.05, \*\*p<0.01, \*\*\*p<0.001.

### **Immune checkpoint blockade therapy recruits enolase-active CD8<sup>+</sup> TIL into tumors**

PD-1 has been reported to inhibit glycolytic metabolism in human CD4<sup>+</sup> T cells(74).

Consistent with this, a recent study has shown that blockade of either PD-1 or CTLA-4 augments the glycolytic metabolism in CD8<sup>+</sup> TIL responding to mouse sarcoma tumors(21). This led us to ask if immune checkpoint signals constrained enolase activity in CD8<sup>+</sup> TIL. We treated mice bearing tumors established for nine days with a combination of checkpoint blocking antibodies (anti-PD-1, anti-CTLA-4 and anti-TIM-3 every three days). This treatment regimen increased the absolute number of CD8<sup>+</sup> TIL in the tumors (Fig. 10A) and constrained tumor outgrowth (Fig. 6B) compared to controls. This combinatorial checkpoint molecule inhibition (CPi) did not have significant effect on the expression of enolase 1 (Fig. 10, C and D). However, the CPi treatment significantly improved enolase activity in CD8<sup>+</sup> TIL (Fig. 10E). To determine the relative contribution of the inhibition of PD-1, CTLA-4, or TIM-3 to the increase in enolase activity, we treated tumor-bearing mice with antibodies targeting individual checkpoint molecules. Checkpoint monotherapies did not significantly improve enolase activity in CD8<sup>+</sup> TIL (Fig. 10F). Together, these results indicating that multiple checkpoint signals contribute to the low enolase activity observed in CD8<sup>+</sup> TIL.

To understand the contribution of enolase activity to the anti-tumor effects of the CPi-treated CD8<sup>+</sup> TIL, we investigated the impact of inhibiting enolase on the cytokines and lytic molecules (perforin) production by the CPi-treated CD8<sup>+</sup> TIL. Treatment of CPi-treated CD8<sup>+</sup> TIL with NaF significantly reduced the capacity of the CPi-treated CD8<sup>+</sup> TIL to produce IFN $\gamma$  and perforin (Fig. 11, A and B). These data suggest that the increase in enolase activity in the CPi-treated CD8<sup>+</sup> TIL contributes to the anti-tumor activity of these cells.

We next investigated whether the CPi treatment increases enolase activity in CD8<sup>+</sup> TIL via reactivation of enolase in pre-existing intratumoral CD8<sup>+</sup> TIL or by inducing/sustaining enolase activity in newly infiltrating CD8<sup>+</sup> TIL. For this study, the CPi experiment was conducted in the presence or absence of a well-known S1PR-agonist FTY-720 that blocks T cells from exiting the secondary lymphoid tissues. FTY-720 treatment abrogated the ability of CPi treatment to increase enolase activity in CD8<sup>+</sup> TIL (Fig. 10G). These data indicate that the combinatorial checkpoint molecule blockade either enhances enolase activity in the recently activated CD8<sup>+</sup> TIL or sustains it in newly the tumor infiltrating T cells, rather than re-activating enolase in the CD8<sup>+</sup> TIL that are already in the tumors.

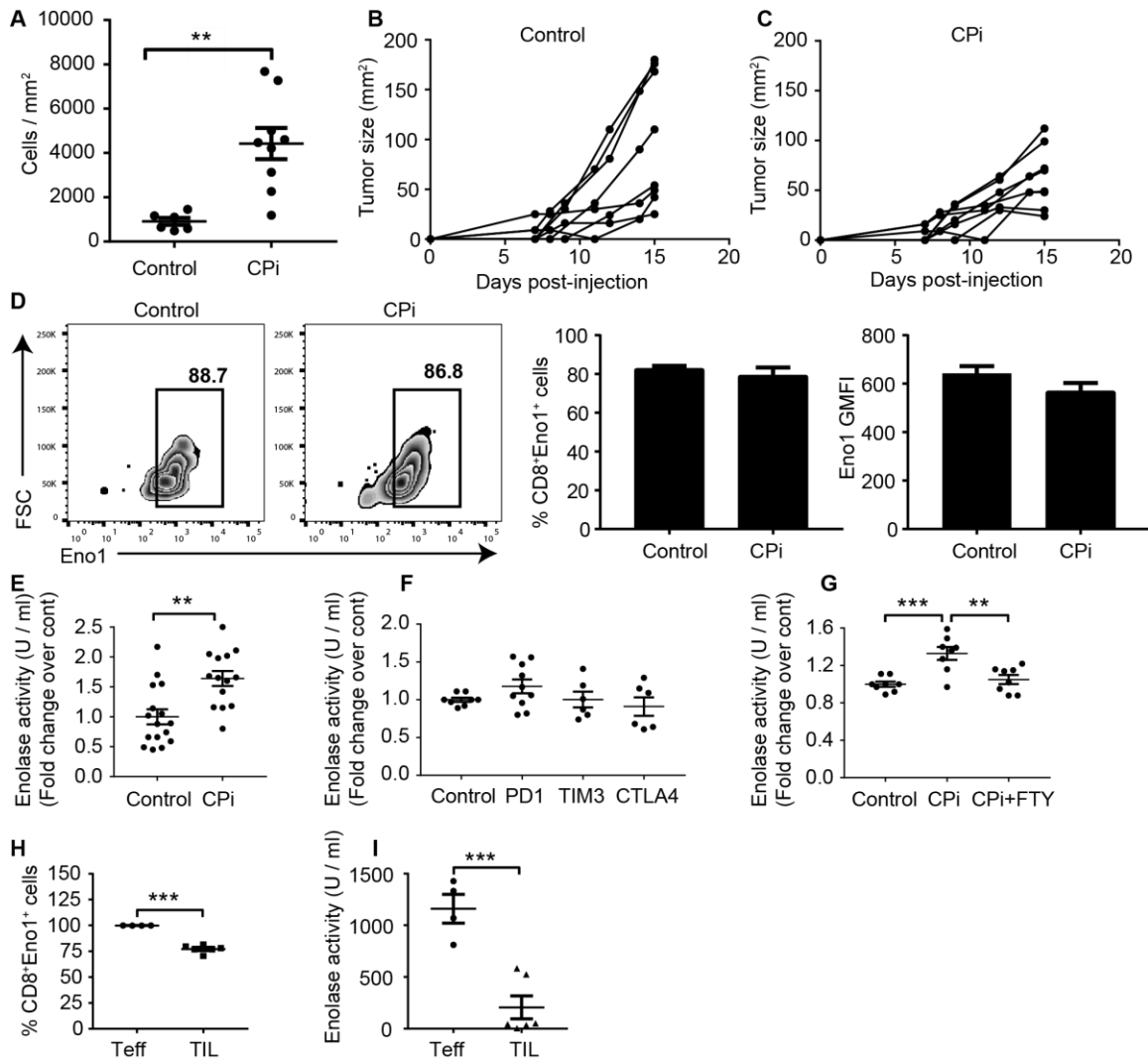


**Figure 10: Checkpoint molecule blockade supports CD8+ TIL enolase function.**

(A - G) B6 mice were s.c. injected with B16cOVA tumor cells and treated with either control, combination of checkpoint inhibitors (CPI: anti-PD-1, anti-CTLA-4, and anti-TIM-3) antibodies or individual antibodies on days 8, 11, and 14. (G) FTY-720 treatment was continuously provided through the drinking water starting on day 8 post-tumor injection. All tumors were harvested on day 15 post-injection. (A) The absolute numbers of antigen-experienced CD8+ TIL per mm<sup>2</sup> tumor. (B) Tumor growth over time. (D) The frequency (left and middle) and intensity of expression (right) of enolase within OVA-specific CD8+CD44<sup>hi</sup> populations from control or combined CPI-treated mice. (E-G) Fluorescent-based spectrophotometric direct enolase activity (PEP formation) measurement in the lysates prepared from FACS-sorted antigen-experienced CD8+ TIL from control, combined-CPI (E and G), or individual-CPI (F) treated mice in the absence (E-G) or presence of FTY720 (G). The enolase activity in panel E and F were normalized to the average of the control replicates for CD8+ TIL to allow cross-experiment comparison. (H and I) Analysis of enolase 1 expression and activity in ex vivo human CD8+ TIL using human healthy

donor PBMC that were *in vitro* stimulated with anti-CD3 and anti-CD28 for three days as a positive control. (H) Frequency of enolase 1 positive cells within CD8+CD45RO+ human Teff and TIL. (I) Fluorescent-based spectrophotometric analysis of the activity of enolase in lysates prepared from FACS-sorted CD8+CD45RO+ human Teff and TIL. Data are representative of three independent experiments (A-D), combined from three to five independent experiments with samples pooled from at least three mice per group (E and F), combined from two independent experiments with at least three mice per group (G), or from two healthy donor PBMC and three melanoma patient TIL (H-I). Data show mean  $\pm$  SEM and analyzed by unpaired student's t-test. \* $p < 0.05$ , \*\* $p < 0.01$ , \*\*\* $p < 0.001$ .

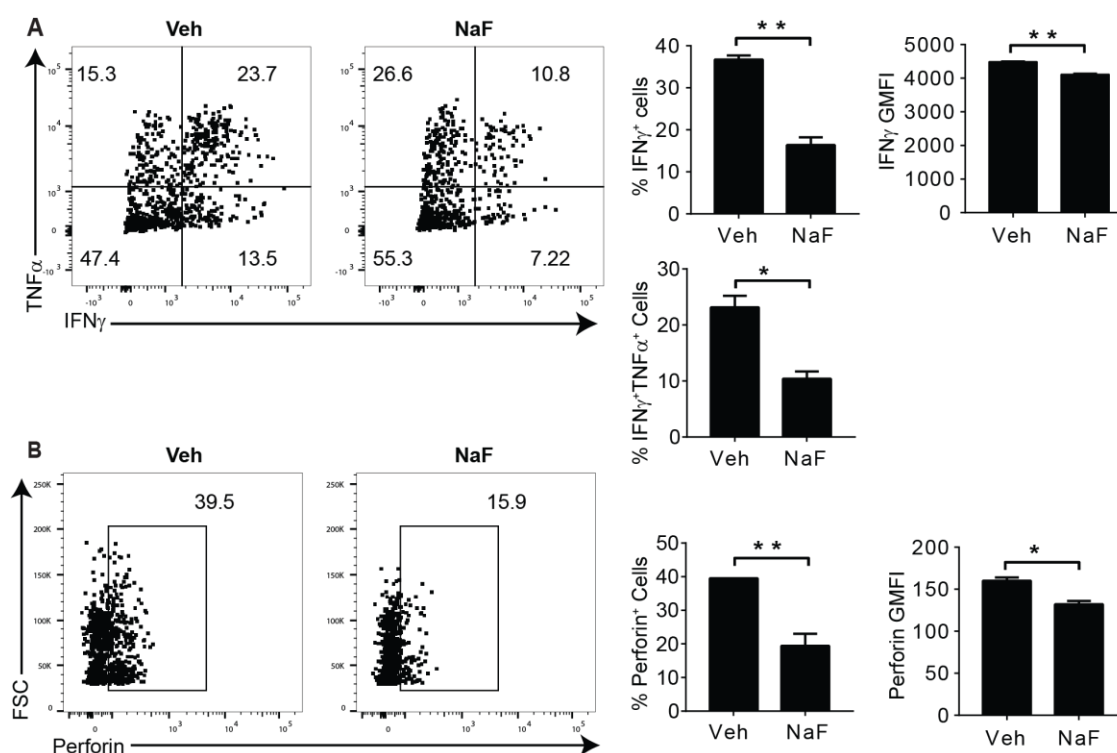


**Figure 11: Enolase activity contributes to the effector function of CPI-treated CD8+ TIL.**

B6 mice were s.c. injected with B16cOVA tumor cells and then treated with a combination of checkpoint inhibitors (CPI: anti-PD-1, anti-CTLA-4, and anti-TIM-3) antibodies on days 8, 11, and 14. Tumors were harvested and FACS sorted on day 15 post-injection. Flow cytometric analysis of TNF $\alpha$  and IFN $\gamma$  (A) or perforin (B) production from the combinatorial CPI-treated CD8+ TIL that were *in vitro* stimulated with 1  $\mu$ g/ml anti-CD3 and 10 IU/ml IL-2 for 24 hours for 24 hours in the presence vehicle (veh: water) or 2  $\mu$ M NaF. Brefeldin A (BFA) was added only for the last 4 hours of the cell culture to enhance cytokine staining. Numbers in the representative dot plots (A and B) show the frequencies of the cells expressing the protein being evaluated. The summary bar graphs (A and B) show either the proportion of CD8+ TIL that express the protein depicted on the Y-axis or the GMFI of the protein labeled on the Y-axis within the expressing

cells. Data are representative of two independent experiments with CD8+ TIL pooled from at least 3 mice per group in each experiment (A and B), and show mean  $\pm$  SEM. Statistical analyses were done by unpaired student's t-test. \* $p < 0.05$ , \*\* $p < 0.01$ , \*\*\* $p < 0.001$ .

### **Human melanoma CD8+ TIL have low enolase activity**

To understand whether enolase activity is altered in CD8+ TIL that infiltrate the human cancers, we sorted antigen experienced (CD45RO+) CD8+ TIL from metastatic melanoma samples. Compared to PBMC from healthy donors that were stimulated *in vitro* to generate Teff, human CD8+ TIL produce limited amount of IFN $\gamma$  after cross-linking the TCR (Fig. 12A). Activation of human healthy donor PMBC also strongly induces (4-fold) their enolase activity as judged by direct analysis of enolase activity within cell lysates (Fig. 12B). Over 80% of the antigen-experienced human CD8+ TIL (Fig. 10H) and about 50% of the antigen-experienced CD4+ TIL express enolase 1 (Fig. 12D)). However, consistent with our murine studies, we found limited enolase activity in both antigen-experienced CD8+ TIL and CD4+ TIL compared to the acutely activated human healthy donor T cells (Fig. 10I and Fig. 12E). Notably, there was a trend towards higher enolase activity in 41BB (CD137)-positive compared to 41BB-negative CD8+ TIL (Fig. 12C), where 41BB expression identifies T cells that may have recently responded to TCR stimulation(123). This suggests that functional enolase may correlate with T cells that maintain functional responsiveness. Thus, we conclude that human melanoma CD8+ TIL have similar low enolase activity as observed in murine models, and that their metabolic activity is likely to be similarly impeded, contributing to the observed defect in effector function.

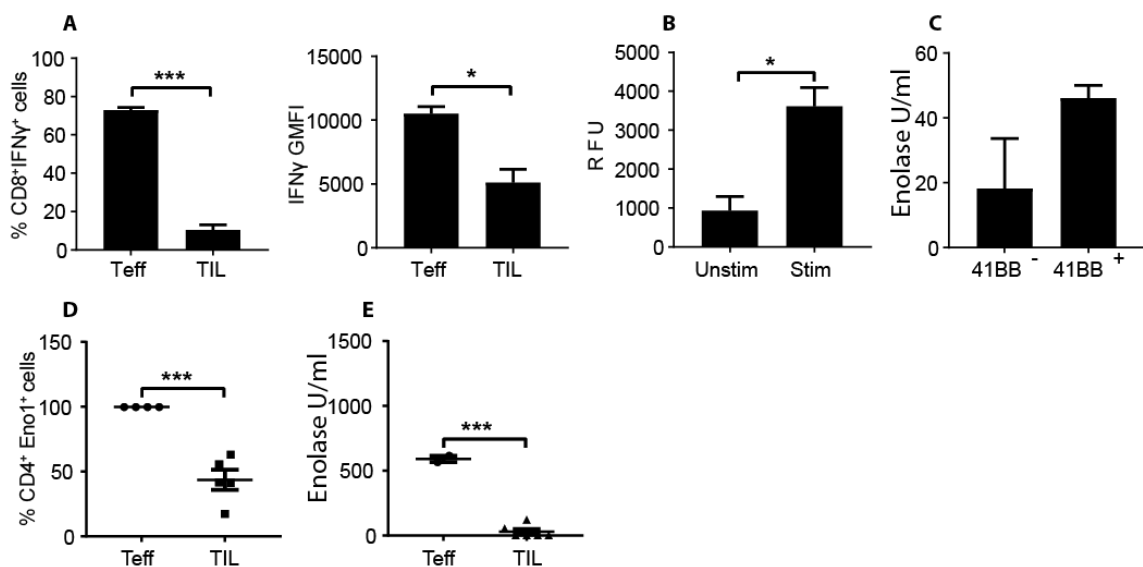


**Figure 12: Human melanoma TIL have low functional and enolase activity.**

(A) Flow cytometric analysis of IFN $\gamma$  production from d3 *in vitro* activated healthy donor CD8 $^+$  PBMC and antigen-experienced *ex vivo* human melanoma CD8 $^+$  TIL after 4 hours anti-CD3 stimulation. (B) The activity of enolase in lysates prepared from quiescent or d4 *in vitro* anti-CD3 and anti-CD28-stimulated human healthy donor PMBC. (C) Enolase activity in FACS sorted 41BB $^-$  or 41BB $^+$  human melanoma CD8 $^+$ CD45RO $^+$  cells. (D) Frequency of Enolase 1 expressing cells of CD4 $^+$ CD45RO $^+$  healthy donor PBMC or TIL. (E) Enolase activity in FACS sorted CD4 $^+$ CD45RO $^+$  healthy donor PBMC or TIL. Data are from 2 healthy donor PBMC and 3 melanoma patients TIL, and show mean  $\pm$  SEM. Statistical analyses were done by unpaired student's t-test. \*p < 0.05, \*\*p < 0.01, \*\*\*p < 0.001.

## DISCUSSION

Elevation of metabolic activity is essential for effector T cells to support their proliferation and function(19, 22, 31). Our data support the developing notion that an underlying basis of TIL dysfunction is insufficient glycolysis and OXPHOS to support strong effector functions(20, 21, 96, 111). This state persists even though CD8 $^+$  TIL are capable of efficiently transporting glucose and have active signaling pathways that normally promote the expression of the enzymes that are involved in glucose

metabolism. This indicates that CD8+ TIL represent a population of cells that are undergoing constant stimulation and that their attenuated metabolic activity is not a function of immunological quiescence. Rather, glucose metabolism is constrained in CD8+ TIL by weak enolase activity, which resulted in limited production of PEP, a vital glycolytic intermediate, and provision of pyruvate or PEP is sufficient to restore some of the metabolic and functional activity of CD8+ TIL. Remarkably, the reduction in enolase activity is regulated post-translationally. Our data show that a checkpoint molecule inhibition protocol that slowed tumor outgrowth results in the infiltration of tumor by CD8+ TIL with improved enolase activity. The low proliferative and functional activity of CD8+ TIL, allied with their limited metabolic activity, could indicate that these cells are simply quiescent. However, compared to naive and late (age-matched) effectors, we find high levels of expression and activation of the PDK1-mTORC1-HIF1 $\alpha$  signaling pathway, which lies downstream of the TCR and cytokine receptors. Indeed, the level of activation of this pathway was equal to, or higher, than seen in acute Teff. Consistent with this, we found no defect in the expression of Glut1, the major transporter of glucose in lymphocytes, or the ability of CD8+ TIL to acquire glucose from their surroundings. Thus, the inability of CD8+ TIL to consume glucose despite the expression of the glycolytic machinery indicates that the glycolytic inactivity of CD8+ TIL is regulated by a functional defect in the glycolytic pathway rather than quiescence or a lack of stimulation. Notably, while the biomarkers (i.e. signaling molecules and molecular components of glycolysis) of T cell glycolysis correlate well with the actual metabolic

activity (as judged by flux assays) of naive and effector CD8<sup>+</sup> T cells, it is important to note that there is not a strong correlation between the activation state of these molecules and the overall metabolic activity of CD8<sup>+</sup> TIL; thus, the sole use of glycolytic biomarkers may over-estimate the metabolic activity of CD8<sup>+</sup> TIL. Importantly, this study pinpointed the mechanism responsible for restraining CD8<sup>+</sup> TIL glycolytic metabolism to weak enolase activity, which resulted in reduced levels of PEP and pyruvate. PEP can support T cell function in two major ways: by promoting cytokine production via calcium signaling(96) and by serving a substrate for pyruvate synthesis(70). A recent study has demonstrated that the anti-tumor activity of *in vitro* activated T cells after adoptive transfer into tumor-bearing mice improves when PEP production is augmented(96). Our findings not only support that report, but also directly show that endogenous CD8<sup>+</sup> TIL have low levels of PEP and that the shortage of this metabolite constrains both the glycolytic and mitochondrial metabolism in CD8<sup>+</sup> TIL. Surprisingly, we did not observe accumulation of glycolytic metabolites upstream of PEP as one might expect from the loss of enolase activity. However, this is not uncommon in a complicated biological systems such as glycolysis, which involves bidirectional reactions, feedback inhibition, and metabolites with multiple possible fates(66, 70). For example, 2-PG (enolase's substrate) can be converted back to upstream metabolite 3-PG(125), which can be taken out of glycolysis and be used for nucleotide and lipid synthesis via serine biosynthesis(70, 81).

Our studies have found no deficiency in enolase protein expression, indicating that post-translational regulation likely impedes enolase enzymatic activity. There are several potential mechanisms of regulation of enolase activity in CD8+ TIL. First, post-translational modifications of enolase 1 have been described, including phosphorylation, acetylation, and methylation(126), though it is unclear whether these modifications influence enolase enzymatic activity. Second, enolase enzymatic activity requires divalent cations and is inhibited by fluoride (127), and thus may be susceptible to ion availability in the tumor microenvironment. Third, in addition to enolase 1's typical cytoplasmic localization where it performs its enzymatic role, enolase 1 can also be directed to the cell surface where it serves as a receptor for plasminogen(126); is recruited to mitochondria where it preserves mitochondrial integrity and membrane potential(128); or expressed as an alternative translational product (Myc Binding Protein -1) that is translocated to the nucleus(56). Thus, the inactivity of enolase in CD8+ TIL may either be a result of regulation of its enzymatic activity or repurposing of enolase away from glycolysis. Pertinently, preliminary mass spectrometry data suggests that enolase 1 isolated from Teff exhibits different acetylation and methylation patterns compared to CD8+ TIL. However, the contribution of any of these regulatory processes to the impaired of enolase activity remains to be determined. We currently do not understand whether the low enolase activity in CD8+ TIL is a function of weak priming or loss within the tumor. We found that concomitant blocking of multiple immune checkpoint molecules increased the presence of CD8+ TIL with more active enolase and

led to a decrease in tumor outgrowth. The increase in enolase-active CD8+ TIL that occurs with CPI was determined to arise from newly infiltrating T cells. We interpret these data to mean that CPI either promotes enolase activity during CD8+ T cell priming or preserves enolase activity in the newly infiltrating CD8+ T cells as they enter the tumor. Currently, there is no assay with sufficient sensitivity to assess the enolase or glycolytic activity of CD8+ TIL in the early stages of their response to tumors in the draining lymph node. Sensitive metabolic assays are also required to investigate whether the weak enolase activity observed in the murine and human TIL is only apparent in those cells embedded within the tumor, or whether tumor-specific or bystander T cells within the stroma, at the periphery of the tumor, or within the circulation are also metabolically compromised.

Our current study identifies augmentation of enolase activity as an avenue for increasing TIL function, though it should be noted that the combination of checkpoint molecules used in this study have yet to be evaluated clinically. We have concluded that the limited glycolysis and enolase activity exhibited by CD8+ TIL contributes to the remaining effector function of these cells as NaF eliminated remaining activity.

Although NaF is a well-characterized inhibitor of enolase, we acknowledge that it could have other enolase-independent impacts on T cells. Further, blocking checkpoint signals or isolating CD8+ TIL from the tumors (as done in the *in vitro* studies) did not fully restore enolase activity, suggesting the existence of additional as yet unidentified

pathways regulating enolase and glycolysis. While PEP and pyruvate were found to enhance TIL function *in vitro* here and in our previous studies on renal cell carcinoma(23), bypassing enolase inactivity *in vivo* with PEP or pyruvate may be challenging as PEP does not cross the cell membrane and pyruvate may be used by tumors. The most likely immediate clinical utility of pyruvate rescue approach will be to support the metabolic activity of TIL or PBMC that are intended to be used in adoptive cell transfer protocols. These limitations of PEP- and pyruvate-based rescue approaches highlight the need to understand how enolase activity is impaired in CD8+ TIL.

Recent studies by others(111) and the data presented here show a low level of OXPHOS in CD8+ TIL. While this could be attributed to low mitochondrial mass or mitochondrial membrane potential(111), the ability of pyruvate to rescue the OXPHOS in CD8+ TIL raises intriguing questions about the contribution of pyruvate deficiency to the loss of mitochondrial function. Interesting, enolase 1 has been previously reported to bind the mitochondrial membrane and prevent loss of membrane potential, which is essential for the OXPHOS(128). Whether mitochondrial binding of enolase 1 supports mitochondrial function by bringing together pyruvate synthesis and mitochondria is an intriguing question that will need to be addressed. In conclusion, restoration of enolase 1 activity might be expected not only to promote glycolysis but also improve the OXPHOS capabilities of TIL, together substantially improving effector activity and durability within tumors.

## **Chapter Four: Advancing the understanding of enolase impairment in CD8+ TIL: studies in different cancer types, investigation of its molecular basis, and development of a reporter for Enolase activity.**

### **INTRODUCTION**

In chapter 3, we showed that the glycolytic metabolism is restrained by post-translational regulation of enolase activity in melanoma infiltrating CD8+ TIL. Here we present studies where we investigated whether dysfunction in T cell glycolysis is evident in other implantable tumor models (4T1, breast cancer; LLC, non-small cell lung cancer; MC38, colorectal cancer) and human tumor samples (NSCLC). Analysis of the glycolytic metabolism and enolase activity in CD8+ TIL that infiltrated different cancer types is necessary to determine if the impairment of enolase activity is unique to the melanoma model or is general characteristic of CD8+ TIL. The former would imply enolase regulation is specific to a particular microenvironment. Further, we considered potential mechanisms to understand the basis by which enolase loses enzymatic activity in tumor-infiltrating lymphocytes. There are multiple potential mechanisms that can post-translationally control enolase activity. For example, divalent cations (especially magnesium ions) are known activators of enolase while fluoride ions inhibit it(127), and thus the availability of these ions in the tumor microenvironment (TME) could have a significant impact on the activity of enolase in CD8+ TIL. Enolase has also been reported to undergo post-translational modifications in cancer cells, including phosphorylation,

acetylation, and methylation(131), though the impact of these PTMs on enolase enzymatic active has not been elucidated. The subcellular localization of enolase can also impact its activity as demonstrated by lack of glycolytic activity of enolase expressed on the cell surface or in the nucleus(129–131). We also considered whether un-sustained TCR stimulation or factors derived from tumors themselves limited elements of the glycolytic pathway. Finally, there is currently no sensitive assay that could be used to identify T cells with impaired enolase activity, hampering studies to determine whether inactivity of enolase occurs due to poor initial priming or as a result of suppression of activity in the TME. For these purposes, we developed an enolase activity reporter by using a cell permeable small molecule (ENOblock) that has been shown to directly bind to enolase (121, 122). The development of the reporter may allow us to segregate cells with minimal enolase activity to more accurately identify the mechanism of regulation.

Here we assessed the glycolytic machinery in CD8+ TIL isolated from different types of murine and human cancers, and identified active mTORC1 signal, a range of glucose uptake potential, and high enolase 1 expression. Consistent with the melanoma model, the enolase activity but not expression level was impaired in colon adenocarcinoma infiltrating CD8+ TIL. Analysis of the potential post-translational regulation of enolase demonstrated that neither weak TCR signaling nor the availability of divalent cations limit enolase activity. Rather, these studies identified multiple differential post-translational modifications of enolase 1 in CD8+ TIL that may be involved in regulated

the activity of this enzyme. We have developed a fluorescent enolase reporter for further investigation of the activity and subcellular localization of this enzyme.

## **RESULTS**

### **A. Interrogation of glycolysis in CD8+ TIL in cancers other than melanoma.**

#### **Lewis lung carcinoma and breast tumor-infiltrating CD8+ TIL have active mTORC1 and glucose uptake potential**

In the previous chapter, we reported that the melanoma tumor-infiltrating CD8+ T cells receive signals that promote glycolysis and that these TIL are capable of effectively taking up glucose. Here we investigated whether these active pro-glycolytic signals and glucose uptake potential are also found in the CD8+ TIL that infiltrate other types of tumors. Similar proportions of Teff and CD8+ TIL isolated from Lewis lung carcinoma (LLC) and from breast cancer (4T1) had p-mTORC1 (detected using antibody specific to Ser2448) (Fig. 13, A and B), a key component of the signaling that sustain glycolysis in CD8+ T cells(49). The per cell amount of p-mTORC1 in LLC and 4T1 CD8+ TIL is significantly higher than the amount observed in naïve CD8+ T cells and at least at the level found in acute Teff (Fig. 13B, right). These data suggest that the pro-glycolytic signal is active in LLC and 4T1 CD8+ TIL, which is consistent with our observations made

in melanoma.

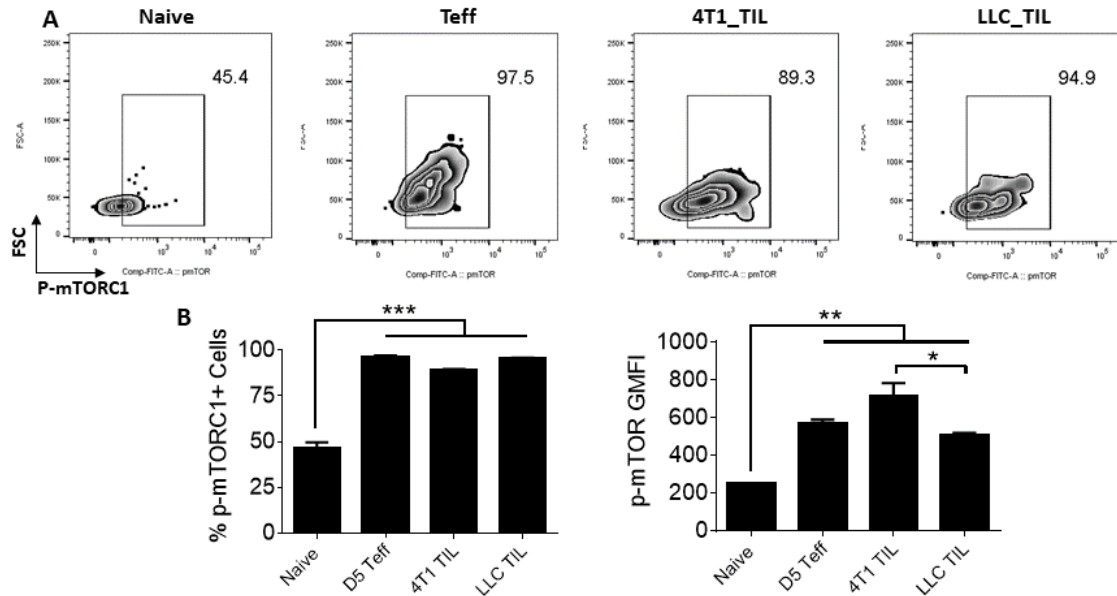


**Figure 13: mTORC1 may be active in the CD8+ TIL that infiltrate the LLC and 4T1 tumors.**

(A-B) d5 Teff were generated in C57BL/6 mice by immunization with a combination of OVA protein, poly I:C, and anti-CD40 and isolated from spleens. TIL were isolated from 4T1 and LLC tumors that developed subcutaneously in C57BL/6 mice for 14 days. Flow cytometric analysis of the phosphorylation mTORC1 was performed on *ex vivo* naive CD8+ T cells, acute Teff, and CD8+ TIL. The numbers within representative dot plots (A) describe the frequency of cells expressing p-mTORC1 for individual samples. Bar graph (B, left graph) shows the overall frequency p-mTORC1<sup>+</sup> cells within naive CD8+CD44<sup>lo</sup> or antigen-experienced (OVA-specific for Teff) Teff or CD8+ TIL. GMFI (B, right graph) is derived from p-mTORC1<sup>+</sup> naive CD8 T cells or antigen-experienced Teff or CD8+ TIL. Data are from three to five mice per group. Error bars represent mean  $\pm$  SEM. P values were calculated using one-way ANOVA, followed by Tukey's Multiple Comparison Test. \* $p < 0.05$ , \*\* $p < 0.01$ , \*\*\* $p < 0.001$ .

Glucose uptake potential is one of the key steps in glucose metabolism. We did not find significant difference in the proportion of cells that took up 2-NBDG between the acute Teff, LLC CD8+ TIL, and 4T1 CD8+ TIL (Fig. 14, A and B). However, the GMFI of 2-NBDG in the CD8+ TIL was significantly lower than that of the acute Teff (Fig. 14B, right),

suggesting that the LLC and 4T1 CD8+ TIL may transport glucose to a lower degree than acute Teff. This observation is different from melanoma CD8+ TIL, which were as capable as acute Teff at taking up 2-NBDG. Further, the reduction in 2-NBDG uptake in 4T1 and LLC TIL is modest, and may not be rate limiting for glycolysis. Surprisingly, although naïve CD8+ T cells are known to be metabolically quiescent cells, they took up more 2-NBDG than the Teff or any of the CD8+ TIL groups (Fig. 14B, right). Although the underlying mechanism for this is still not understood, other groups have also previously reported high 2-NBDG uptake potential of *ex vivo* naïve T cells(132). The inconsistency between the uptake and metabolism of glucose in *ex vivo* naïve CD8+ T cells further supports the notion that glucose uptake potential does not always reflect the actual glycolytic activity of cells as we described in chapter 3. Further studies are required to determine whether the Lewis lung carcinoma and breast tumor-infiltrating CD8+ TIL

have attenuated glycolytic activity and to understand if glucose uptake is limiting glycolysis in these cells.

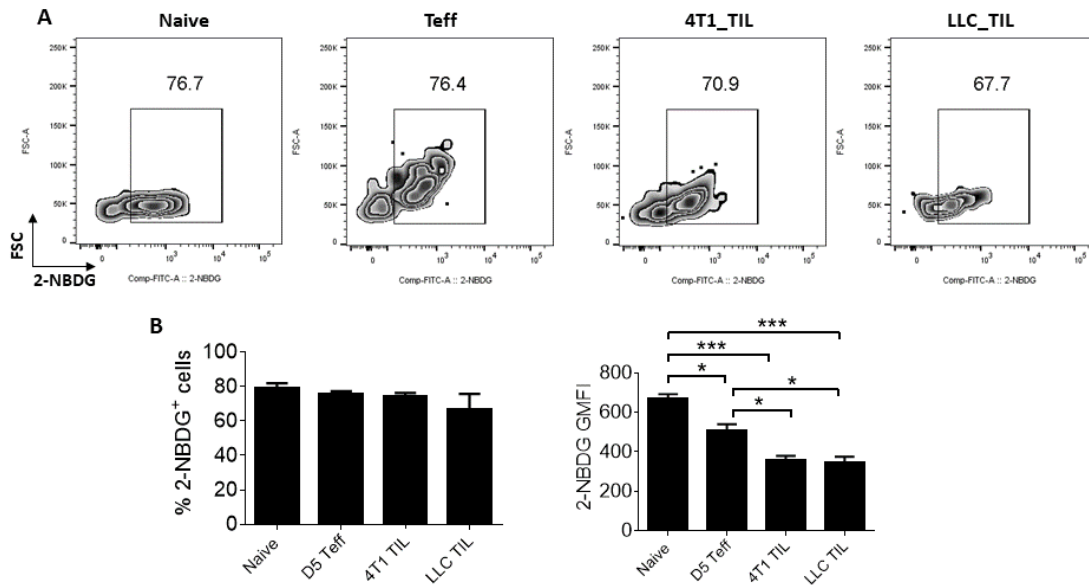


**Figure 14: LLC and 4T1 CD8<sup>+</sup> TIL take up 2-NBDG although not as efficiently as splenic CD8<sup>+</sup> T cells.**

Samples of T cells were prepared as in Figure 13 for all panels. Glucose uptake potential of ex vivo naive, d5 Teff, and d14 CD8<sup>+</sup> TIL isolated from 4T1 and LLC tumors as measured by flow cytometry after pulsing the cells with fluorescent glucose analog, 2-NBDG. The numbers within representative dot plots (A) describe the frequency of 2-NBDG<sup>+</sup> cells for individual samples. Bar graphs show the overall frequency (B, left) 2-NBDG<sup>+</sup> cells within naive CD8<sup>+</sup>CD44<sup>lo</sup> or OVA-specific Teff or antigen-experienced CD8<sup>+</sup> TIL. GMFI (B, right) is derived from 2-NBDG<sup>+</sup> naive CD8<sup>+</sup> T cells, Teff, or CD8<sup>+</sup> TIL. Data are from three to five mice per group. Error bars represent mean  $\pm$  SEM. P values were calculated using one-way ANOVA, followed by Tukey's Multiple Comparison Test. \*p < 0.05, \*\*p < 0.01, \*\*\*p < 0.001.

### **CD8<sup>+</sup> TIL from different tumor types have impaired enolase activity, but not expression.**

Although the melanoma-infiltrating CD8<sup>+</sup> TIL could efficiently take up glucose, they were unable to completely process it through glycolysis due to impaired enolase activity

as we described in chapter 3. Here we investigated the expression and activity of enolase 1 in CD8+ TIL from different types of cancers to understand if the impairment of enolase activity is a general characteristic of CD8+ TIL or a unique feature of the melanoma model. We found that similar proportions of human melanoma and non-small cell lung cancer (NSCLC) infiltrating CD8+ TIL and antigen-experienced (CD45RO+) CD8+ T cells in the healthy donors PBMC express enolase 1 (Fig. 15, A and B). The per cell amount of (GMFI) of enolase 1 in both CD8+ TIL populations were also similar to each other, but were considerable higher than the level observed in antigen-experienced CD8+ T cells in healthy donors PBMC (Fig. 15A, bottom left). Moreover, we found equivalent expression of enolase 1 in melanoma and NSCLC CD8+ TIL that express 4-1BB, a marker of cells that may have recently received TCR stimulation<sup>(123)</sup>, (Fig. 15B). Together, these data indicated that high level of enolase 1 expression seen in CD8+ TIL is consistent across multiple human tumor types. It remains to be determined whether the enolase 1 in the NSCLC infiltrating CD8+ TIL is functional.

We used MC38 colon adenocarcinoma to investigate whether enolase activity is impaired in CD8+ TIL that infiltrate murine tumor models other than melanoma. Consistent with the B16 melanoma model, a similar proportion of MC38 infiltrating CD8+ TIL and acute Teff expressed enolase 1 (Fig. 16A). Furthermore, the per cell expression of enolase 1 in these two cell populations were also equivalent (Fig. 16A, right graph). Importantly, we found that MC38 infiltrating CD8+ TIL had significantly less

enolase activity than acute Teff (Fig. 16B), similar to the observation made in the melanoma model. Taken together, these data suggest that impaired enolase activity may limit the metabolic and effector activities of CD8+ TIL in a general manner and not be unique to melanoma.

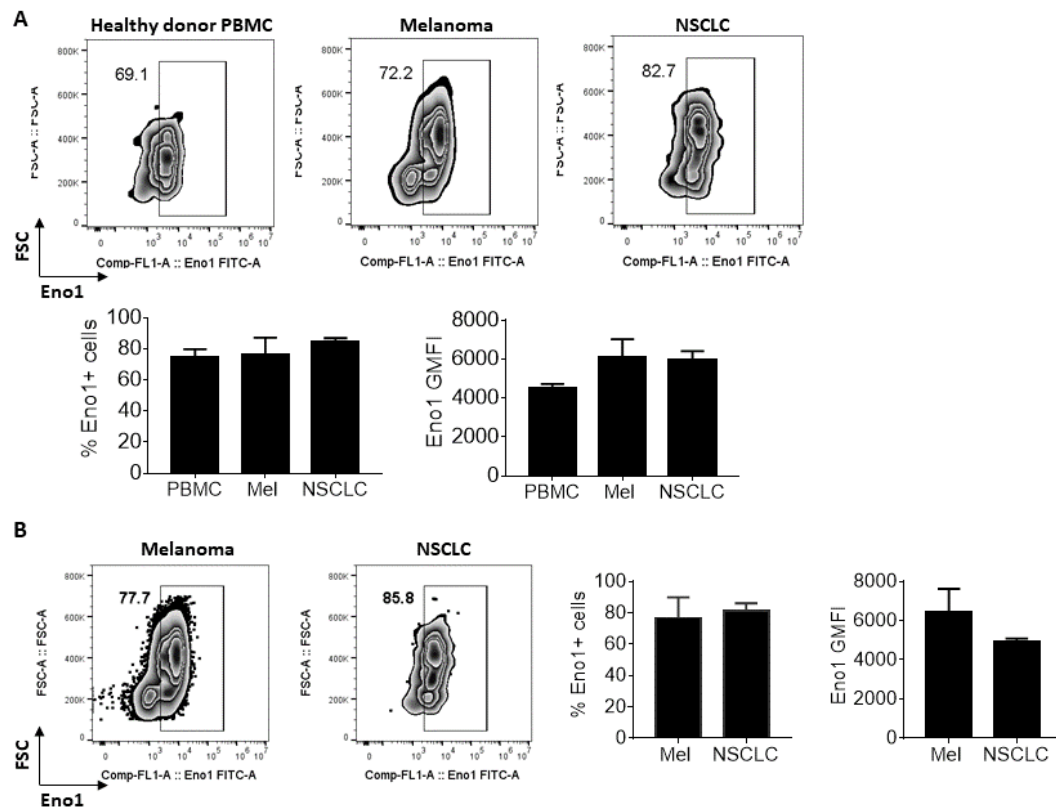


**Figure 15: CD8+ TIL in human melanoma and NSCLC tumors express similar amount of enolase 1.**

(A-B) Flow cytometric analysis of enolase 1 protein expression in antigen-experienced CD8 T cells in healthy donor PBMC and CD8+ TIL in human melanoma and NSCLC patient samples. The numbers within representative dot plots describe the frequency of Eno1+ cells for individual samples. Bar graphs show the overall frequency of Eno1-positive cells within CD8+CD45RO+ cells (A, left) or CD8+CD45RO+41BB+ cells (B, left), and the GMFI of enolase 1 on Eno1+CD8+CD45RO+ (A, right) or Eno1+CD8+CD45RO+41BB+ cells (B, right) in the indicated samples. Data are from two healthy donor PBMC, three melanoma patient TIL, and three NSCLC patient TIL. Error bars represent mean  $\pm$  SEM.

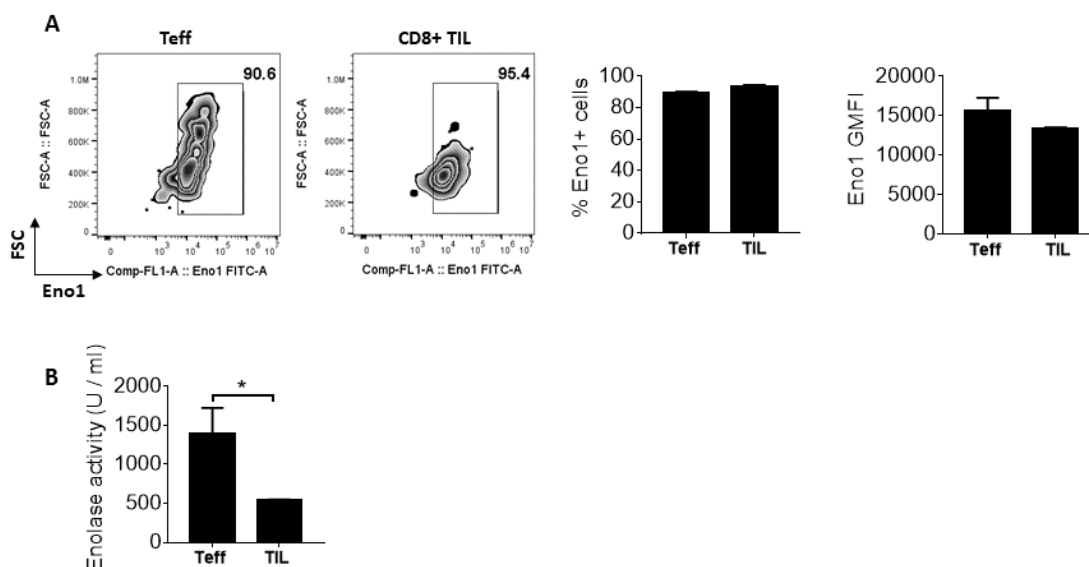


**Figure 16: Enolase is post-translationally regulated in the CD8+ TIL that infiltrated MC38 tumors.**

(A) Flow cytometric analysis of enolase 1 protein expression in d5 Teff and d14 MC38 CD8+ TIL. The frequencies of cells that express enolase 1 within OVA-specific CD8+CD44hi Teff or CD8+CD44hi TIL are indicated. GMFI is derived from enolase 1-expressing OVA-specific CD8+CD44hi Teff or CD8+CD44hi TIL. (B) Fluorescence-based spectrophotometric analysis of enolase activity (PEP formation) measured in lysates prepared from FACS-sorted d5 Teff and CD8+ TIL. Data are representative of two independent experiments with at least three mice per group in each(A) or on samples pooled from three vaccinated mice and five tumor-bearing mice (B). Error bars represent mean  $\pm$  SEM. P values were calculated by unpaired Student's *t*-test. \* $p < 0.05$ .

## B. Establishing a mechanistic basis for the loss of enolase enzymatic activity

### In vitro stimulation increases the expression, but not the function of glucose transporters in CD8+ TIL

TCR stimulation is known to strongly induce glucose transporter expression and glucose uptake in T cells(40). We hypothesized that one of the reasons that CD8+ TIL had limited glycolysis was an inability to increase glucose transport in response to TCR stimulation.

This could lead to a negative feedback loop on enolase activity. To investigate this, we *in vitro* stimulated CD8+ TIL and age-matched Teff with anti-CD3 and anti-CD28. The proportion of CD8+ TIL and Teff that express Glut1 remained unchanged after *in vitro* stimulation (Fig. 17, A and B). However, the stimulation significantly increased the per cell expression of Glut1 in both CD8+ TIL and Teff (Fig. 17B, right), showing that CD8+ TIL can increase expression of glucose transporters in response to TCR stimulation.

Next, we tested whether *in vitro* stimulation also induced glucose uptake in CD8+ TIL and age-matched Teff. *In vitro* stimulation of late Teff resulted in a significant increase in the proportion of cells that took up 2-NBDG and in the per cell amount of 2-NBDG they took up compared to the unstimulated late Teff (Fig. 17, C and D). However, *in vitro* stimulation did not further increase the frequency of CD8+ TIL that took up 2-NBDG (Fig. 17, C and D), which was already high (~75%). Interestingly, while *in vitro* stimulation strongly increased the GMFI of 2-NBDG in the late Teff, it did not have significant impact in CD8+ TIL (Fig. 17D, right). These data indicate that *in vitro* stimulation failed to enhance glucose uptake and/or retention in CD8+ TIL. Thus, TIL are competent at taking up glucose. However, relatively quiescent T cells can disproportionately increase their expression of Glut1 and ultimately the amount of glucose they can acquire compared to TIL. The basis of this is unclear, and could perhaps reflect a disconnection between TCR stimulation and Glut1 expression in TIL, and the use of additional glucose transporters by non-TIL.

Although the CD8<sup>+</sup> TIL in the above study were isolated from the tumor by density gradient separation, this technique does not completely remove the tumor cells. Hence, we asked whether the tumor cells actively suppress the glucose uptake potential of CD8<sup>+</sup> TIL during the *in vitro* co-culture. While competition for 2-NBDG between the tumor cells and the T cells could also limit 2-NBDG uptake by the CD8<sup>+</sup> TIL, it is unlikely that this occurs in these experiments given the short assay time (20 min) and the use of 100nM of 2-NBDG. To test the potential active suppression of glucose uptake, we *in vitro* stimulated *ex vivo* late Teff for 3 days in the presence or absence of tumor cells (B16cOVA). We observed equivalent induction of Glut1 expression as well 2-NBDG uptake in the late Teff stimulated in the presence or absence of the tumor cells (Fig. 18, A and B). Interestingly, there were modest trends toward increase in the 2-NBDG uptake of unstimulated late Teff co-culture with B16cOVA compared to the late Teff cultured alone (Fig. 18B), which might be due to stimulation of these cells by the OVA antigens on the B16cOVA. These data indicated that interaction with tumor cell does not acutely limit the ability of Teff to increase Glut1 expression and to transport glucose, suggesting that the lower ability of CD8<sup>+</sup> TIL to induce glucose uptake during *in vitro* stimulation may be associated with a TIL-intrinsic defect rather than being repressed by signals derived from the tumor cells. Further studies are required to determine whether CD8<sup>+</sup> TIL could increase glucose uptake if they are purified prior to *in vitro* stimulation, and whether *in vitro* stimulation can induce glycolytic metabolism in these cells.

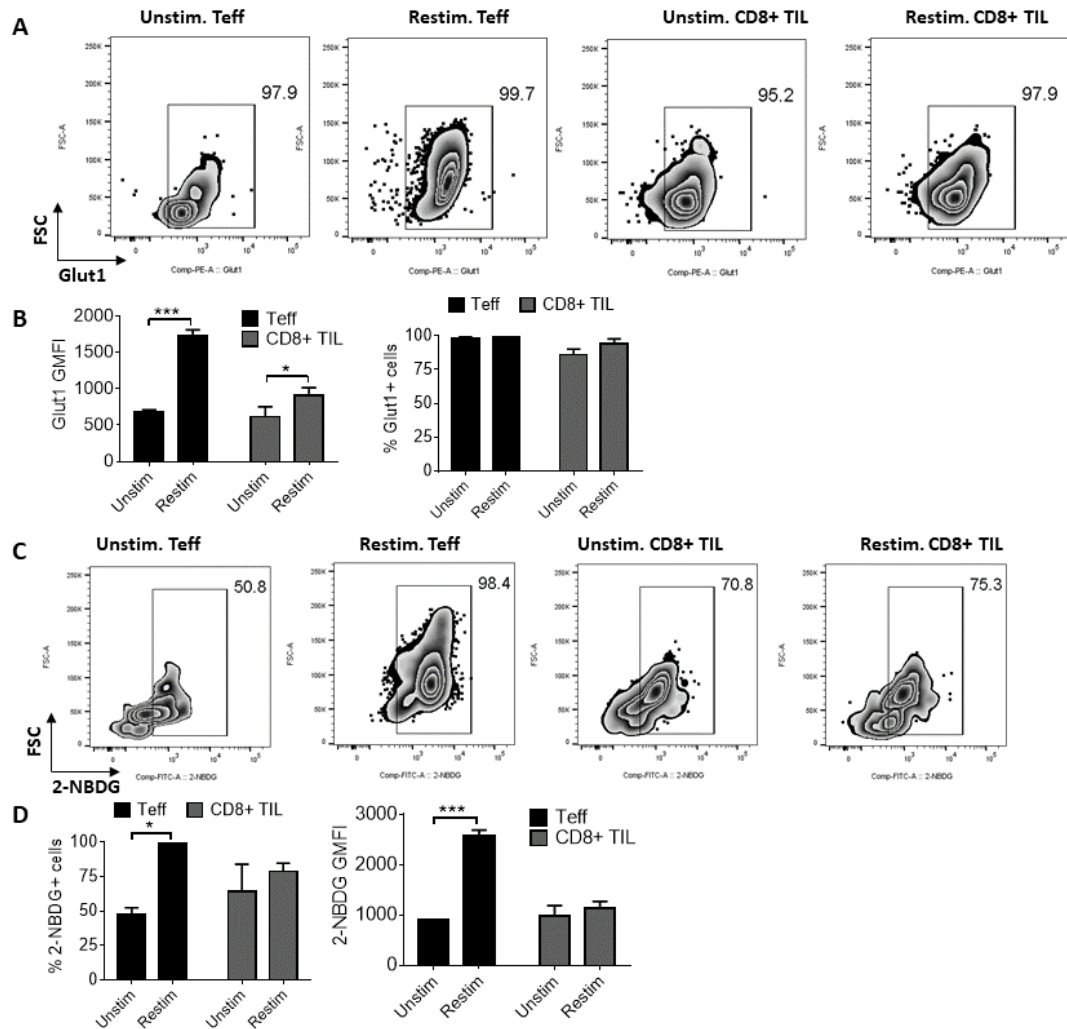


**Figure 17: In vitro restimulation of CD8+ TIL modestly increases Glut1 expression, but not glucose uptake.**

(A-D) Splenocytes harvested from mice immunized with a combination of OVA protein, poly I:C, and anti-CD40 12 days prior and TIL isolated from d12 B16cOVA tumor-bearing mice were *in vitro* stimulated with anti-CD3/CD28 and IL-2 or cultured in IL-2 for 2 days. (A-B) Flow cytometric analysis of glucose transporter 1 (Glut1) protein expression in unstimulated and restimulated Teff and CD8+ TIL. The numbers within representative dot plots(A) describe the frequency of Glut1<sup>+</sup> cells for individual samples. Bar graphs show the overall frequency (B, left) of Glut1<sup>+</sup> cells within CD8<sup>+</sup>CD44<sup>hi</sup> Teff or TIL, and GMFI (B, right) Glut1<sup>+</sup> on Glut1<sup>+</sup>CD8<sup>+</sup>CD44<sup>hi</sup> Teff or TIL. (C-D) Glucose uptake potential of *in vitro* cultured or restimulated Teff and CD8+ TIL as measured by flow cytometry after pulsing the cells with 2-NBDG. Bar graphs (D, left) show the overall frequency 2-NBDG<sup>+</sup> cells within the CD8<sup>+</sup>CD44<sup>hi</sup> Teff or TIL. GMFI (D, right) is derived from 2-NBDG<sup>+</sup>CD8<sup>+</sup>CD44<sup>hi</sup> Teff or TIL. Data are representative of three independent experiments with

samples pooled from at least three mice per group in each experiment. Error bars represent mean  $\pm$  SEM. P values were calculated by unpaired Student's *t*-test. \* $p < 0.05$ , \*\*\* $p < 0.001$ .

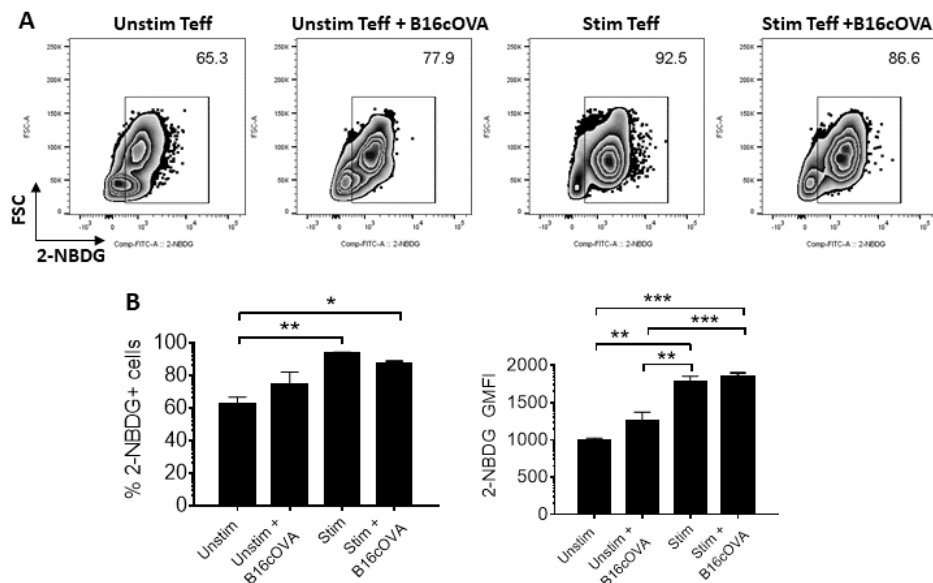


**Figure 18: Tumor cells do not prevent induction of glucose uptake potential in Teff during *in vitro* coculture.**

Splenocytes prepared as in Figure 13 were *restimulated in vitro* with anti-CD3/CD28 and IL-2 in the presence or absence of B16cOVA cells or cultured in IL-2 in the presence or absence of B16COVA cells for 2 days. 2-NBDG uptake was assess by flow cytometry. The numbers within representative dot plots (A) describe the frequency of 2-NBDG<sup>+</sup> cells for individual samples. Bar graphs show the frequency of 2-NBDG<sup>+</sup> cells within the CD8<sup>+</sup>CD44<sup>hi</sup> Teff (B, left) and the GMFI of 2-NBDG on 2-NBDG<sup>+</sup>CD8<sup>+</sup>CD44<sup>hi</sup> Teff (B, right). Data are representative of two independent experiments with samples pooled from at least three mice per group in each experiment. Error bars represent mean  $\pm$  SEM. P values were calculated by unpaired Student's *t*-test. \* $p < 0.05$ , \*\*\* $p < 0.001$ .

### Post-translational modifications may contribute to low enolase activity in CD8<sup>+</sup> TIL

Given the importance of enolase activity for the T cell's metabolic and effector function, identifying the post-translational mechanism responsible for its impairment in CD8<sup>+</sup> TIL is critical to develop interventions that can restore or preserve the activity of this enzyme. *In vitro* stimulation via TCR engagement was insufficient to improve enolase

activity in CD8+ TIL as we described in chapter 3. Another potential mechanism that could regulate enolase activity is the availability of magnesium ions and, to a lesser extent, other divalent cations such as zinc and manganese ions, which have been reported to be needed for enolase enzymatic activity(127). Therefore, we assessed whether  $Mg^{2+}$  supplementation could improve enolase activity in CD8+ TIL. *In vitro* stimulation of CD8+ TIL in the presence of  $MgSO_4$  had no effect on the enolase activity in these cells (Fig. 19), suggesting that  $Mg^{2+}$  availability is not limiting enolase activity in CD8+ TIL. It should be noted that although we have not assessed  $Mg^{2+}$  uptake, we used the amount (5mM) of  $MgSO_4$  that has been reported to increase intracellular free  $Mg^{2+}$  in T cells(133).

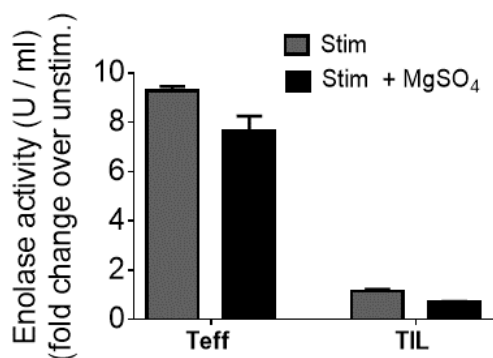


**Figure 19:  $Mg^{2+}$  availability may not be limiting the activity of enolase in CD8+ TIL.**

FACS-sorted CD8 T cells and CD8+ TIL were *in vitro* cultured in IL-2 or stimulated with anti-CD3/CD28 and IL-2 in the presence or absence of  $MgSO_4$  for three days. Fluorescence-based spectrophotometric analysis of enolase activity (PEP formation) was performed on lysates prepared from the *in vitro* maintained or stimulated Teff and CD8+ TIL. Data are representative of two independent experiments with three to five mice per group in each experiment. Error bars represent mean  $\pm$  SEM.

Regulation of enolase activity by post-translational modifications (PTMs) is an alternative hypothesis. Although the impact of PTMs on enolase activity is unknown,

enolase has been reported to undergo phosphorylation, methylation, and acetylation(129, 131) in other cell types. Our Western blot experiments (shown in chapter 3) determined that enolase 1 from Teff and CD8+ TIL had similar molecular weight, suggesting that it is unlikely that a change in conserved large molecular weight PTMs such as the gain or loss of multiple phosphorylations is the cause of the impaired enolase activity in CD8+ TIL. However, this observation does not rule out potential changes in PTMs that are below the detection limit of electrophoretic shift on Western blotting, including single phosphorylation or de-phosphorylation, or changes that ultimately balance each other out. Therefore, to further address this question, we (in collaboration with Dr. Ku-Lung Hsu and his graduate student Adam Borne) performed a preliminary mass spectrometric analysis of PTMs comparing Teff and CD8+ TIL. We found multiple differences in methylation and acetylation PTMs between Teff and CD8+ TIL, some of which were found only in Teff or only TIL (Fig. 20). Further studies are required to validate and to manipulate these complex PTMs in order to understand whether they are involved in impairing enolase activity in CD8+ TIL.

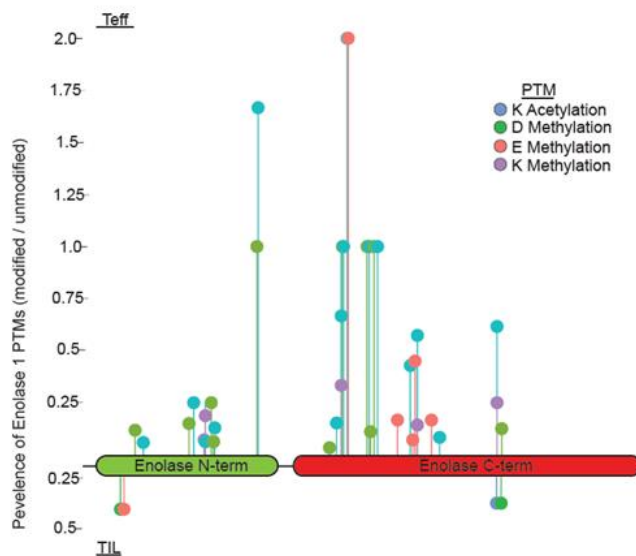


**Figure 20: Differential post-translational modifications of enolase 1 in acute Teff and CD8+ TIL.**

Enolase is enriched by immunoprecipitation from lysates of FACS-sorted ex vivo CD8+ TIL and *in vitro* generated CD8+ Teff, and subjected to mass spectrometric analysis of posttranslational modifications (PTMs). Differential PTMs is shown in different colors. The number of spectra for each modified peptide is normalized to the number of unmodified spectra in the y-axis and the position on enolase 1 on the x-axis. The pfam domains are shown along the length of the protein sequence.

### **C. The development of a chemical probe that allows a robust enolase expression/activity analysis**

Currently, there is no assay with a sufficient sensitivity to allow assessment of enolase activity in the limited number of TIL that could be obtained from the early stage murine tumors and limited human samples. Analysis of enolase activity in the CD8+ TIL from early stage tumors or tumor draining lymph nodes is important to understand whether these cells fail to induce enolase activity during the activation phase or lose it during the effector phase upon entrance into the tumor (as suggested by the checkpoint inhibitor + FTY720 experiments). Therefore, developing a reporter or a chemical probe that would

allow a robust, single cell analysis of enolase activity would be very useful for such investigation. A compound known as ENOblock has been reported to cross the cell membrane and to directly bind to enolase(121, 122). Initial *in vitro* studies(122) and subsequent *in vivo* analysis(121) have demonstrated that ENOblock inhibits enolase activity. Based on these findings, the authors suggested that ENOblock could be “used as a probe to characterize enolase activity in biological systems.”(121, 122). This led us to ask if conjugating ENOblock with fluorophores such as rhodamine would give us a fluorescent reporter that can be used to detect active enolase within the cells by flow cytometry. We collaborated with Dr. Ku-Lung Hsu and his postdoctoral fellow Jeffery Bulet in the Department of Chemistry and Pharmacology at the University of Virginia to generate the fluorophore-conjugated ENOblock and named it REPO. This was achieved by labeling ENOblock with an amine-reactive fluorescent probe 5-Carboxy-tetramethylrhodamine N-succinimidyl ester (5-TAMRA NHS ester). The ENOblock-rhodamine conjugate was purified by reverse-phase HPLC (High performance Liquid chromatography) and assessed for purity by HPLC, which determined that the conjugate was >95% pure (Fig. 21A).

Flow cytometric analysis determined that the ENOblock itself did not have significant auto-fluorescence that could interfere with its use for the enolase 1 reporter (Fig. 21B). We pulsed naive CD8 T cells and effector CD8 T cells with different concentrations of REPO and determined that the optimal concentration (the amount REPO that gave a low background and a wide separation in the peak of signal between naive and effector T

cells) required for labeling cells was between 2.5  $\mu\text{M}$  and 5  $\mu\text{M}$  (Fig. 21C). Competition analysis using free (non-fluorescent bound) ENOblock significantly reduced REPO staining in Teff, confirming the specificity of REPO for its binding site (Fig. 21D). Taken together, these data indicate that conjugating ENOblock with the rhodamine (5-TAMRA NHS ester) provided a fluorescent reporter of enolase activity without impairing the specificity of ENOblock for its binding site.

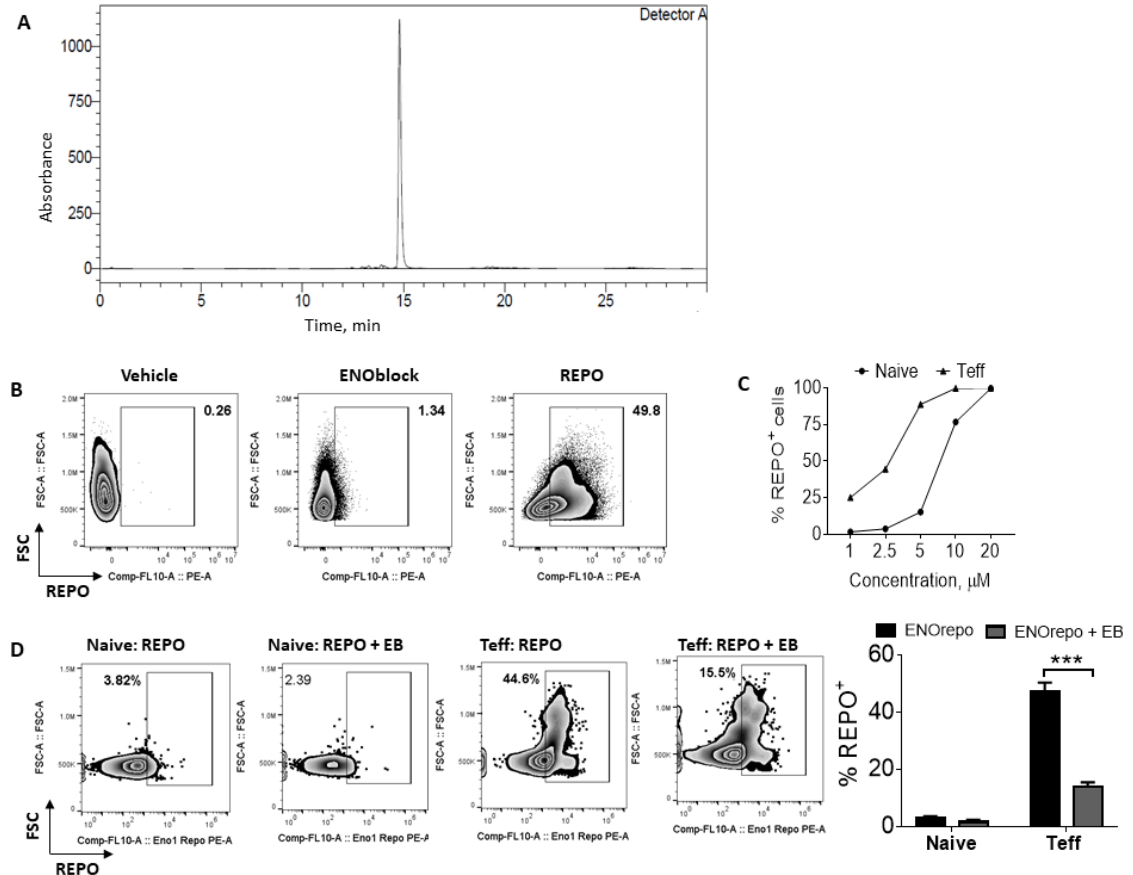


**Figure 21: Development and analysis of enolase reporter.**

(A) HPLC analysis of the purity of enolase reporter (REPO) that was generated by conjugating ENOblock with 5-TAMRA NHS ester. (B-D) Flow cytometric analysis of REPO staining in the splenocytes harvested from mice vaccinated with OVA/poly I:C/anti-CD40 and *ex vivo* pulsed

with vehicle (media), 2.5  $\mu$ M ENOblock, or 2.5  $\mu$ M REPO for 15min. (B) The frequency of REPO-positive cells within OVA-specific CD8+CD44<sup>hi</sup> T cells. (C) REPO titration as determined by comparing the labeling of naïve CD8 T cells and acute Teff with the indicated amounts of the reporter. (D) The specificity of REPO for its binding site as determined by competition analysis using free ENOblock as a competitor for binding site. Error bars represent mean  $\pm$  SEM. P values were calculated by unpaired Student's *t*-test. \*\*\**p* <0.001.

Next, we assessed whether REPO can report on enolase 1 activity at single cell level. To do this, we probed murine naïve CD8<sup>+</sup> T cells, Teff, and CD8<sup>+</sup> TIL, which we have shown to have different levels of enolase activity in chapter 3. Consistent with their low enolase 1 expression and activity, naïve T cells were weakly stained with REPO (Fig. 22A). More importantly, the frequency of REPO-positive cells and the GMFI of the REPO staining were significantly lower in CD8<sup>+</sup> TIL than Teff (Fig. 22A). These observations suggest that the REPO reports on the activity of enolase 1 since CD8<sup>+</sup>TIL and Teff express similar amount enolase 1, but the former has weaker enolase activity than the latter as shown in chapter 3. Consistent with the murine studies, human melanoma CD8<sup>+</sup> TIL also weakly stained with REPO compared to the antigen-experienced CD8<sup>+</sup> T cells in the healthy donors PMBC (Fig. 6B). Together, these data strongly argue for the capacity of REPO to label enolase 1 in an activity dependent manner although it remains to be further validated by future studies.

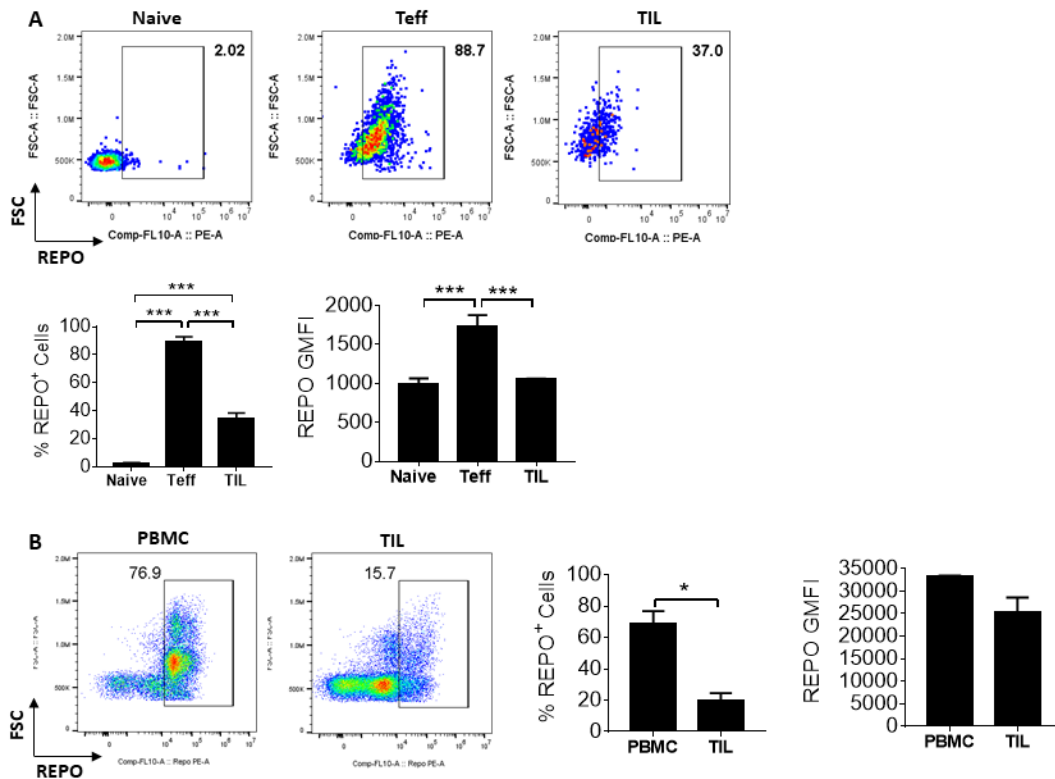


**Figure 22: Murine and human CD8+TIL weakly stained with the enolase reporter.**

(A) Flow cytometric analysis of REPO staining in *ex vivo* naive CD8 T cells, acute Teff, and B16OVA infiltrating CD8+TIL after the cells were pulsed with 5  $\mu$ M REPO for 15min. The numbers within representative dot plots describe the frequency of REPO<sup>+</sup> cells for individual samples. Bar graphs (left) show the overall frequency REPO<sup>+</sup> cells within naive CD8+CD44<sup>lo</sup> or OVA-specific Teff or CD8+ TIL. GMFI (A, right) is derived from REPO<sup>+</sup> naive CD8 T cells, OVA-specific Teff, or OVA-specific CD8+ TIL. (B) The frequency (dot plot and left graph) of REPO<sup>+</sup> cells within CD8+CD45RO<sup>+</sup> healthy donor PBMC or human melanoma patient TIL is indicated. GMFI of REPO (B, right graph) was derived from REPO<sup>+</sup>CD8+CD45RO<sup>+</sup> PBMC or human TIL. Data are representative of two experiments (A) or are on samples from two healthy donor PBMC and three melanoma patient TIL. Error bars represent mean  $\pm$  SEM. P values are calculated by one-way ANOVA, followed by Tukey's Multiple Comparison Test (A) or unpaired student's *t*-test (B). \**p* < 0.05, \*\**p* < 0.01, \*\*\**p* < 0.001.

## DISCUSSION

Our investigation of the glycolytic metabolism in the melanoma infiltrating CD8+ T cells has demonstrated that this metabolic program was restrained by the impairment of enolase activity even though several components of the glycolytic machinery were well-expressed and functional. The studies described in this chapter recapitulated some of these findings in different types of cancers. For example, the CD8+ TIL that infiltrated 4T1 and LLC tumors had high level of phosphorylated mTORC1, a key player in signaling that maintains the glycolytic metabolism(49). This suggests that the induced activity the pro-glycolytic signaling observed in melanoma CD8+ TIL may also be present in the CD8+ TIL that infiltrate other tumor types. The 4T1 and LLC CD8+ TIL were also capable of acquiring glucose from their environment, albeit with less efficiency than Teff. Importantly, we found that enolase 1 was well-expressed in CD8+ TIL that infiltrate the human melanoma and NSCLC tumors, and the murine MC38 tumors. Consistent with the melanoma model, the activity enolase in the MC38 CD8+ TIL was post-translationally regulated. This was demonstrated by fact that the MC38 CD8+ TIL had significantly lower enolase activity than the Teff, which express equivalent amount of the protein. Hence, it is likely that impairment of enolase activity limits the metabolic and effector function of CD8+ TIL found in different types cancers. Further study using more tumor types will be necessary to confirm this conclusion. It also remains to be determined whether post-translational regulation of enolase activity is one of mechanisms by which the T cell response is curtailed after the resolution of infection and/or is involved in the exhaustion T cells in chronic viral infection.

The preliminary analysis of the post-translational modifications of enolase 1 as a potential regulator of its activity detected multiple differential acetylations and methylations in this enzyme. While it remains to be determined if these modifications are involved in impairing enolase activity, PTMs have been reported to regulate the activity of other metabolic enzymes (125, 134, 135). For example, deacetylation has been shown to repress the activity of the glycolytic enzyme phosphoglycerate mutase 1 (PGAM1)(125). Lysine acetylation has also been shown to either positively or negatively regulate the activities of enzymes involved in the metabolic programs such as TCA cycle, gluconeogenesis, and urea cycle(134). Therefore, it is possible that the change in acetylation state of enolase 1 lysine residues contributes to the impairment of its activity in CD8+ TIL.

It is currently unclear whether enolase activity is not induced during the priming of CD8+ TIL or if it is repressed in these cells as they enter the TME. To aid the analysis of enolase activity in the limited amount of samples in the TDLNs or early stage tumors in order to address these questions, we developed a cell permeable reporter that is capable of detecting enolase at a single cell level. This reporter is highly likely to label enolase in an activity-dependent manner since it accumulates more in the T<sub>H</sub>1 that have strong enolase active than in the CD8+ TIL in which the enzyme is significantly less active. Naïve

CD8<sup>+</sup> T cells weakly stained with the reporter, which could be due their limited enolase 1 expression and/or activity. More experiments will be necessary to further validate the activity-dependency of this reporter and to identify whether the reporter binding inhibits enolase activity. Currently, there are inconsistencies in the literature regarding whether the small molecule (ENOblock) used to develop the enolase reporter inhibits the enzymatic activity of enolase 1(121, 122, 136). The fact that it can differentially label active and inactive enolase at a single cell level makes this reporter a powerful tool for the analysis of enolase activity whether the binding is inhibitory or not. Furthermore, this reagent could allow analysis of enolase in living cells as well as sorting of cells based on enolase activity since it is cell permeable. It could also be useful for rapid, simultaneous analysis of enolase subcellular location including its expression on the cell surface, in the cytoplasm, and on the mitochondria membrane all of which have been reported in different cell types(127, 137, 138).

## Chapter Five: Analysis of mitochondria metabolism in CD8+ TIL

### INTRODUCTION

Although effector T cells primarily depend on glycolytic metabolism, it is now clear that T cell activation also induces mitochondrial metabolism, which plays several important roles in these cells. In fact it has been reported that TCR engagement immediately induces mitochondrial metabolism prior to the initiation of a strong dependency on the glycolytic metabolism(139). In addition to being an efficient source of ATP, mitochondria also produce biosynthetic precursors that support cellular proliferation and reactive oxygen species that serve as signaling molecules(41). Studies have also demonstrated that mitochondrial metabolism is important for T cell activation and to initiate proliferation in activated T cells(41, 84, 140). However, the role of mitochondria metabolism in the activated T cells is not limited to the initial activation and proliferation, but is also crucial for memory T cell development, longevity, and the rapid, high magnitude recall response(132, 140). Furthermore, mitochondrial metabolism is the major metabolic program that supports the functional activities of chronically activated T cells found in graft-versus-host responses(92, 141) and T cells in some autoimmune diseases(72, 142). The importance of mitochondrial metabolism for the longevity of antigen-experienced T cells and the function of chronically activated T cells may suggest that engaging this metabolic program could be beneficial for the CD8+

TIL, which are known to undergo progressive loss of function and to receive chronic stimulation in the TME.

In the previous chapters, we showed that both glycolytic and mitochondrial oxidative phosphorylation (OXPHOS) are attenuated in CD8<sup>+</sup> TIL when compared to Teff. Our investigation of the basis for suppression of glycolytic metabolism has identified impaired enolase activity as a mediator of glycolytic deficiency of these cells. In addition to glycolysis, weak enolase activity could limit mitochondrial metabolism since its product phosphoenolpyruvate (PEP) is a precursor for the synthesis of pyruvate, which is one of substrates for mitochondrial metabolism. Interestingly, enolase 1 has also been reported to bind to mitochondria and to regulate their function(138). In cardiomyocytes, the mitochondrial binding of enolase 1 has been reported to prevent Ca<sup>2+</sup> overload into the mitochondria resulting in a loss of the membrane potential(138). In T cells, the metabolic product of enolase 1 (PEP) has been shown to regulate the cytoplasmic pool of Ca<sup>2+</sup> via inhibition of its uptake into the endoplasmic reticulum(22). Hence, if PEP also regulates mitochondrial Ca<sup>2+</sup> channels, the lack of enolase activity in CD8<sup>+</sup> TIL may contribute to the deficiency in OXPHOS observed in these cells although we have not investigated this possibility. However, the OXPHOS deficiency observed in the CD8<sup>+</sup> TIL cannot be fully explained by limited availability of glycolysis-derived pyruvate alone, since other nutrients such as glutamine and fatty acid could also fuel the mitochondrial metabolism(64). There are multiple potential causes of OXPHOS

deficiency in CD8<sup>+</sup> TIL including limited nutrients availability, lack of metabolic plasticity, and loss of mitochondrial mass and/or function.

It is well established that different nutrients feed into mitochondria via different metabolic pathways(64). For example, as mentioned above, glucose is processed through glycolysis to produce pyruvate, some of which enters the mitochondria and is converted into acetyl-CoA by the pyruvate dehydrogenase (PDH) complex (64). Acetyl-CoA then enters the tricarboxylic acid (TCA) cycle and is used to produce intermediary metabolites and high energy molecules NADH and FADH<sub>2</sub>, which donate electrons to the mitochondrial electron transport chain (ETC) of OXPHOS to drive ATP production(69, 75). Alloreactive effector T cells(141) and memory T cells(132, 140) metabolize fatty acid via fatty acid oxidation (FAO) in the mitochondria to produce acetyl-CoA, which is consumed in the TCA cycle similar to the pyruvate-derived acetyl-CoA to fuel OXPHOS. Glutamine is another important nutrient that is known to fuel OXPHOS in effector T cells(35, 41, 82). Glutamine is converted into  $\alpha$ -ketoglutarate in the metabolic process known as glutaminolysis and directly enters mitochondria TCA cycle(35, 64). The activation of T cells has been reported to strongly induce glutaminolysis(35).

It has become increasingly clear that T cells have significant metabolic plasticity that would allow them to switch between different metabolic programs or substrate utilization under conditions of nutrient limitation or metabolic stress(37, 73, 82, 87). For example, CD8<sup>+</sup> effector T cells increase OXPHOS and glutaminolysis when glucose or glycolysis is restricted(82). This understanding raises an interesting question regarding

why CD8+ TIL fail to upregulate OXPHOS by inducing glutaminolysis or the consumption of other nutrients while they have low glycolytic activity. One of the hypotheses that could explain this scenario is that CD8+ TIL either lack metabolic plasticity or have a mitochondrial alteration that hinders induction/maintenance of OXPHOS.

Here we investigated the mechanisms that impede CD8+ TIL from inducing OXPHOS to compensate for their glycolytic deficiency. We found that CD8+ retain low OXPHOS in the presence of different nutrients that can fuel mitochondria, suggesting that mitochondrial substrate availability is not the major limited factor for OXPHOS in CD8+ TIL. Rather, CD8+ TIL possess low mitochondrial mass and severe deficiency of mitochondrial membrane potential that restrict their OXPHOS capacity irrespective of the availability of nutrients. This is consistent with the ability of exogenous pyruvate to at least partially rescue OXPHOS in these cells as described in chapter 3.

## **RESULTS**

### **Effector CD8+ T cells induce mitochondrial metabolism in addition to glycolysis**

Although glycolysis is thought to be the primary metabolic choice of effector T cells, it has recently been appreciated that mitochondrial metabolism is also induced and plays an important role in effect T cells(72, 92, 141, 142). To test whether the *ex vivo* effector T cells generated by our model system (vaccination strategy) utilize both glycolytic and OXPHOS metabolism, we assessed the ECAR and OCR of CD8+ Teff. As

expected, CD8+ Teff had significantly higher ECAR and OCR than naïve CD8+ T cells (Fig. 23, A and B). In chapter 3, we have shown that CD8+ TIL have low ECAR and OXPHOS compared to CD8+ Teff, and that bypassing glycolysis via pyruvate provision improves the ECAR, OXPHOS, and functional activity of CD8+ TIL. The improved effector function observed in pyruvate treated CD8+ TIL could presumably be a combined-effect of the glycolytic and mitochondrial metabolism. To determine the contribution of OXPHOS to the effector function of CD8+ TIL during pyruvate treatment, we assessed the impact of inhibiting OXPHOS (oligomycin treatment) on cytokine production from pyruvate-treated CD8+ TIL. The inhibitor significantly reduced IFN $\gamma$  production from pyruvate-treated CD8+ TIL (Fig. 24, A and B), indicating that augmenting mitochondria metabolism could improve effector function of CD8+ TIL. However, pyruvate was not sufficient to fully rescue OXPHOS in CD8+ TIL as show in chapter 3. This suggests that there are additional factors that limit the mitochondria metabolism in CD8+ TIL.

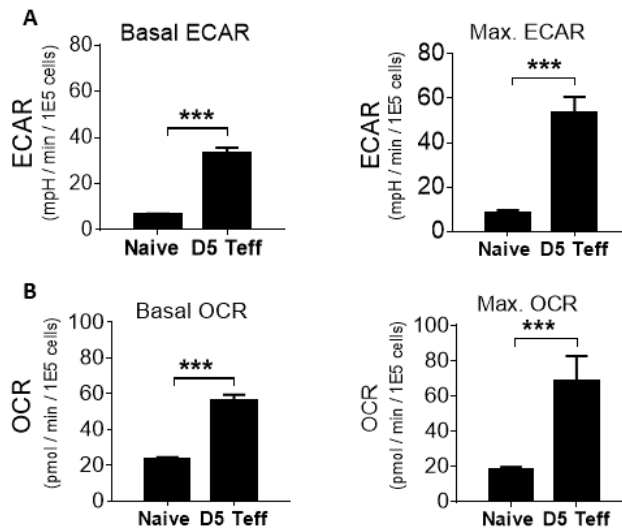


**Figure 23: Activation of CD8 T cells induces both glycolysis and OXPHOS.**

(A-B) Naive and d5 antigen-specific effector CD8<sup>+</sup> T cells were FACS-sorted from the spleens of C57Bl/6 mice immunized with OVA protein, poly I:C, and anti-CD40. (A) *Ex vivo* T cell glycolytic metabolism as measured by the extracellular acidification rate (ECAR) during the Seahorse assay. Basal ECAR was measured in unmanipulated cells while the maximum (Max.) ECAR was quantified after exposing cells to a mitochondrial ATP synthase inhibitor (1  $\mu$ M oligomycin) during the extracellular flux assay. (B) Oxidative phosphorylation (OXPHOS) of the cells in A as measured by oxygen consumption rate (OCR) assessed via Seahorse assay. Basal OCR was measured in cells under steady state while maximum OCR determined after cells were exposed to un-coupler of mitochondrial OXPHOS (1  $\mu$ M FCCP). Data are representative of four independent experiments with n=3 mice per group in each experiment. Error bars represent mean  $\pm$  SEM. P values were calculated by unpaired student's *t*-test. \*\*\*p<0.001.

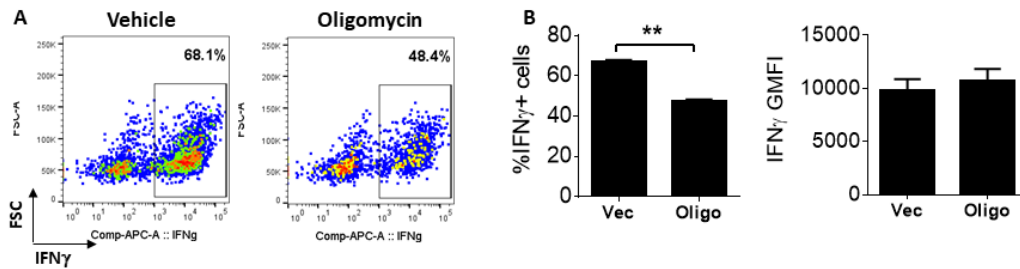


**Figure 24: OXPHOS contributes to CD8<sup>+</sup> TIL function.**

(A-B) Flow cytometric analysis of IFN $\gamma$  production from FACS-sorted CD8<sup>+</sup> TIL that were cultured overnight in the media containing 2mM pyruvate and then *in vitro* restimulated with 1  $\mu$ g/ml anti-CD3 for 4 hours in the presence of vehicle (Veh., DMSO) or 1  $\mu$ M oligomycin (oligo). (A) Representative dot plots with the frequency IFN $\gamma$ <sup>+</sup> CD8<sup>+</sup> TIL from each sample indicated. (B)

Overall frequency (left bar graph) of IFN $\gamma$ <sup>+</sup> cells of CD8<sup>+</sup>CD44<sup>hi</sup> TIL and the GMFI (right bar graph) of IFN $\gamma$  on the IFN $\gamma$ <sup>+</sup>CD8<sup>+</sup>CD44<sup>hi</sup> TIL. Data are representative of two independent experiments with samples pooled from n= 5-7 mice per group in each experiment. Error bars represent mean  $\pm$  SEM. P values were calculated by unpaired student's *t*-test. \*\**p*<0.01

### **Nutrient availability is not the major limiting factor in CD8<sup>+</sup> TIL mitochondrial metabolism**

Glucose fuels the mitochondrial metabolism through pyruvate, which is completely oxidized in the TCA cycle and results in efficient ATP production. Hence, it would be expected that CD8<sup>+</sup> TIL oxidize most of their pyruvate in the mitochondria, rather than converting it to lactate, since they have a deficiency in ATP as shown in chapter 3. We assessed the capacity of CD8<sup>+</sup> TIL to oxidize glucose by measuring the amount of CO<sub>2</sub> liberated from radioactive glucose-derived pyruvate during its oxidation in the TCA cycle(35). Interestingly, the level of glucose oxidation in CD8<sup>+</sup> TIL was similar to that of metabolically quiescent naïve CD8<sup>+</sup> T cells and significantly lower than that of the age-matched Teff (Fig. 25A), which had low overall metabolic activity as demonstrated in chapter 3. The amount of glucose-derived carbon that CD8<sup>+</sup> TIL incorporated into fatty acid during *de novo* lipogenesis, which occurs through the consumption of TCA cycle intermediate citrate(143), was also very similar to that of the metabolically quiescent T cells (Fig. 25B). This may further support the notion that CD8<sup>+</sup> TIL do not efficiently oxidize glucose.

There are multiple nutrients other than glucose/pyruvate that can fuel the mitochondria. It has been reported that T cells induce glutamine metabolism during

activation and that effector T cells can use glutamine as fuel source under glucose deprivation condition(35, 82). Hence, we tested whether CD8+ TIL can efficiently engage glutaminolysis (the metabolism of glutamine in the mitochondria), which could indicate that glutamine availability is limiting the mitochondrial metabolism in CD8+ TIL. We found similar levels of glutamine oxidized in CD8+ TIL and the metabolically quiescent naïve and late effector CD8+ T cells (Fig. 25C). These cell populations had also incorporated similar amount of glutamine-derived carbons into fatty acid during de novo lipogenesis (Fig. 25D), supporting the notion that these cells have similar levels of glutamine oxidation. Together these data suggest that CD8+ TIL consume glutamine at an equivalent rate of quiescent cells. Thus, CD8+ TIL do not appear to have engaged glutaminolysis to compensate for low glucose metabolism.

Fatty acid is another nutrient that can fuel the mitochondrial metabolism(63, 141). Previous unpublished studies from our laboratory identified enhanced fatty acid accumulation in CD8+ TIL compared to CD8 T cells in the spleens of tumor-bearing mice and dendritic cells (DC) (Fig. 26A), indicating that fatty acid availability is not a limiting factor in mitochondrial fatty acid oxidation (FAO) or OXPHOS. Fatty acid accumulation has been associated with dysfunction of DC found in the tumors(144), but whether it is involved in CD8+ TIL is dysfunction is unknown. T cells can either synthesize fatty acids or acquire it from their environment(145). The de novo synthesis of fatty acid is rate limited by acetyl-CoA carboxylase 1 (ACC1)(146, 147). To begin to understand if de novo

lipogenesis contributes to CD8+ TIL dysfunction, we generated a Granzyme B-Cre x ACC1<sup>fl/fl</sup> mouse model in which ACC1 would be deleted after T cells become active and start expressing granzyme B. In a preliminary study, the deletion of ACC1 resulted in significantly slower tumor outgrowth (Fig. 26B), suggesting that synthesis of FA may be limiting the ability of CD8+ T cell to control tumors. Future experiments will confirm whether ACC1 deletion promotes the antitumor activity of CD8+ TIL, and whether this is directly related to reducing fatty acid accumulation.

The oxidation of fatty acid is rate-limited by a key enzyme known as CPT1a, which is critical for the uptake of fatty acids into the mitochondrial to enter FAO(148). The frequency of cells that express CTP1a and the per cell amount of this protein are significant higher in CD8+ TIL than naive CD8 T cells and age-matched Teff (Fig. 26, C and D). However, CD8+ TIL express less CPT1a than acute Teff (Fig. 26, C and D), which may reduce FAO and contribute to the accumulation of fatty acid in CD8+ TIL. However, more in-depth analysis of FAO is required to confirm this conclusion since nutrient uptake potential is not always a reflective of the actual metabolic activity of cells as we demonstrated in the previous chapter with glucose uptake and glycolysis.

Collectively, the above studies and the glucose transport analysis in the chapter 3 indicated that the availability and uptake of the nutrients that can fuel mitochondrial metabolism were not the major limiting factors for OXPHOS in CD8+ TIL.

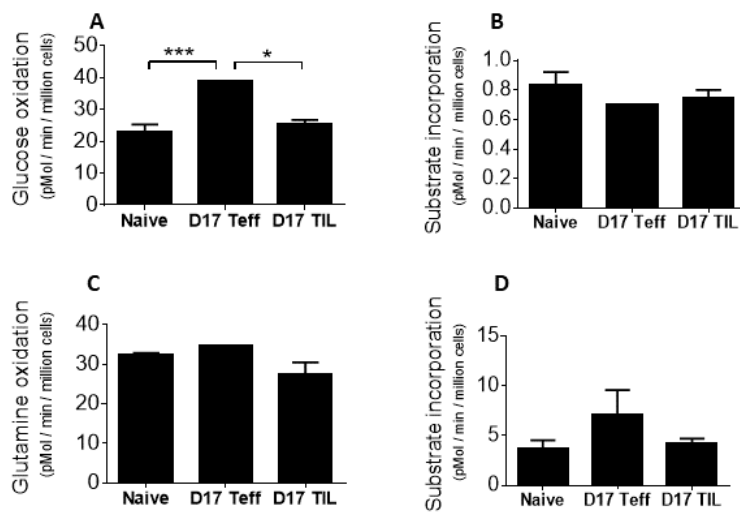


**Figure 25: The availability of glucose or glutamine may not be the major limiting factor in CD8+ TIL mitochondrial metabolism.**

(A-D) Naive and d17 antigen-specific CD8+ T cells were FACS sorted from the spleens of C57Bl/6 mice immunized with OVA protein, poly I:C, and anti-CD40 while antigen-experienced CD8+ TIL were FACS sorted from d17 B16cOVA-bearing mice. (A) Glucose oxidation as measured by the generation of  $^{14}\text{CO}_2$  from  $[^{14}\text{C}]$  glucose in the TCA cycle. (B) The incorporation of glucose-derived carbon into lipid during *de novo* lipogenesis was measured by radiotracer-based assay. (C) Glutamine oxidation as quantified by the generation of  $^{14}\text{CO}_2$  from  $[^{14}\text{C}]$  glutamine. (D) The incorporation carbon derived from  $[\text{U-}^{14}\text{C}]$ -glutamine into lipid was determined by radiotracer assay. Data are on three mice per group. Error bars represent mean  $\pm$  SEM. P values were calculated using one-way ANOVA, followed by Tukey's Multiple Comparison Test. \* $p < 0.05$ , \*\*\* $p < 0.001$ .

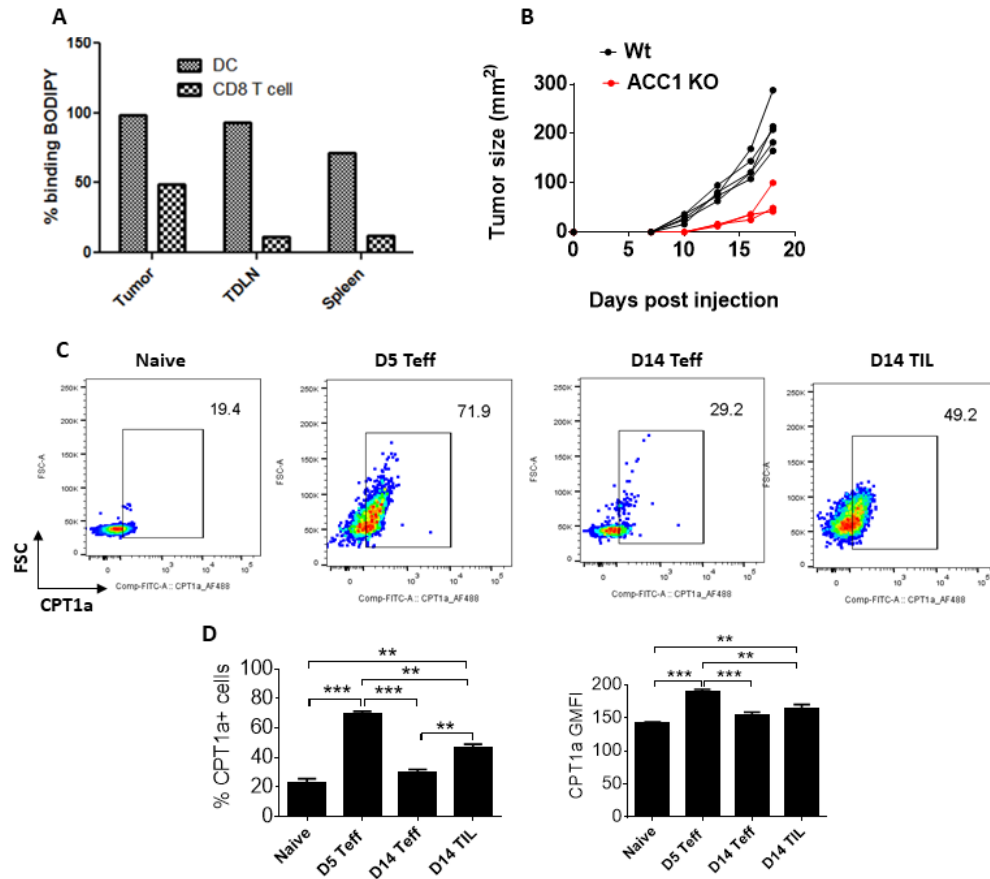


**Figure 26: CD8+ TIL do not exhibit fatty acid deficiency.**

(A) Flow cytometric analysis of fatty acid accumulation (BODIPY labeling) in the CD8 T cells and dendritic cells (DC) isolated from the spleens, tumor draining lymph nodes, and tumors of d17 B16cOVA-bearing. (B) B16cOVA tumor outgrowth in wild type (WT) mice and ACC1 knockout (ACC1 KO) mice. (C-D) Flow cytometric analysis of CPT1a expression in naïve and effector CD8 T cells isolated from the spleens of mice immunized five days prior as in Figure 25 and in CD8+ TIL prepared from d14 B16cOVA tumors developed subcutaneously in C57BL/6 mice. Frequency (C and D, left) of CPT1<sup>+</sup> cells among naïve CD8+CD44<sup>lo</sup>, OVA-specific Teff, or OVA-specific CD8+ TIL and GMFI (D, right) of CPT1 on CPT1-expressing naïve CD8+CD44<sup>lo</sup>, OVA-specific Teff or OVA-specific CD8+ TIL are indicated. Error bars represent mean  $\pm$  SEM. P values were calculated using one-way ANOVA, followed by Tukey's Multiple Comparison Test. \* $p < 0.05$ , \*\*\* $p < 0.001$ .

**The mitochondrial content and function of CD8+ TIL are consistent with their low OXPHOS capability**

Although CD8<sup>+</sup> TIL have attenuated glycolytic activity, they fail to engage a compensatory increase in mitochondrial metabolism even when provided different types of nutrients that can feed into the mitochondria. This led us to reason that CD8<sup>+</sup> TIL may have limited mitochondrial content and/or function that prevent them from engaging strong mitochondrial metabolism. To test this possibility, we measured mitochondrial content by using MitoTracker Green (MTG, fluorescent dye), which labels mitochondria irrespective of their functional status (membrane potential) by binding to the free thiol groups of cysteine residues in the mitochondria proteins(76). This assay identified that CD8<sup>+</sup> TIL have significant lower amount of mitochondrial mass compared to acute Teff (Fig. 27, A and B). However, CD8<sup>+</sup> TIL have more mitochondria than naïve CD8<sup>+</sup> T cells (Fig. 27, A and B), which is consistent with higher OXPHOS in CD8<sup>+</sup> TIL than naïve CD8 T cells. To determine the functional status of the mitochondria in these cells, we measured mitochondrial membrane potential with tetra-methylrhodamine ester (TMRE), a membrane potential-sensitive cationic fluorescent dye, which preferentially accumulates in the matrix of polarized mitochondria due to their more negative inner membrane potential(76). Impressively, while all of the Teff stained with TMRE, only about half of the CD8<sup>+</sup> TIL were found to be TMRE-positive (Fig. 27, C and D), suggesting that some of the CD8<sup>+</sup> TIL do not have the mitochondrial membrane potential that is critical for OXPHOS. Furthermore, there was about 4-fold higher level of TMRE staining in the Teff than CD8<sup>+</sup> TIL at per cell level (GMFI) among the cells that stained positive for the dye (Fig. 27D) indicating less functional mitochondria in each CD8<sup>+</sup> TIL. To

demonstrate that difference in TMRE GMFI is not simply the result of difference in total mitochondria (assessed by MTG), we normalized the TMRE data of each population by their prospective MTG GMFI. This analysis determined significantly lower normalized TMRE GMFI in CD8+ TIL than Teff (Fig. 27E), suggesting that the lower mitochondrial membrane potential observed in CD8+ TIL is a characteristic of these cells rather than being a function of their lower mitochondrial mass.

To further understand the comparative mitochondrial metabolic activity of CD8+ TIL and acute Teff, we assessed the relative composition of metabolic intermediates that are produced in the TCA cycle. This investigation determined 2-4-fold lower TCA intermediates in CD8+ TIL than acute Teff (Fig. 28), confirming the reduced mitochondrial function of CD8+ TIL determined by the TMRE staining.

In the above studies, we compared naïve CD8+ T cells, acute Teff, and day 14 CD8+ TIL. Therefore, we wondered whether the low mitochondrial content and function observed in CD8+ TIL are associated with the notion that these cells are old effectors. To investigate this concern, we assessed mitochondrial content and membrane potential of age-matched Teff and CD8+ TIL. These experiments determined higher MTG staining in CD8+ TIL than in age-matched Teff (Fig. 29A), which argues against age-associated loss of mitochondrial mass in CD8+ TIL. Furthermore, the proportion of CD8+ TIL that stained

with TMRE and the GMFI of TMRE in CD8+ TIL are significantly higher than the levels observed in age-matched Teff (Fig. 29B), in agreement with the higher OXPHOS in CD8+ TIL than age-matched Teff shown in chapter 3. These observations are also consistent with the notion that although CD8+ TIL have low metabolic activity compared to acute Teff, they are not metabolically quiescent like naïve T cells.

To understand the functional state of mitochondria in the CD8+ TIL in human cancer, we conducted the TMRE analysis in healthy donors PBMC and human melanoma TIL. Only about 50% of the human CD8+ TIL stained with TMRE, and the frequency and intensity of TMRE staining in these cells were similar to that observed in resting antigen-experienced CD8+ T cells in healthy donor PBMC (Fig. 30), which are expected to have low metabolic activity because of their quiescent state(64, 149). Hence, the human melanoma CD8+ TIL may have low mitochondrial metabolic activity similar to the CD8+ TIL that infiltrate murine melanoma tumors. However, more accurate experiments such as measurement of OXPHOS or nutrient oxidation are necessary to support this conclusion. Collectively, our mitochondrial studies indicated that the availability and function of these critical organelles might be a major limiting factor in CD8+ TIL OXPHOS.

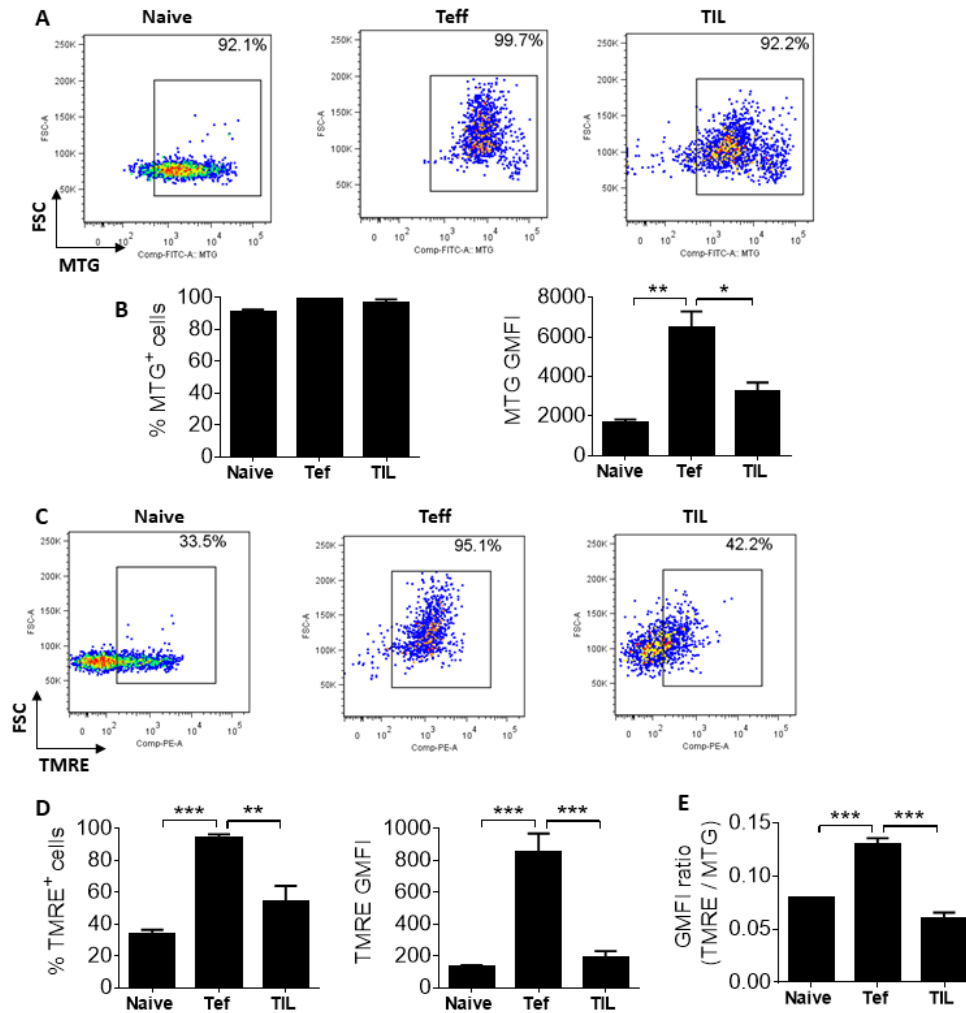


**Figure 27: CD8<sup>+</sup> TIL have low mitochondria mass and function, which are constituent with their limited OXPHOS capability.**

(A-E) Naive CD8 T cells, Teff, and CD8<sup>+</sup> TIL were prepared as in Figure 26C. (A-B) Flow cytometric analysis of mitochondrial mass through measurement of the accumulation of MitoTracker Green (MTG), membrane potential independent mitochondrial labeling dye. Frequency (A and B, left) of MTG<sup>+</sup> cells among naïve CD8<sup>+</sup>CD44<sup>lo</sup>, OVA-specific Teff, or OVA-specific CD8<sup>+</sup> TIL, and GMFI (B, right) of MTG on MTG-positive naïve CD8<sup>+</sup>CD44<sup>lo</sup>, OVA-specific Teff, or OVA-specific CD8<sup>+</sup> TIL are indicated. (C-D) Mitochondrial membrane potential as determined by potentiometric dye TMRE accumulation in the indicated cells. Frequency (C and D, left) of TMRE<sup>+</sup> cells among naïve CD8<sup>+</sup>CD44<sup>lo</sup>, OVA-specific Teff, or OVA-specific CD8<sup>+</sup> TIL, and GMFI (D, right) of TMRE on TMRE-positive naïve CD8<sup>+</sup>CD44<sup>lo</sup>, OVA-specific Teff, or OVA-specific CD8<sup>+</sup> TIL are indicated. (E) Ratio of the GMFI of TMRE (from panel D, right) to GMFI of MTG (from panel B, right). Error bars represent mean  $\pm$  SEM. P values were calculated using one-way ANOVA, followed by Tukey's Multiple Comparison Test. \* $p < 0.05$ , \*\* $p < 0.01$ , \*\*\* $p < 0.001$ .

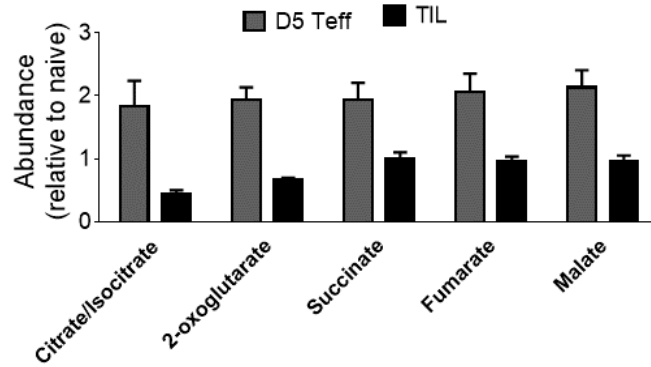


**Figure 28: CD8+ TIL have low TCA cycle active compared to acute Teff.**

Metabolomic analysis of the relative TCA cycle metabolites composition of d5 Teff and d14 CD8+ TIL normalized to that of naive CD8+ T cells. Metabolites were extracted from FACS-sorted naïve, d5 Teff, and CD8+ TIL that were prepared and subjected to mass spectrometric analysis as in Figure 4.

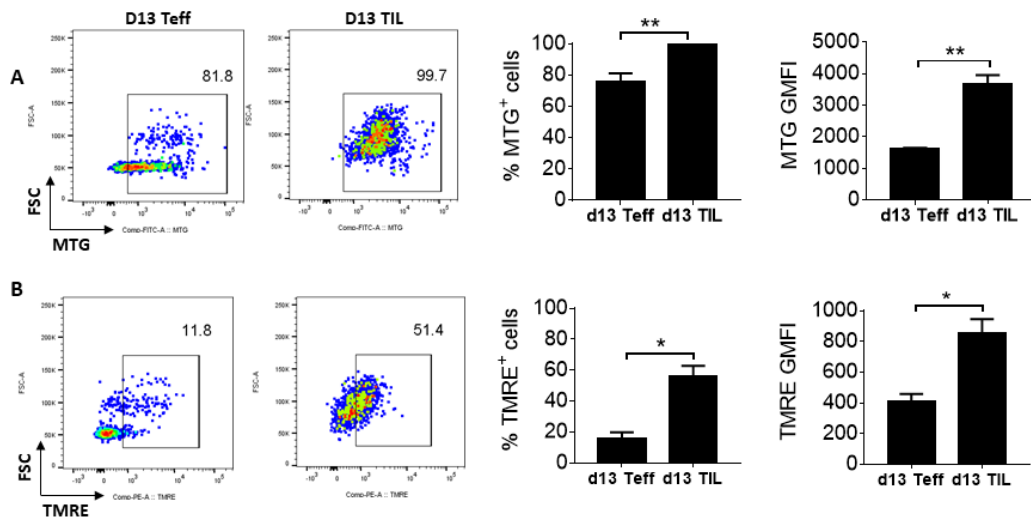


**Figure 29: Mitochondrial dysfunction may not be associated with the age of CD8+ TIL.**

(A-B) MTG and TMRE analysis was done as in Figure 28. d13 Teff were isolated from the spleens of mice immunized with OVA protein, poly I:C, and anti-CD40 while d13 TIL were isolated from B16cOVA tumor-bearing mice. Data are representative of two independent experiments with three mice per group in each. Error bars represent mean  $\pm$  SEM. P values were calculated by unpaired student's *t*-test. \*\* $p < 0.01$  \* $p < 0.05$ .

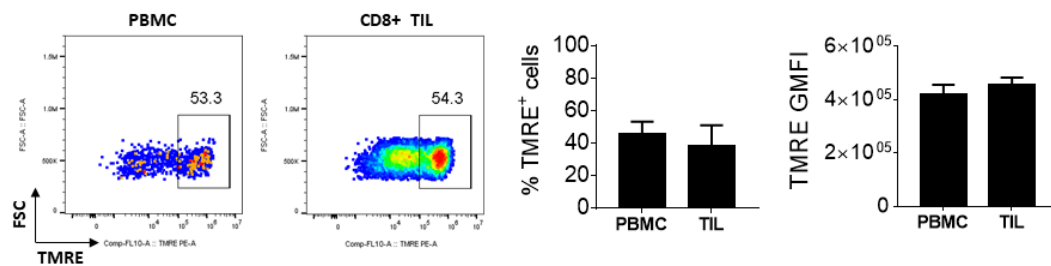


**Figure 30: Human melanoma CD8+TIL have similar level membrane potential as quiescent antigen-experience CD8 T cells in healthy donors PBMC.**

Mitochondrial membrane potential of antigen-experienced CD8 T cells in the healthy donor PBMC and melanoma TIL was determined by measuring TMRE staining with flow cytometry. Frequency (dot plots and left graph) of TMRE<sup>+</sup> cells among CD8+CD45RO<sup>+</sup> T cells and GMFI of TMRE on TMRE<sup>+</sup>CD8+CD45RO<sup>+</sup> cells are indicated. Data are on samples from two healthy donors and three melanoma patients. Error bars represent mean  $\pm$  SEM.

## DISCUSSION

Mitochondrial metabolism can support the generation and function of effector T cells (41, 84, 92, 140, 141). However, the activity of this metabolic program was compromised in CD8+ TIL as we showed in chapter 3 and others have also reported(23, 24). The mitochondrial metabolic deficiency of CD8+ TIL was partly linked to the inability of the glycolytic metabolism to efficiently produce pyruvate. This was demonstrated

with our glycolysis bypassing approach in which the provision of exogenous pyruvate significantly increased OXPHOS and cytokine production capability of CD8+ TIL, indicating that mitochondria in TIL have some residual activity. Inhibition of OXPHOS reduced the capacity of pyruvate to rescue cytokine production in CD8+ TIL, which indirectly showed that the glycolytic deficiency constrained the mitochondrial function. However, pyruvate was able to only partial rescue the OXPHOS in CD8+ TIL (chapter 3), suggesting the existence of additional mechanisms that limit mitochondrial metabolism in these cells.

In addition to glucose, mitochondria can consume glutamine and fatty acid to support OXPHOS(35, 64). The entry of glutamine and fatty acid into mitochondria metabolism does not require glycolytic activity since these nutrients are not processed by glycolysis. In fact, repression of glycolysis or glucose deprivation leads to a compensatory increase in glutamine metabolism(82). Our analysis of the consumption of glucose and glutamine in the mitochondrial TCA cycle determined that CD8+TIL metabolized these nutrients at an equivalent rate as other quiescent T cells. These studies suggest that nutrient availability was also not limiting the OXPHOS in CD8+ TIL.

Mitochondrial dysfunction may be a major mediator of the OXPHOS deficiency in CD8+ TIL. These cells exhibited a striking deficiency of mitochondrial membrane potential, a

critical component of the OXPHOS. CD8+ TIL also had reduced mitochondrial mass compared to acute Teff, and others have also reported even larger loss of mitochondrial mass in CD8+ TIL(24). We have also previously reported loss of membrane potential in the TIL that infiltrate the human renal cancer although these TIL did not exhibit a reduction in mitochondrial mass(23). Interestingly, enolase 1 has been reported to play an important role in stabilizing mitochondrial membrane(138) and in promoting acquisition of mitochondria morphology that is suitable for engagement of enhanced OXPHOS(150). It is currently unclear whether enolase activity is necessary for its role in the regulation mitochondria. However, it is tempting to hypothesize that the impairment of enolase activity in CD8+ TIL contributes to the mitochondrial dysfunction not only by limiting pyruvate availability, but also by repressing mitochondrial membrane potential. Other studies in the lab are currently investigating the basis of mitochondrial dysfunction in TIL, and have observed a hyper-punctate phenotype that is consistent with damaged mitochondria with reduced OXPHOS capabilities (Marissa Gonzales, personal communication). Thus, approaches that promote elongation of mitochondria might be anticipated to increase OXPHOS capabilities and work with enolase-reactivation to promote overall metabolic fitness of CD8+ TIL.

## Chapter 6: Conclusions and Future Directions

### Metabolic activity of CD8+ TIL

The link between immunological and metabolic activities of T cells has recently become an area of intense investigation in the field of immunology. Such studies have established that elevated metabolic activity is critical for the growth, proliferation, survival and effector function of activated T cells(38–42). In this work, we investigated whether CD8+ TIL have a metabolic insufficiency that either underlies or contributes to their dysfunction. Collectively, our work has demonstrated that CD8+ TIL have attenuated glycolytic and oxidative metabolic activity, and that these metabolic limitations constrain their effector functions by limiting the availability of cellular metabolites that are essential for T cell function (Fig. 31). Furthermore, we discovered that post-translational regulation of the activity of enolase 1, a key glycolytic enzyme, limits glycolytic metabolism at the level of phosphoenolpyruvate production in CD8+ TIL. Phosphoenolpyruvate deficiency constrained the production of a downstream metabolite pyruvate, and impeded the metabolic and effector function of CD8+ TIL. Impaired enolase activity is also evident in the T cells that infiltrate the human melanoma tumors. Our studies have also demonstrated that an immune checkpoint blockade therapy that promoted antitumor immunity generated CD8+ TIL with stronger enolase activity. The improved enolase activity of checkpoint-treated CD8+ TIL was important for their effector function. Furthermore, we showed that the impairment of

enolase activity also diminished the OXPHOS capability of CD8+ TIL via limitation of glucose-derived pyruvate that fed into mitochondrial metabolism. CD8+ TIL also have reduced mitochondrial content and function, which contributes to their repressed oxidative metabolism.

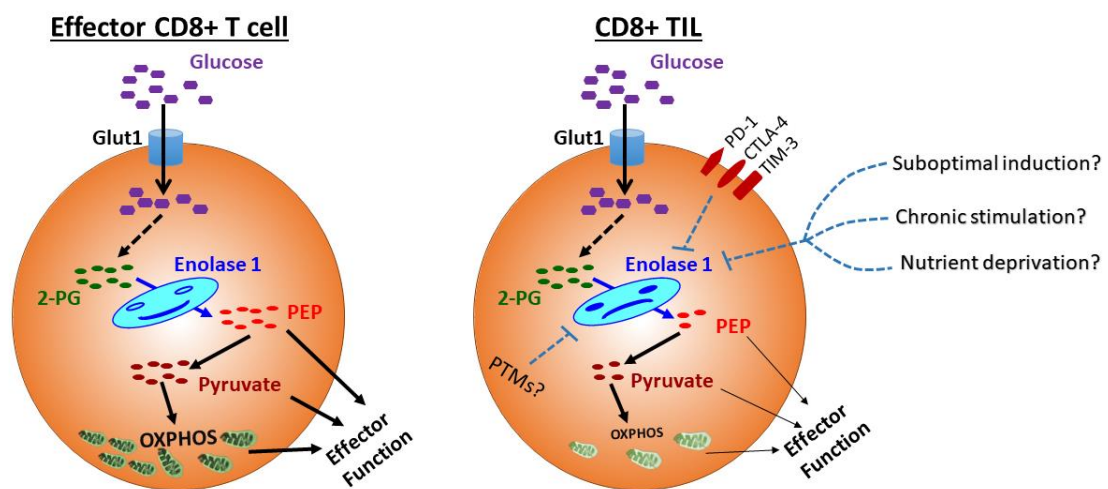


**Figure 31: Model of CD8+ TIL metabolic and effector function restraint by impaired enolase activity.**

Impaired enolase activity represses glycolytic metabolism at the level of phosphoenolpyruvate (PEP) production and dampens OXPHOS by limiting pyruvate availability. Hence, loss of enolase activity contributes the dysfunction of CD8+ TIL by diminishing the ability of glycolytic metabolism (PEP and pyruvate) and OXPHOS to support effector function. Loss of mitochondrial mass (represent by number of mitochondria) and membrane potential (represented by change in color of mitochondrial, lighter green) also restrict the OXPHOS capability of CD8+ TIL. Potential mechanisms of enolase impairment, including the checkpoint molecules and PTMs we assessed in this work, are represented by dash lines.

## **Role of competition for glucose and cell-intrinsic mechanism in controlling the metabolic activity of CD8+ TIL**

High glycolytic activity is a metabolic characteristic of both tumor cells(151, 152) and activated T cells(35, 152). Such understanding led to the hypothesis that competition for glucose between the tumor cells and TIL would result in attenuated glycolytic activity in the CD8+ TIL. A recent work has attempted to test this hypothesis by studying the effect of glucose-deprivation on T cells responding to murine sarcoma cell lines with low or high glycolytic activity(21). That study found a lower glycolytic activity in CD8+ TIL isolated from the more glycolytic tumors (less glucose in the TME) compared to the CD8+ TIL from the tumors with lower glycolytic activity (more glucose in the TME), supporting the competition hypothesis. Another recent study has provided more support for this hypothesis by showing that the TME has limited amount of glucose compared to spleen and blood, and that such nutrient restriction could negatively impact the glycolytic and effector function of T cells(22). Our work identified a novel cell-intrinsic mechanism of regulation of the glycolytic metabolism in CD8+ TIL. We found that even though these cells could effectively take up glucose, they retained low glycolytic activity under *ex vivo* conditions that allowed access to physiological amount of glucose and removed competition from other cells (by FACS-purification). These findings indicated that a cell-intrinsic regulatory mechanism, rather than simply glucose deprivation, restrains the glycolytic activity of CD8+ TIL. Our investigation of this

mechanism has determined that impairment of enolase activity is a mediator of the attenuated glycolytic activity in CD8<sup>+</sup> TIL. Bypassing enolase activity significantly improved the metabolic and effector function of CD8<sup>+</sup> TIL, further supporting the role of processes other than simple unavailability of glucose in impacting the glycolytic activity of CD8<sup>+</sup> TIL. However, it is tempting to speculate that the prolonged glucose deprivation that the CD8<sup>+</sup> TIL experience in the TME initiates the impairment of enolase activity. In support of this notion, glucose restriction has been reported to repress the activities of other metabolic enzymes in different cells(125, 134). To test the impact of prolonged glucose restriction on the enolase and glycolytic activity of T cells, we could culture *in vitro* activated CD8 T cells in media containing either the amount of glucose reported in TME (0.6 mM) or physiological amount (10 mM) of glucose that has been reported in the spleen of mice(22). T cells would be provided physiological amounts of glucose during the initial activation to mimic the access to glucose that might be available in the lymph node, and then further cultured in IL-2 and 0.6 mM or 10 mM glucose. Enolase and glycolytic activity would be assessed every two days while the cells that remain in culture would receive fresh media containing IL-2 and the appropriate amount of glucose at each time point. This study will clarify if there is a link between the impairment of enolase activity and the glucose deprivation, which may explain the relationship between the model based on competition for glucose and our work.

### **Failure to induce glycolysis versus loss of glycolytic activity in CD8+ TIL**

The glycolytic deficiency of CD8+ TIL could be a result of either failed induction during the T cell priming phase or a failure to sustain in the TME. The results of our investigation of several cellular programs that are activated during metabolic induction are consistent with dysregulation or suppression of glycolysis, rather than a failure in its initial induction in CD8+ T cells being activated in the TDLN. For example, our analysis of glucose transport determined that CD8+ TIL expressed high levels of glucose transporters and are capable of effectively taking up glucose, indicating successful mobilization of glucose transport machinery. We also observed that CD8+ TIL had active cellular signals that are important for maintenance of elevated glycolytic activity(40, 44, 51, 77, 78), and expressed high levels of key glycolytic enzymes. More importantly, our metabolomics analysis determined that the majority of the steps involved in glycolysis were as active in CD8+ TIL as in Teff as judged by the relative amounts of intermediary metabolites they produced compared to similar steps in effector T cells that were highly glycolytic. Finally, T cells responding to tumors after checkpoint inhibition has relatively high enolase activity, suggesting appropriate induction of glycolysis.

Direct investigation of whether the priming of CD8+ TIL induces glycolytic metabolism is currently technically challenging since there is no sensitive metabolic assay that can be used to interrogate glycolytic activity in the limited number of antigen-specific CD8 T

cells in the tumor draining lymph nodes or in early stage tumors. While the enolase reporter we have developed in this work has the sensitivity to study glycolysis at the level of the reaction catalyzed by this enolase 1, it cannot determine the potential repression of glycolysis by other mechanisms and we do not know when enolase itself becomes impaired. Hence, assessing the overall glycolytic activity may be important when investigating the induction and maintenance of this metabolic program in CD8+ TIL. Such studies can be done in couple of ways if sensitive metabolic assays are developed. One of the approaches is to assess the glycolytic activity of CD8+ TIL at different time points starting when tumors becomes first palpable, which is around day 7 post-tumor injection for B16cOVA. The second approach is to use adoptive T cell transfer experiment in which TCR-transgenic (OT-I or Pmel) CD8+ T cells would be transferred into B16cOVA tumor-bearing mice or vaccinated mice in the presence or absence of FTY-720 treatment. The vaccination cohort will be included to generate T<sub>eff</sub> for positive control while the FTY-720 treatment will be important to assess if CD8+ TIL lose glycolytic activity when they enter the TME. The transferred cells would be re-isolated from the tumor draining lymph nodes (TDLN), tumors, and spleens at different time points beginning on day 3 post-transfer and subjected to analysis of glycolytic activity. Even though it might not fully address the question about lack of induction versus repression of glycolysis by itself, assessing enolase activity in the above experiments could provide insight into whether CD8+ TIL fail to activate enolase during priming or are unable to sustain its activity in the TME. Whether these studies identify a

defect in the induction or repression in the TME as the mediator of the glycolytic insufficiency of CD8+ TIL, they will shed some light on the mechanism of regulation of glycolysis and provide important foundations for designing approaches to promote this metabolic program.

### **Mechanism of enolase impairment**

Our investigation of the mechanisms of impairment of enolase activity in CD8+ TIL have determined that this enzyme is post-translationally regulated since we did not observe any alteration in Eno1 gene transcription or mRNA translation. We have also determined that enolase cannot be reactivated in CD8+ TIL by providing a stimulation condition that was capable of further increasing the activity of this enzyme in Teff. However, we have not assessed the potential contribution of chronic antigen exposure to the impairment of enolase activity in CD8+ TIL. Notably, chronic stimulation of T cells by viral (153) or tumor(24) antigens has been shown to alter the metabolic activity of T cells. The impact on chronic antigen exposure on enolase activity could be tested by using the chronic lymphocytic choriomeningitis virus (LCMV) infection or *in vitro* chronic stimulation. In LCMV studies, we could infect mice with LCMV Armstrong, which would be acutely cleared, or LCMV clone 13 to generate chronic infection(153). Enolase expression and activity would be assessed at different time-point including day 8 post-infection, a time-point at which CD8+ T cells responding to the chronic LCMV have been

shown to have repressed glycolysis(153). Alternatively, repetitive *in vitro* stimulation of CD8+ T cells could be employed as a model for chronic antigen exposure(154) to study whether persistent stimulation impairs enolase activity. Although the *in vitro* chronic stimulation conditions would not necessarily reflect the physiological environment of tumors, it allows elimination of factors other than antigen availability (such as generation of new wave of effectors and change in viral load and cytokine milieu) that may impact the LCMV Clone 13 model.

While the above studies may shed some light on the immunological basis for the initiation of impaired enolase enzymatic activity, they will not address the potential biochemical mechanisms that regulates the activity of this enzyme. Little is known about how enolase activity is post-translationally regulated. Divalent cations such as magnesium ions are known cofactors for enolase(127, 131). However, we did not observe significant change in enolase activity following *in vitro* treatment of CD8+ TIL with MgSO<sub>4</sub>, suggesting that the availability of Mg<sup>2+</sup> was not limiting enolase activity in these cells. Other potential post-translational regulators of enolase activity are post-translational modifications (PTMs) since enolase has reported to undergo acetylation, methylation, and phosphorylation in highly glycolytic tumor cells(129, 131). Our preliminary analysis of PTMs of enolase 1 from CD8+ TIL and acute Teff identified differential acetylation of lysine and methylation of lysine, aspartic acid, and glutamic acid. Some of these modifications were present either only the CD8+ TIL or Teff. These

modifications need to be confirmed with repeat experiments and targeted mass spectrometric analysis. If they are real, there are multiple literature reports indicating the potential of such PTMs to regulate protein functions. Particularly, lysine acetylation has been reported to activate some metabolic enzymes while they inhibit others(125, 134, 135). Therefore, we hypothesize that the differential acetylation of lysine residues identified in enolase 1 from CD8+ TIL contributes to the inactivity of this enzyme. This hypothesis could be tested by using recombinant enolase 1 proteins others have previous used to directly assess enolase activity(122, 136). During the generation the recombinant enolase 1, we would substitute one or more of the lysine residues that were differentially acetylated in CD8+ TIL with arginine or glutamine and assess the impact of deacetylation or acetylation of lysine on enolase activity. It has been reported that lysine to arginine substitution mimics lysine deacetylation while lysine to glutamine mutation mimics lysine acetylation(125). Alternatively, the impact of enolase 1 acetylation on its activity might be assessed by treating CD8+ TIL *in vitro* with lysine deacetylase (KDAC) inhibitors such as trichostatin A (TSA) and/or nicotinamide (NAM), which have been shown to increase the acetylation of other enzymes(125, 134). We could also prepare cell lysate from CD8+ TIL and *in vitro* treat it with deacetylase inhibitors(134) if *in vitro* culture of CD8+ TIL interferes with enolase acetylation. The potential regulation of enolase activity by the differential methylations observed in enolase 1 isolated from CD8+ TIL could also be assessed by introducing point mutations

in the recombinant protein or by conducting *in vitro* CD8+ TIL treatment with pan-protein demethylase inhibitors(155).

Interestingly, studies have shown that glucose availability can modulate the activities of metabolic enzymes via regulation of their acetylation state(125, 134). For example, glucose deprivation has been reported to induce the expression of deacetylase Sirt1 and cause deacetylation that represses the activity of the glycolytic enzyme phosphoglycerate mutase 1 (PGAM1)(125). Glucose has also be reported to promote lysine acetylation that regulates the enzymatic activity of malate dehydrogenase (MDH) in the TCA cycle, phosphoenolpyruvate carboxykinase 1 (PEPCK1) in the gluconeogenesis, and argininosuccinate lyase (ASL)in the urea cycle(134). Therefore, if the studies in the above paragraph link the lysine deacetylation to the impairment of enolase activity in CD8+ TIL, we would hypothesize that the limited availability of glucose in the TME regulates enolase activity via lysine deacetylation. This hypothesis could be tested by conducting PTM analysis on *in vitro* activate CD8 T cells that were cultured in a range of glucose concentrations varying from no glucose to supraphysiological amounts. Assessing the expression of Sirt1, whose expression level could be induce by glucose restriction(125), and other lysine deacetylases in CD8+ TIL or *in vitro* Teff that were exposed to different amount glucose might also shed some light on the role of glucose availability of enolase acetylation. The role of Sirt1 in the regulation of enolase activity could be examine by using Sirt1 knockout mouse model

that have previously described(156). T cells from these mice could be *in vitro* stimulated and subjected to glucose deprivation followed by analysis of enolase acetylation and activity, or transferred to tumor-bearing mice and subject to a similar assessment. Another useful approach would be to overexpress FLAG-tagged enolase 1 in *ex vivo* CD8+ TIL and examine its acetylation status by western blot. However, this approach might be challenging since CD8+ TIL are not very amenable to transduction protocol because of their dysfunction and fragility. If these studies determine that PTMs are involved in regulation of enolase activity, they will provide mechanisms that could be targeted to rescue the activity of this enzyme in CD8+ TIL or to prevent its inactivation in the T cells used for adoptive cell therapy.

### **Immune checkpoint signals and impaired enolase activity**

Previous studies have reported that immune checkpoint (CP) signals alter glycolytic metabolism(21, 74) in T cells, but the details of the molecular mechanism by which these inhibitors disrupt glycolysis is still poorly understood. Our work has determined that the regulation of enolase activity is a possible novel mechanism by which checkpoint signaling can suppress glycolytic metabolism. We found that inhibition of multiple immune checkpoint signals (CPI) generated CD8+ TIL with a stronger enolase activity, and active enolase played a critical role in supporting their effector function as demonstrated by the capacity of enolase inhibitor to suppress cytokines and lytic

molecule production from these cells. Furthermore, our investigation ascribed the increased enolase activity to the new CD8<sup>+</sup> TIL generated in response to the checkpoint blockade, rather to the reactivation of enolase in the pre-existing cells. However, it is unclear whether the CPI improves enolase activity by promoting its induction during the activation of the newly generated CD8<sup>+</sup> TIL in the tumor draining lymph nodes and/or by preventing its inactivation in the TME. Among the checkpoint molecules targeted by our combinatorial CPI therapy, the impact of CTLA-4 is thought to be mainly on the priming of T cells in the lymph nodes(157, 158). Hence, its blockade may relieve a potential interference of CTLA-4 with the initial induction of enolase activity.

Alternatively, CTLA-4 has also been shown to support Treg function, and its activity in this context may reflect a contribution of Treg to effector T cell glycolytic metabolism. Blockade of PD-1 and TIM-3, on the other hand, may render CD8<sup>+</sup> TIL unable to maintain the activity of enolase in the TME since these checkpoint molecules are thought to act late at the effector stage of T cell activation(157–160).

To test if CPI treatment influences the induction and/or maintenance of enolase activity in CD8<sup>+</sup> TIL, we could perform FTY-720 treatment and adoptively transfer of TCR-transgenic (OT-I or Pmel) CD8<sup>+</sup> T cells into melanoma tumor-bearing mice, and then treat the mice with the combinatorial CPI or control antibody. If we observe stronger enolase activity in CD8<sup>+</sup> T cell recovered from TDLNs of CPI-treated mice than control-treated mice, this would suggest that the combinatorial CPI treatment enhances enolase activity by promoting its induction during T cell priming. If we do not observe a significant

difference in the activity of enolase in CD8 T cells from TDLNs of CPi- or control-treated mice, this might suggest that the CPi treatment works by preserving enolase activity in CD8+ TIL in the TME. This could be further investigated by conducting the above experiment without the FTY-720 treatment and comparing the activity of enolase in CD8+ TIL recovered from CPi- and control-treated mice. If we observe stronger enolase activity in the CD8+ TIL recovered from CPi-treated mice than control-treated mice, this would indicate that the checkpoint blockades work by preventing loss of enolase activity in the TME. However, it is also possible that the combinatorial CPi treatment involves in both the induction and maintenance of enolase activity in CD8+ TIL. This possibility is supported by the premise that the different checkpoint molecules are active in different anatomical locations and stages of T cell activation as described above. The role of the CPi treatment in the induction enolase activity could be determined by the TDLN analysis outlined above. However, deciphering the contribution of this treatment to the maintenance of enolase activity from its effect on the induction of the activity of this enzyme in *in vivo* or *ex vivo* setting will be very hard when the treatment supports both processes. Such analysis could be done by using *in vitro* assays where enolase-active effector CD8 T cells could be cocultured with tumor cells in the presence or absence of the combination of CPi antibodies.

The molecular mechanism by which the combinatorial CPi treatment improved enolase activity in CD8+ TIL also remains to be determined. Based on our studies that suggest

potential regulation of enolase 1 activity by PTMs, it possible that the CPi works by influencing the PTMs status of enolase 1 in CD8+ TIL. This might be tested by assessing the PTM repertoire (e.g. acetylations) of enolase 1 isolated (immunoprecipitated) from CPi- and control-treated CD8+ TIL.

### **Validation and usage of enolase reporter**

The enolase reporter we developed in this work has the potential to allow a rapid analysis of enolase activity at single cell level. Our current data showed strong association between the strength of enolase activity and the level of enolase reporter staining. However, whether the reporter binds to enolase in an activity-dependent manner should be further validated prior to using this reagent for analysis of enolase activity. This might be done by comparing the capacity of enolase reporter to differentially label enzymatically active and inactive enolase 1. It has been reported that mutation of any of the highly conserved amino acid residues (Glu168, Glu211, Lys345 or Lys396) in the active site of enolase 1 renders this enzyme catalytic inactive(161–163). Therefore, we could transduce cells to overexpress wild type or the catalytically-inactivity enolase 1, and then conduct enolase functional and reporter assays. The impact of endogenous enolase on the outcome of this experiment can be reduced by using cells that have weak enolase activity such as naive T cells or late effectors, or possibly by knocking out enolase 1 in parent cell lines such as 3T3 cells. We would

expect to observe higher reporter staining in the cells transduced with the wild enolase 1 than in the ones transduced with the inactive enolase 1. As an alternative experiment, we could treat effector T cells with enolase inhibitor (NaF) or vehicle, and measure enolase activity by using both the reporter assay and direct enolase activity assays. A potential concern with this experiment is that we do not know whether the change in the conformation of enolase 1 due to fluoride binding(164) itself would impact the binding of the reporter to enolase 1. Collectively, the results of these studies will be useful in guiding how the enolase reporter should be used because this reagent can serve different purposes based on whether it labels enolase 1 in an activity-dependent or -independent manner. If the reporter is activity-dependent, it will offer a quick and sensitive approach for the assessment of enolase activity, which may be a biomarker of glycolytic metabolism. If the reporter does not require enzymatic activity of enolase 1 for labeling, it will offer a robust approach for the analysis of total enolase 1 expression. Such robustness may have an important implication in clinical cancer tests where the expression of enolase has been investigated for a diagnostic marker(165, 166). Furthermore, this reporter can be used for staining of enolase 1 in the living cells due to its ability to cross the cell membrane without any manipulation as a result of the cell permeable small molecule (ENOblock)(122) we used to develop it. This could be important for enolase 1-based cell sorting and for co-staining in assays that have to be done in living cells, such as mitochondrial function analysis. Additionally, the presence of rhodamine on the reporter allows anti-rhodamine to be used for subcellular localization

and purification assays, to identify potential binding partners and subcellular localization of enolase. However, the impact of ENOblock on the activity of enolase should be considered when using in living cell assays. Although current studies agree that ENOblock binds enolase 1, whether the binding leads to inhibition of enolase activity has been controversial(121, 122, 136). ENOblock did not have a significant impact on enolase activity in our model system during preliminary studies (data not shown). However, a more thorough investigation involving multiple concentrations, time points, and control samples will be necessary to support this finding since two papers have reported the inhibitory effect of ENOblock(121, 122). It should be noted that ENOblock is a reversible inhibitor and therefore even if inhibition of enolase is observed, it will not preclude using the reporter to isolate different T cell populations for further analysis. Dr. Hsu's lab is in the process of developing a photoactivatable cross-linking version of enolase reporter which will allow its use in T cell functional assays.

Another potential use of the enolase 1 reporter is for the analysis of the subcellular localization of this enzyme. Although enolase is known to be expressed in the cytoplasm of every cells, it has also been reported to be expressed on the cell surface of different types of cells(127) including CD4 T cells (167) and cancer cells (127, 137). Based on its cell permeable nature, we expect that this reporter would be able to simultaneous stain enolase 1 on the surface as well in the cytoplasm of a cell. The cells that express enolase 1 on their surface and in their cytoplasm can be a great model system to test this

notion. Conveniently, different pancreatic ductal adenocarcinoma cell lines (PDAC) have been shown to express variable levels of the enolase 1 on their surfaces in addition to expressing in their cytoplasm(168). Therefore, we could conduct enolase reporter staining in PDAC cell lines that express high (T3M4, CFPAC-1 and L3.6pl), medium (MIA PaCa-2, Hs766T, and PT45), and no (BxPC-3 and PANC-1 cells) surface enolase(168) and assess the labeling of enolase by using image stream or confocal microscopy.

### **Potential fates of glycolytic intermediate in CD8+ TIL with impaired enolase activity**

Despite their limited glycolytic and oxidative metabolic activities, CD8+ TIL efficiently take up and retain glucose. Moreover, these cells could successfully process glucose through the steps of glycolysis that are found upstream of the reaction catalyzed by enolase 1 as demonstrated by our metabolomics analysis. These findings raise an important question: why is there no buildup of 2-phosphoglycerate (2-PG, substrate of enolase 1) in CD8+ TIL while their enolase is not working? There are several possible explanations for this including the conversion of 2-PG back to the upstream metabolite (3-phosphoglycerate, 3-PG), shunting of 2-PG away from glycolysis, and/or feedback inhibition. 2-PG can be converted back to 3-PG(169), which could be removed from glycolysis and be used for serine synthesis(65, 80). Serine plays a critical role in supporting active T cells via production of glycine and one-carbon units that are

important for nucleotide synthesis(170). Interestingly, 2-PG can also promote the consumption of 3-PG in the serine synthesis pathway by directly activating 3-PG dehydrogenase (PHGDH), which catalyzes the conversion 3-PG into serine precursors(125, 171). Therefore, we hypothesize that the lack of accumulation of glycolytic metabolites upstream of PEP despite the impairment of enolase activity in CD8+ TIL is due to 2-PG/3-PG shunting into serine synthesis. To test this hypothesis, we could treat *ex vivo* CD8+ TIL with a recently identified PHGDH inhibitor(172) to block 3-PG commitment to serine biosynthesis and measure the amount of 3-PG and 2-PG in the lysate prepared from these cells. 3-PG and 2-PG could be measured by a spectrophotometric-based approach that others have previously described(171). Alternatively, we could track glucose-derived metabolites by using stable isotopic labeled glucose (<sup>13</sup>C-glucose) tracer assay(82). For this assay, CD8+ TIL would be acutely cultured in the media containing <sup>13</sup>C-glucose in the presence and absence of PHGDH inhibitor. Although this assay requires more cells, it could provide more detailed information about the usage of 3-PG in serine synthesis pathway as well as the consumption of glucose-derived metabolites in other metabolic programs.

Another mechanism that could prevents glycolytic intermediate buildup in CD8+ TIL, is the induction of a metabolic program known as pentose phosphate pathway (PPP). Once glucose is taken up by cells, it is converted into glucose-6-phosphate (G6P) by the activity of hexokinases(63). G6P is then either further processed by the glycolytic pathway or removed from glycolysis and be used to fuel the PPP(63). The consumption

of G6P in PPP could impact the abundance of all the downstream glycolytic intermediates. Interestingly, 3-PG has been reported to be a negative regulator of PPP by directly inhibiting a key enzyme (6-phosphogluconate dehydrogenase (6PGD)) in the pathway(173). More importantly, the 2-PG-mediated induction of 3-PG consumption in the serine synthesis pathway (described above) has been reported to promote PPP activity(173). Therefore, the impaired enolase activity may lead to a simultaneous activation of the serine synthesis pathway and PPP in CD8+ TIL. This might be assessed by tracking the intermediary metabolites of both pathways with <sup>13</sup>C-glucose tracer experiment describe above. We could also determine PPP activity by measuring the rate of <sup>14</sup>CO<sub>2</sub> released from [1-<sup>14</sup>C]-glucose during PPP as previously described by others(35). If these studies reveal high PPP activity in CD8+ TIL, further investigation would determine its utility for these cells beyond the regulation of glycolytic metabolites. PPP is generally known for its ability to produce macromolecules that support lipid and nucleic acids synthesis and antioxidants that are important for prevention damage caused by reactive oxygen species (ROS)(174). All of these could be very beneficial for CD8+ TIL given their altered metabolic activity and localization in environment rich in ROS(175). Collectively, these studies will provide further insight into the mechanisms of glucose utilization in CD8+ TIL, and may in fact identify a novel “survival” metabolic adaptation taken by T cells within the TME.

Blocking enolase activity could also be a mechanism by which CD8+ TIL are trying to preserve/shunt glycolytic intermediates that are produced upstream of PEP into

biosynthetic pathways in order to improve their proliferation. This is a similar concept to the use of catalytically less active pyruvate kinase M2 (PKM2) in cancer cells to reduce the conversion of PEP to pyruvate, a process that is known as a mechanism of channeling glycolytic intermediates away from mitochondrial ATP production into biosynthetic pathways(65). Repressing the activity of enolase, as oppose to other enzymes that serve upstream in glycolysis, may allow the CD8+ TIL to produce the most glycolytic intermediates that can feed into different anabolic pathways described above and also in chapter 1 (Fig. II).

### **Mechanism of pyruvate rescue of cytokine production in CD8+ TIL**

Pyruvate can impact cytokine production by multiple mechanisms. First, it can promote OXPHOS in CD8 TIL and allow it to support cytokine production as demonstrated by our assay where inhibition of OXPHOS reduced the ability of pyruvate to rescue cytokine production. Second, the consumption of pyruvate in the mitochondria can produce a TCA cycle intermediate oxaloacetate, which has been reported to be serve as a substrate for regeneration of PEP(96). PEP can then be used to drive cytokine production through the maintenance  $Ca^{2+}$ -NFAT signaling(96). Third, pyruvate can be converted to acetyl-Coenzyme A (acetyl-CoA), which have been shown to promote cytokine (IFN $\gamma$ ) production by serving as a substrate for histone acetylation (more specifically by promoting histone H3 at lysine 27 acetylation (H3K27Ac))(67).

The treatment of CD8+ TIL with PEP or pyruvate resulted in a similar level of improved cytokine production in CD8+ TIL, suggesting that in our model system PEP may exert its effect by being converted to pyruvate, rather than by sustaining  $\text{Ca}^{2+}$ -NFAT signaling. Pyruvate has to be converted to acetyl-CoA in the mitochondria in order to support the effector function of T cells through OXPHOS and/or acetyl-CoA-mediated enhancement of histone acetylation and cytokine gene transcription(65, 67). Therefore, we hypothesize that pyruvate treatment improves cytokine production in CD8+ TIL by increasing the amount of acetyl-CoA in the cells to support both OXPHOS and histone acetylation. Whether pyruvate treatment increases acetyl-CoA concentration in the CD8+ TIL could be tested by measuring acetyl-CoA after *ex vivo* treatment of the cells with pyruvate. To determine whether pyruvate improves cytokine production via histone acetylation, we could perform cytokine measurement after treating of CD8+ TIL with pyruvate in the presence or absence of histone acetyltransferases (HATs) inhibitors. The inhibitors should reduce or abrogate pyruvate-mediated improvement of cytokine production if pyruvate acts through modulation of histone acetylation.

### **Pyruvate availability and mitochondrial alterations as mediators of OXPHOS deficiency in CD8+ TIL**

In addition of their glycolytic deficiency, CD8+ TIL also had reduced mitochondrial metabolic activity compared to functional effector T cells. Mitochondrial metabolism

can support CD8+ TIL function as demonstrated by our studies, which showed that the ability of exogenous pyruvate to enhance the effector function of these cells is partially dependent of OXPHOS. Other groups have also demonstrated that promoting mitochondria biogenesis in CD8+ TIL can enhance their antitumor activity(24).

Therefore, further understanding of the basis for the mitochondrial metabolic deficiency of CD8+ TIL is of interest to tumor immunology. We identified two mechanisms by which the mitochondrial metabolism was restrained in CD8+ TIL. First, the impairment of enolase activity hinders efficient production of pyruvate, which fuels mitochondrial metabolism. In support for this conclusion, we showed that provision of exogenous pyruvate could significantly improve OXPHOS capability of CD8+ TIL. Secondly, we showed that CD8+ TIL have reduced mitochondrial content and membrane potential, both of which could also directly impact the level of OXPHOS these cells could engage. Consistent with this, exogenous pyruvate only partially rescued OXPHOS in CD8+ TIL. Furthermore, CD8+ TIL retained low mitochondrial metabolism while exposed to nutrients such as glutamine, which can directly feed into the mitochondria and reduce the effects of inefficient glycolysis. Hence, mitochondrial alterations may be a major barrier for the engagement of OXPHOS in CD8+ TIL.

The activation of T cells increases the mitochondrial mass by inducing mitochondrial biogenesis (176). Scharping et al reported that chronic stimulation represses mitochondria biogenesis and results in loss of mitochondrial mass in T cells in the TME(24). These authors determined that chronic antigen exposure in the TME leads to

Akt-mediated inhibition of the expression of PGC1a, which regulates mitochondrial biogenesis. We found that the Akt is active in our CD8+ TIL. Therefore, a similar mechanism of repression might be responsible for the reduced mitochondrial content of CD8+ TIL we found in our model system, although we did not observe the level of mitochondrial loss Scharping et al have reported. This could be investigated by assessing the Akt-mediated phosphorylation Foxo1, which has been reported to inhibit PGC1 $\alpha$  expression(24), and the expression PGC1 $\alpha$  itself in the CD8+ TIL.

Although the decrease in mitochondrial mass of CD8+ TIL could contribute to their low OXPHOS, the functional impairment of their existing mitochondria might play a bigger role in limiting the activity of this metabolic program. In support of this conclusion, we observed significantly lower membrane potential in CD8+ TIL than acute Teff even when we normalized the difference in mitochondrial mass. Disruption of mitochondrial membrane potential without loss of mitochondrial mass has also been reported in CD8+ TIL that infiltrate the human renal cancer(23). One of the key players in the establishment of mitochondrial membrane potential is NADH, which is produced by the activity of TCA cycle and donate electrons to the electron transport chain (ETC) to drive the electrochemical gradient across the mitochondrial inner membrane(38). Our metabolomics analysis has shown that CD8+ TIL have limited TCA cycle activity. Therefore, one of the potential causes of low mitochondrial membrane potential in CD8+ TIL could be NADH deficiency. This could be tested by performing

spectrophotometric-based quantification of NADH and NAD<sup>+</sup>(148) in lysate of FACS-sorted CD8<sup>+</sup> TIL and acute Teff. If this experiment shows significantly lower NADH and higher NAD<sup>+</sup>/NADH ratio in the CD8<sup>+</sup> TIL than Teff, it may suggest that there is inefficient conversion of NAD<sup>+</sup> to NADH by the TCA cycle, thus limiting the mitochondrial membrane potential. Although such data could also be interpreted as enhanced oxidation of NADH to NAD<sup>+</sup> by the ETC, this is unlikely to happen in CD8<sup>+</sup> TIL as it would be more consistent with high rather low membrane potential. Nevertheless, whether ETC depletes NADH could be tested by blocking the conversion of NADH to NAD<sup>+</sup> in the mitochondria by using ETC inhibitors(148) and measuring NADH accumulation.

Other potential mechanisms that could be responsible for the reduced membrane potential of CD8<sup>+</sup> TIL are the expression and organization of ETC proteins. The expression of the different complexes of the ETC proteins could be assessed by western blot(148). However, even if the ETC proteins are well expressed in CD8<sup>+</sup> TIL, the organization of the mitochondria cristae that they are localized to could have significant impact on the ETC activity(177). Tightly packed cristae have been associated with enhanced ETC activity, while loosely packed cristae have been linked to inefficient electron transfer through the ETC(177). The morphology of cristae in CD8<sup>+</sup> TIL and acute Teff could be assessed by using electron microscopy (EM) (177, 178). We expect that the CD8<sup>+</sup> TIL mitochondrial cristae would be looser than that of the acute Teff based on the

higher OXPHOS in Teff than CD8+ TIL and the association of tight cristae with higher OXPHOS(177, 178).

There may be a link between the loss of mitochondria membrane potential and the impaired enolase activity in CD8+ TIL. Enolase 1 has been reported to bind to the mitochondria and to stabilize mitochondrial membrane in cardiomyocytes(138). Furthermore, enolase 1 has also recently been shown to play a critical role in giving dendritic cells (DC) the mitochondria morphological (tubular and fused shape, and tighten cristae) that has been associated with enhanced OXPHOS(150). The authors presumed that enolase 1 influenced mitochondria morphology via pyruvate production, which might be one of the mechanisms by which our pyruvate treatment increased OXPHOS in CD8+ TIL. This could be directly tested by performing mitochondrial morphology analysis after *ex vivo* treatment of CD8+ TIL with pyruvate. Moreover, if the studies of mitochondrial morphology of CD8+ TIL outlined in the above paragraph determine any alteration, we could assess if it is mediated by relocalization of enolase 1 to the mitochondria. The localization of enolase 1 to the mitochondrial surface could be assessed by confocal/electron microscopy(138) and subcellular fractionation. It is unclear whether the enzymatic activity of enolase 1 is necessary for its localization to the mitochondria. Therefore, it is possible that enzymatically impaired enolase 1 in CD8+ TIL has the capacity to bind to the mitochondria, but fail to support their morphology (due to the lack of activity). Hence, it may be necessary to also conduct the above

experiment in the Teff exposed to enolase inhibitors or cells overexpressing catalytically inactive or active enolase 1. Together, these studies might expand our understanding of the mechanisms that regulate mitochondrial metabolism in CD8+ TIL, and provide some insight into the role of enolase in such processes.

### **Contribution of this work to the understanding of CD8+ TIL metabolism**

There is a growing interest in understanding the detail of how cellular metabolism fuels T cell effector function and how its dysregulation may contribute to the dysfunction of TIL. Studies have described multiple mechanisms by which the glycolytic metabolism promote effector function of T cells. For example, when the glycolytic enzyme GAPDH is not involved in the glycolysis pathway, it has been shown to bind to the 3' untranslated region (3'UTR) of IFN $\gamma$  mRNA and to inhibit its translation(84). As a result, the elevated glycolytic activity of effector T cells is thought to prevent GAPDH from inhibiting cytokine production by keeping it more involved in glycolysis. The glycolytic metabolism has also been shown to support the production of effector cytokines by a 3'UTR-independent mechanism that involves increased production acetyl-CoA, which serve as a substrate for acetylation of histone H3 at the lysine 9 residue (H3K27Ac) that have been reported to enhance IFN $\gamma$  production(67). Glucose-derived pyruvate is one of the major source of acetyl-CoA in cells(65). Therefore, the pyruvate deficiency we observed in CD8+ TIL may contribute to impaired cytokine production by impacting histone

acetylation. On the other hand, it is unlikely that the cytokine production is impacted by GAPDH in CD8+ TIL since the glycolytic steps upstream of enolase 1 are active (as demonstrated by our metabolomics analysis) and are expected to keep GAPDH engaged in its enzymatic role.

Another mechanism by which the glycolytic metabolism promote effector function of T cells is through production of phosphoenolpyruvate (PEP). PEP has been shown to mediate the activation and effector function of T cells by sustaining the TCR-mediated activation of Ca<sup>2+</sup>-NFAT signaling(96). Augmentation of PEP production via overexpression an enzyme (phosphoenolpyruvate carboxykinase 1) that produces PEP from a TCA cycle intermediate oxaloacetate significantly improved the antitumor activity CD4+ TIL and CD8+ T cells upon adoptive transfer of the cells into tumor-bearing mice(96). While this observation suggested that increasing PEP production in TIL can enhance their antitumor activity, whether endogenous TIL had PEP deficiency was unknown. Our work has demonstrated that the endogenous CD8+ TIL do have PEP deficiency. More importantly, we discovered that the PEP deficiency was mediated by impaired enolase activity in CD8+ TIL.

While other groups have described that competition for glucose between tumor cells and T cells as a mediator of glycolytic deficiency of CD8+ TIL(21, 96), our work identified

impaired enolase activity as a cell-intrinsic mechanism that attenuates glycolysis in these cells. Consistently, CD8<sup>+</sup> TIL had attenuated glycolytic activity even though we assessed their metabolism after FACS-purifying them to remove a potential role of competition for glucose and also provided the cells access physiological (10 mM) amount of glucose reported in the spleen of mouse. Interestingly, in the paper that described the competition-model, the glycolytically deficient CD8<sup>+</sup> TIL retained their attenuated glycolysis in the presence of supra-physiological amount of glucose during *ex vivo* analysis(21). We interpreted that data to mean that glycolysis was repressed by cell-intrinsic mechanism although the authors did not reach the same conclusion.

Whether competition for glucose in the tumor microenvironment is involved in initiating or establishing the impairment of enolase activity in CD8<sup>+</sup> TIL is currently unknown. Our current data indicate that checkpoint blocking antibodies enhance the recruitment of enolase-active T cells, suggesting that loss of enolase function likely happens in the TME.

Immune checkpoint is another mechanism that have been reported to inhibit glycolytic metabolism, but the molecular detail of this mechanism is poorly understood. *In vitro* studies have shown that PD-1 signal inhibits glycolysis in effector T cells(74). Treatment of tumor-bearing mice with anti-PD-1 and/or anti-CTLA-4 have been reported to improve glycolytic metabolism in CD8<sup>+</sup> TIL(21). In this work, we showed that one of the mechanisms by which checkpoint molecule suppress glycolytic metabolism is through regulation of enolase activity. This was demonstrated by the ability of checkpoint

inhibitors (anti-PD-1, anti-CTLA-4, and anti-TIM-3) to improve of enolase activity in CD8+ TIL. As such our work indicates that enolase is a novel target of checkpoint molecules and that approaches that can improve enolase activity could enhance cancer immunotherapy.

Another area where our work contributes to further the understanding of TIL metabolism is through shedding some light on how mitochondria metabolism is regulated in CD8+ TIL. Previous studies have reported loss of mitochondria mass<sup>(111)</sup> and/or membrane potential<sup>(23, 111)</sup> in CD8 TIL. However, whether mitochondria dysfunction of these cells is linked to their glycolytic deficiency is not understood. Our work has confirmed mitochondrial dysfunction in CD8+ TIL that infiltrated the murine and human melanoma tumors. More importantly, we described that impaired enolase activity contributes to the mitochondrial dysfunction of CD8+ TIL by limiting the availability of pyruvate that could fuel mitochondrial metabolism. In support of this, treatment of CD8+ TIL *ex vivo* with pyruvate partially rescued their OXPHOS capability. Therefore, mitochondrial dysfunction is at least partly linked to glycolytic inefficiency in CD8+ TIL.

Lastly, this work (in collaboration with Hsu lab) developed a chemical probe that can be used for a robust analysis of the expression of active enolase in live cell at single cell

level. This reagent offers a powerful approach that can be taken to further investigate the regulation of enolase activity including in samples that limited in availability such human TIL and early stage murine tumors. Currently there is no assay with sufficient sensitivity to allow study glycolysis in a low number of cells. The sensitivity the enolase probe may also facilitate analysis of the potential use of enolase as a biomarker of TIL metabolism and function.

### **Translational/clinical relevance of manipulation of enolase activity in T cells**

Our work has identified the regulation of metabolic enzyme activity as novel mechanism by which T cell function could be controlled. Modulation of T cell metabolism has strong translational significance and potential clinical utility. Its inhibition offers an approach by which pathologic T cell responses could be suppressed in diseases such as autoimmunity and graft-versus-host disease(72, 92). Enhancing T cell metabolism, on the other hand, has the potential to promote immune response to chronic viral infections and cancers(21, 22, 24, 83). Therefore, identification of novel targets that can be manipulated to positively or negative regulate T cells and other actors in innate and adaptive immunity is of interest to field of immunology. Enolase activity may offer such a target as our work demonstrated that its inhibition suppresses the function of T cells while bypassing its inactivity improves the metabolic and effector function of CD8+ TIL. Importantly, manipulation of enolase activity provides an approach by which both the glycolytic and oxidative metabolism can be influenced.

There are multiple ways by which this work can contribute to the advancement of the translational aspects of T cell metabolism. First, the development of interventions that could prevent the loss of function or restore the activity of enolase may be considered as approaches to augment the efficacy of cancer immunotherapy. This has high potential clinical utility since the TIL that infiltrate human melanoma also exhibit impaired enolase activity. Second, bypassing of enolase inactivity with pyruvate could be useful for the *ex vivo* maintenance of TIL and the expansion CAR-T cells used in adoptive cell therapy. Third, the enolase reporter we developed may be clinically useful as a biomarker of TIL metabolism and function. This reporter may also be used for analysis of enolase 1 in other cells types including cancer cells, where this enzyme has been investigated as a diagnostic marker(165, 166).

In summary, this body of work has demonstrated that metabolic dysfunction is a major contributor to the functional impairment of CD8+ TIL. We have shown that the metabolism of glucose, which is critical for the generation and function of effector T cells, is repressed by impaired enolase activity in CD8+ TIL. In addition to glycolysis, the impaired enolase activity also contributed to the loss of OXPHOS in these cells by limiting pyruvate availability. Enolase activity is post-translationally regulated by mechanism that has yet to be fully defined. Our studies have shown that checkpoint

signals played some role in controlling enolase activity in CD8+TIL, and that post-translational modifications of enolase may be the mechanistic basis for regulating its enzymatic activity. Further understanding of how enolase activity is regulated in T cells could provide a foundation for developing interventions that could activate this enzyme and promote the metabolic and effector function of CD8+ TIL, or that might be used to inhibit enolase activity to suppress the pathologic T cells function.

## References

1. N. Rezaei, M. Hedayat, A. Aghamohammadi, K. E. Nichols, Primary immunodeficiency diseases associated with increased susceptibility to viral infections and malignancies., *J. Allergy Clin. Immunol.* **127**, 1329-41.e2; quiz 1342–3 (2011).
2. J. F. Buell, T. G. Gross, E. S. Woodle, Malignancy after Transplantation, *Transplantation* **80**, S254–S264 (2005).
3. D. H. Kaplan, V. Shankaran, a S. Dighe, E. Stockert, M. Aguet, L. J. Old, R. D. Schreiber, Demonstration of an interferon gamma-dependent tumor surveillance system in immunocompetent mice., *Proc. Natl. Acad. Sci. U. S. A.* **95**, 7556–61 (1998).
4. V. Shankaran, H. Ikeda, a T. Bruce, J. M. White, P. E. Swanson, L. J. Old, R. D. Schreiber, IFNgamma and lymphocytes prevent primary tumour development and shape tumour immunogenicity., *Nature* **410**, 1107–11 (2001).
5. C. M. Koebel, W. Vermi, J. B. Swann, N. Zerafa, S. J. Rodig, L. J. Old, M. J. Smyth, R. D. Schreiber, Adaptive immunity maintains occult cancer in an equilibrium state., *Nature* **450**, 903–7 (2007).
6. T. Boon, P. G. Coulie, B. J. Van den Eynde, P. van der Bruggen, Human T cell responses against melanoma., *Annu. Rev. Immunol.* **24**, 175–208 (2006).
7. I. S. van Houdt, B. J. R. Sluijter, L. M. Moesbergen, W. M. Vos, T. D. de Gruijl, B. G. Molenkamp, A. J. M. van den Eertwegh, E. Hooijberg, P. A. M. van Leeuwen, C. J. L. M.

Meijer, J. J. Oudejans, Favorable outcome in clinically stage II melanoma patients is associated with the presence of activated tumor infiltrating T-lymphocytes and preserved MHC class I antigen expression, *Int. J. Cancer* **123**, 609–615 (2008).

8. C. G. Clemente, M. C. Mihm, R. Bufalino, S. Zurrida, P. Collini, N. Cascinelli, Prognostic value of tumor infiltrating lymphocytes in the vertical growth phase of primary cutaneous melanoma., *Cancer* **77**, 1303–10 (1996).

9. E. Sato, S. H. Olson, J. Ahn, B. Bundy, H. Nishikawa, F. Qian, A. A. Jungbluth, D. Frosina, S. Gnjjatic, C. Ambrosone, J. Kepner, T. Odunsi, G. Ritter, S. Lele, Y.-T. Chen, H. Ohtani, L. J. Old, K. Odunsi, Intraepithelial CD8+ tumor-infiltrating lymphocytes and a high CD8+/regulatory T cell ratio are associated with favorable prognosis in ovarian cancer, *Proc. Natl. Acad. Sci.* **102**, 18538–18543 (2005).

10. L. Zhang, J. R. Conejo-Garcia, D. Katsaros, P. a Gimotty, M. Massobrio, G. Regnani, A. Makrigiannakis, H. Gray, K. Schlienger, M. N. Liebman, S. C. Rubin, G. Coukos, Intratumoral T Cells, Recurrence, and Survival in Epithelial Ovarian Cancer, *N. Engl. J. Med.* **348**, 203–213 (2003).

11. F. Pagès, A. Berger, M. Camus, F. Sanchez-Cabo, A. Costes, R. Molidor, B. Mlecnik, A. Kirilovsky, M. Nilsson, D. Damotte, T. Meatchi, P. Bruneval, P.-H. Cugnenc, Z. Trajanoski, W.-H. Fridman, J. Galon, Effector memory T cells, early metastasis, and survival in colorectal cancer., *N. Engl. J. Med.* **353**, 2654–66 (2005).

12. Y. Naito, K. Saito, K. Shiiba, A. Ohuchi, K. Saigenji, H. Nagura, H. Ohtani, CD8+ T cells

infiltrated within cancer cell nests as a prognostic factor in human colorectal cancer., *Cancer Res.* **58**, 3491–4 (1998).

13. G. Wieërs, N. Demotte, D. Godelaine, P. Van der Bruggen, Immune Suppression in Tumors as a Surmountable Obstacle to Clinical Efficacy of Cancer Vaccines, *Cancers (Basel)*. **3**, 2904–2954 (2011).

14. D. S. Chen, I. Mellman, Oncology Meets Immunology: The Cancer-Immunity Cycle, *Immunity* **39**, 1–10 (2013).

15. J. Crespo, H. Sun, T. H. Welling, Z. Tian, W. Zou, T cell anergy, exhaustion, senescence, and stemness in the tumor microenvironment., *Curr. Opin. Immunol.* **25**, 214–21 (2013).

16. M. Ahmadzadeh, L. a Johnson, B. Heemskerk, J. R. Wunderlich, M. E. Dudley, D. E. White, S. a Rosenberg, Tumor antigen-specific CD8 T cells infiltrating the tumor express high levels of PD-1 and are functionally impaired., *Blood* **114**, 1537–44 (2009).

17. T. J. Stewart, M. J. Smyth, Improving cancer immunotherapy by targeting tumor-induced immune suppression, *Cancer Metastasis Rev.* **30**, 125–140 (2011).

18. T. L. Whiteside, What are regulatory T cells (Treg) regulating in cancer and why?, *Semin. Cancer Biol.* **22**, 327–334 (2012).

19. S. Pilon-Thomas, K. N. Kodumudi, A. E. El-Kenawi, S. Russell, A. M. Weber, K. Luddy, M. Damaghi, J. W. Wojtkowiak, J. J. Mul??, A. Ibrahim-Hashim, R. J. Gillies,

Neutralization of tumor acidity improves antitumor responses to immunotherapy, *Cancer Res.* **76**, 1381–1390 (2016).

20. N. E. Scharping, A. V. Menk, R. D. Whetstone, X. Zeng, G. M. Delgoffe, Efficacy of PD-1 Blockade Is Potentiated by Metformin-Induced Reduction of Tumor Hypoxia, *Cancer Immunol. Res.* **5**, 9–16 (2017).

21. C.-H. Chang, J. Qiu, D. O’Sullivan, M. D. Buck, T. Noguchi, J. D. Curtis, Q. Chen, M. Gindin, M. M. Gubin, G. J. W. van der Windt, E. Tonc, R. D. Schreiber, E. J. Pearce, E. L. Pearce, Metabolic Competition in the Tumor Microenvironment Is a Driver of Cancer Progression, *Cell* **162**, 1229–1241 (2015).

22. P.-C. Ho, J. D. Bihuniak, A. N. Macintyre, M. Staron, X. Liu, R. Amezcua, Y.-C. Tsui, G. Cui, G. Micevic, J. C. Perales, S. H. Kleinstein, E. D. Abel, K. L. Insogna, S. Feske, J. W. Locasale, M. W. Bosenberg, J. C. Rathmell, S. M. Kaech, Phosphoenolpyruvate Is a Metabolic Checkpoint of Anti-tumor T Cell Responses, *Cell* **162**, 1217–1228 (2015).

23. P. J. Siska, K. E. Beckermann, F. M. Mason, G. Andrejeva, A. R. Greenplate, A. B. Sendor, Y. J. Chiang, A. L. Corona, L. F. Gemta, B. G. Vincent, R. C. Wang, B. Kim, J. Hong, C. Chen, T. N. Bullock, J. M. Irish, W. K. Rathmell, J. C. Rathmell, Mitochondrial dysregulation and glycolytic insufficiency functionally impair CD8 T cells infiltrating human renal cell carcinoma, *JCI Insight* **2**, 1–13 (2017).

24. N. E. Scharping, A. V. Menk, R. S. Moreci, S. C. Watkins, R. L. Ferris, G. M. Delgoffe  
Correspondence, R. D. Whetstone, R. E. Dadey, G. M. Delgoffe, The Tumor

Microenvironment Represses T Cell Mitochondrial Biogenesis to Drive Intratumoral T Cell Metabolic Insufficiency and Dysfunction, *Immunity* **45**, 374–388 (2016).

25. E. J. Wherry, T cell exhaustion, *Nat. Immunol.* **131**, 492–499 (2011).

26. N. Nakamoto, H. Cho, A. Shaked, K. Olthoff, M. E. Valiga, M. Kaminski, E. Gostick, D. a Price, G. J. Freeman, E. J. Wherry, K.-M. Chang, Synergistic reversal of intrahepatic HCV-specific CD8 T cell exhaustion by combined PD-1/CTLA-4 blockade., *PLoS Pathog.* **5**, e1000313 (2009).

27. P. a Prieto, J. C. Yang, R. M. Sherry, M. S. Hughes, U. S. Kammula, D. E. White, C. L. Levy, S. a Rosenberg, G. Q. Phan, CTLA-4 blockade with ipilimumab: long-term follow-up of 177 patients with metastatic melanoma., *Clin. Cancer Res.* **18**, 2039–47 (2012).

28. O. Hamid, C. Robert, A. Daud, F. S. Hodi, W.-J. Hwu, R. Kefford, J. D. Wolchok, P. Hersey, R. W. Joseph, J. S. Weber, R. Dronca, T. C. Gangadhar, A. Patnaik, H. Zarour, A. M. Joshua, K. Gergich, J. Elassaiss-Schaap, A. Algazi, C. Mateus, P. Boasberg, P. C. Tumeah, B. Chmielowski, S. W. Ebbinghaus, X. N. Li, S. P. Kang, A. Ribas, Safety and Tumor Responses with LAMBROLIZUMAB (Anti-PD-1) in Melanoma, *N. Engl. J. Med.* **369**, 134–144 (2013).

29. S. L. Topalian, F. S. Hodi, J. R. Brahmer, S. N. Gettinger, D. C. Smith, D. F. McDermott, J. D. Powderly, R. D. Carvajal, J. A. Sosman, M. B. Atkins, P. D. Leming, D. R. Spigel, S. J. Antonia, L. Horn, C. G. Drake, D. M. Pardoll, L. Chen, W. H. Sharfman, R. A. Anders, J. M. Taube, T. L. McMiller, H. Xu, A. J. Korman, M. Jure-Kunkel, S. Agrawal, D. McDonald, G.

- D. Kolia, A. Gupta, J. M. Wigginton, M. Sznol, Safety, Activity, and Immune Correlates of Anti-PD-1 Antibody in Cancer, *N. Engl. J. Med.* **366**, 2443–2454 (2012).
30. J. D. Wolchok, B. Neyns, G. Linette, S. Negrier, J. Lutzky, L. Thomas, W. Waterfield, D. Schadendorf, M. Smylie, T. Guthrie, J.-J. Grob, J. Chesney, K. Chin, K. Chen, A. Hoos, S. J. O'Day, C. Lebbé, Ipilimumab monotherapy in patients with pretreated advanced melanoma: a randomised, double-blind, multicentre, phase 2, dose-ranging study, *Lancet Oncol.* **11**, 155–164 (2010).
31. J. D. Wolchok, H. Kluger, M. K. Callahan, M. a Postow, N. a Rizvi, A. M. Lesokhin, N. H. Segal, C. E. Ariyan, R.-A. Gordon, K. Reed, M. M. Burke, A. Caldwell, S. a Kronenberg, B. U. Agunwamba, X. Zhang, I. Lowy, H. D. Inzunza, W. Feely, C. E. Horak, Q. Hong, A. J. Korman, J. M. Wigginton, A. Gupta, M. Sznol, Nivolumab plus Ipilimumab in Advanced Melanoma, *N. Engl. J. Med.* **369**, 122–133 (2013).
32. R. Newton, B. Priyadharshini, L. A. Turka, Immunometabolism of regulatory T cells, *Nat. Immunol.* **17**, 618–625 (2016).
33. C. Cammann, T cell Metabolism—Regulating Energy, *J. Clin. Cell. Immunol.* **01** (2013), doi:10.4172/2155-9899.S12-012.
34. D. Finlay, D. a Cantrell, Metabolism, migration and memory in cytotoxic T cells., *Nat. Rev. Immunol.* **11**, 109–17 (2011).
35. R. Wang, C. P. Dillon, L. Z. Shi, S. Milasta, R. Carter, D. Finkelstein, L. L. McCormick, P. Fitzgerald, H. Chi, J. Munger, D. R. Green, The Transcription Factor Myc Controls

- Metabolic Reprogramming upon T Lymphocyte Activation, *Immunity* **35**, 871–882 (2011).
36. N. J. MacIver, R. D. Michalek, J. C. Rathmell, Metabolic Regulation of T Lymphocytes, *Annu. Rev. Immunol.* **31**, 259–283 (2013).
37. K. Renner, K. Singer, G. E. Koehl, E. K. Geissler, K. Peter, P. J. Siska, M. Kreutz, Metabolic hallmarks of tumor and immune cells in the tumor microenvironment, *Front. Immunol.* **8**, 1–11 (2017).
38. N. J. Maciver, S. R. Jacobs, H. L. Wieman, J. a Wofford, J. L. Coloff, J. C. Rathmell, Glucose metabolism in lymphocytes is a regulated process with significant effects on immune cell function and survival., *J. Leukoc. Biol.* **84**, 949–957 (2008).
39. I. Kareva, P. Hahnfeldt, The Emerging “Hallmarks” of Metabolic Reprogramming and Immune Evasion: Distinct or Linked?, *Cancer Res.* **73**, 2737–2742 (2013).
40. S. R. Jacobs, C. E. Herman, N. J. MacIver, J. a Wofford, H. L. Wieman, J. J. Hammen, J. C. Rathmell, Glucose Uptake Is Limiting in T Cell Activation and Requires CD28-Mediated Akt-Dependent and Independent Pathways, *J. Immunol.* **180**, 4476–4486 (2008).
41. L. a Sena, S. Li, A. Jairaman, M. Prakriya, T. Ezponda, D. a Hildeman, C.-R. Wang, P. T. Schumacker, J. D. Licht, H. Perlman, P. J. Bryce, N. S. Chandel, Mitochondria are required for antigen-specific T cell activation through reactive oxygen species signaling., *Immunity* **38**, 225–36 (2013).

42. R. Dziurla, T. Gaber, M. Fangradt, M. Hahne, R. Tripmacher, P. Kolar, C. M. Spies, G. R. Burmester, F. Buttgerit, Effects of hypoxia and/or lack of glucose on cellular energy metabolism and cytokine production in stimulated human CD4<sup>+</sup> T lymphocytes, *Immunol. Lett.* **131**, 97–105 (2010).
43. V. a Gerriets, J. C. Rathmell, Metabolic pathways in T cell fate and function, *Trends Immunol.* **33**, 168–173 (2012).
44. A. T. Waickman, J. D. Powell, mTOR, metabolism, and the regulation of T-cell differentiation and function, *Immunol. Rev.* **249**, 43–58 (2012).
45. D. a. Chisolm, A. S. Weinmann, TCR-Signaling Events in Cellular Metabolism and Specialization, *Front. Immunol.* **6**, 10–14 (2015).
46. K. a Frauwirth, J. L. Riley, M. H. Harris, R. V Parry, J. C. Rathmell, D. R. Plas, R. L. Elstrom, C. H. June, C. B. Thompson, The CD28 signaling pathway regulates glucose metabolism., *Immunity* **16**, 769–77 (2002).
47. C. Cammann, A. Rath, U. Reichl, H. Lingel, M. Brunner-Weinzierl, L. Simeoni, B. Schraven, J. A. Lindquist, Early changes in the metabolic profile of activated CD8<sup>+</sup> T cells, *BMC Cell Biol.* **17**, 28 (2016).
48. P. M. Gubser, G. R. Bantug, L. Razik, M. Fischer, S. Dimeloe, G. Hoenger, B. Durovic, A. Jauch, C. Hess, Rapid effector function of memory CD8<sup>+</sup> T cells requires an immediate-early glycolytic switch, *Nat. Immunol.* **14**, 1064–1072 (2013).

49. D. K. Finlay, E. Rosenzweig, L. V Sinclair, C. Feijoo-Carnero, J. L. Hukelmann, J. Rolf, A. Panteleyev, K. Okkenhaug, D. Cantrell, PDK1 regulation of mTOR and hypoxia-inducible factor 1 integrate metabolism and migration of CD8 + T cells, *J. Exp. Med.* **209**, 2441–2453 (2012).
50. A. N. Macintyre, D. Finlay, G. Preston, L. V Sinclair, C. M. Waugh, P. Tamas, C. Feijoo, K. Okkenhaug, D. Cantrell, Protein kinase B controls transcriptional programs that direct cytotoxic T cell fate but is dispensable for T cell metabolism., *Immunity* **34**, 224–36 (2011).
51. C. C. Hudson, M. Liu, G. G. Chiang, D. M. Otterness, D. C. Loomis, F. Kaper, A. J. Giaccia, R. T. Abraham, Regulation of Hypoxia-Inducible Factor 1 Expression and Function by the Mammalian Target of Rapamycin, *Mol. Cell. Biol.* **22**, 7004–7014 (2002).
52. F. O. Nestle, G. Burg, J. Fäh, T. Wrone-Smith, B. J. Nickoloff, Human sunlight-induced basal-cell-carcinoma-associated dendritic cells are deficient in T cell co-stimulatory molecules and are impaired as antigen-presenting cells., *Am. J. Pathol.* **150**, 641–51 (1997).
53. A. Pinzon-Charry, T. Maxwell, J. A. López, Dendritic cell dysfunction in cancer: a mechanism for immunosuppression., *Immunol. Cell Biol.* **83**, 451–61 (2005).
54. P. Chaux, N. Favre, M. Martin, F. Martin, Tumor-infiltrating dendritic cells are defective in their antigen-presenting function and inducible B7 expression in rats., *Int. J. Cancer* **72**, 619–24 (1997).

55. R. V Parry, J. M. Chemnitz, K. A. Frauwirth, A. R. Lanfranco, I. Braunstein, S. V Kobayashi, P. S. Linsley, C. B. Thompson, J. L. Riley, CTLA-4 and PD-1 Receptors Inhibit T-Cell Activation by Distinct Mechanisms †, **25**, 9543–9553 (2005).
56. T. Bopp, H. C. Probst, M. Radsak, E. Schmitt, M. Stassen, H. Schild, S. Tenzer, C. M. Britten, S. Kreiter, M. Diken, H.-G. Rammensee, Eds. Cancer Immunotherapy Meets Oncology, , 21–27 (2014).
57. G. J. Freeman, a J. Long, Y. Iwai, K. Bourque, T. Chernova, H. Nishimura, L. J. Fitz, N. Malenkovich, T. Okazaki, M. C. Byrne, H. F. Horton, L. Fouser, L. Carter, V. Ling, M. R. Bowman, B. M. Carreno, M. Collins, C. R. Wood, T. Honjo, Engagement of the PD-1 immunoinhibitory receptor by a novel B7 family member leads to negative regulation of lymphocyte activation., *J. Exp. Med.* **192**, 1027–34 (2000).
58. N. Orleans, M. Clinic, Blockade of B7-H1 improves myeloid dendritic cell – mediated antitumor immunity, **9**, 5–10 (2003).
59. C. Blank, A. Mackensen, Contribution of the PD-L1/PD-1 pathway to T-cell exhaustion: an update on implications for chronic infections and tumor evasion., *Cancer Immunol. Immunother.* **56**, 739–45 (2007).
60. T. Höfer, O. Krichevsky, G. Altan-Bonnet, Competition for IL-2 between Regulatory and Effector T Cells to Chisel Immune Responses., *Front. Immunol.* **3**, 268 (2012).
61. J. D. Bui, R. Uppaluri, C.-S. Hsieh, R. D. Schreiber, Comparative analysis of regulatory and effector T cells in progressively growing versus rejecting tumors of similar origins.,

*Cancer Res.* **66**, 7301–9 (2006).

62. M. Chehtane, A. R. Khaled, Interleukin-7 mediates glucose utilization in lymphocytes through transcriptional regulation of the hexokinase II gene., *Am. J. Physiol. Cell Physiol.* **298**, C1560-71 (2010).

63. K. Ganeshan, A. Chawla, Metabolic Regulation of Immune Responses, *Annu. Rev. Immunol.* **32**, 609–634 (2014).

64. E. L. Pearce, M. C. Poffenberger, C.-H. Chang, R. G. Jones, Fueling immunity: insights into metabolism and lymphocyte function., *Science* **342**, 1242454 (2013).

65. S. Y. Lunt, M. G. Vander Heiden, Aerobic glycolysis: meeting the metabolic requirements of cell proliferation., *Annu. Rev. Cell Dev. Biol.* **27**, 441–64 (2011).

66. M. G. Vander Heiden, L. C. Cantley, C. B. Thompson, Understanding the Warburg effect: the metabolic requirements of cell proliferation., *Science* **324**, 1029–33 (2009).

67. M. Peng, N. Yin, S. Chhangawala, K. Xu, C. S. Leslie, M. O. Li, Aerobic glycolysis promotes T helper 1 cell differentiation through an epigenetic mechanism, *Science* (80-.). **354**, 481–484 (2016).

68. E. L. Pearce, M. C. Walsh, P. J. Cejas, G. M. Harms, H. Shen, L.-S. Wang, R. G. Jones, Y. Choi, Enhancing CD8 T-cell memory by modulating fatty acid metabolism., *Nature* **460**, 103–7 (2009).

69. C. J. Fox, P. S. Hammerman, C. B. Thompson, Fuel feeds function: energy metabolism

- and the T-cell response., *Nat. Rev. Immunol.* **5**, 844–52 (2005).
70. S. Y. Lunt, M. G. Vander Heiden, Aerobic glycolysis: meeting the metabolic requirements of cell proliferation., *Annu. Rev. Cell Dev. Biol.* **27**, 441–64 (2011).
71. R. G. Jones, C. B. Thompson, Revving the engine: signal transduction fuels T cell activation., *Immunity* **27**, 173–8 (2007).
72. Y. Yin, S.-C. Choi, Z. Xu, D. J. Perry, H. Seay, B. P. Croker, E. S. Sobel, T. M. Brusko, L. Morel, Normalization of CD4 + T cell metabolism reverses lupus, *Sci. Transl. Med.* **7**, 274ra18-274ra18 (2015).
73. K. Renner, A.-L. Geiselhöringer, M. Fante, C. Bruss, S. Färber, G. Schönhammer, K. Peter, K. Singer, R. Andreesen, P. Hoffmann, P. Oefner, W. Herr, M. Kreutz, Metabolic plasticity of human T cells: Preserved cytokine production under glucose deprivation or mitochondrial restriction, but 2-deoxy-glucose affects effector functions, *Eur. J. Immunol.* **45**, 2504–2516 (2015).
74. N. Patsoukis, K. Bardhan, P. Chatterjee, D. Sari, B. Liu, L. N. Bell, E. D. Karoly, G. J. Freeman, V. Petkova, P. Seth, L. Li, V. a. Boussiotis, PD-1 alters T-cell metabolic reprogramming by inhibiting glycolysis and promoting lipolysis and fatty acid oxidation, *Nat. Commun.* **6**, 6692 (2015).
75. E. L. Pearce, E. J. Pearce, Metabolic pathways in immune cell activation and quiescence., *Immunity* **38**, 633–43 (2013).

76. C. Cottet-Rousselle, X. Ronot, X. Leverve, J.-F. Mayol, Cytometric assessment of mitochondria using fluorescent probes., *Cytometry. A* **79**, 405–25 (2011).
77. D. K. Finlay, Regulation of glucose metabolism in T cells: new insight into the role of Phosphoinositide 3-kinases., *Front. Immunol.* **3**, 247 (2012).
78. C. M. Cham, T. F. Gajewski, Glucose availability regulates IFN-gamma production and p70S6 kinase activation in CD8+ effector T cells., *J. Immunol.* **174**, 4670–7 (2005).
79. L. L. Policastro, I. L. Ibañez, C. Notcovich, H. A. Duran, O. L. Podhajcer, The Tumor Microenvironment: Characterization, Redox Considerations, and Novel Approaches for Reactive Oxygen Species-Targeted Gene Therapy, *Antioxid. Redox Signal.* **19**, 854–895 (2013).
80. T. Hitosugi, L. Zhou, S. Elf, J. Fan, H. B. Kang, J. H. Seo, C. Shan, Q. Dai, L. Zhang, J. Xie, T. L. Gu, P. Jin, M. Alečković, G. LeRoy, Y. Kang, J. A. Sudderth, R. J. DeBerardinis, C. H. Luan, G. Z. Chen, S. Muller, D. M. Shin, T. K. Owonikoko, S. Lonial, M. L. Arellano, H. J. Khoury, F. R. Khuri, B. H. Lee, K. Ye, T. J. Boggon, S. Kang, C. He, J. Chen, Phosphoglycerate Mutase 1 Coordinates Glycolysis and Biosynthesis to Promote Tumor Growth, *Cancer Cell* **22**, 585–600 (2012).
81. T. Hitosugi, L. Zhou, S. Elf, J. Fan, H.-B. Kang, J. H. Seo, C. Shan, Q. Dai, L. Zhang, J. Xie, T.-L. Gu, P. Jin, M. Alečković, G. LeRoy, Y. Kang, J. A. Sudderth, R. J. DeBerardinis, C.-H. Luan, G. Z. Chen, S. Muller, D. M. Shin, T. K. Owonikoko, S. Lonial, M. L. Arellano, H. J. Khoury, F. R. Khuri, B. H. Lee, K. Ye, T. J. Boggon, S. Kang, C. He, J. Chen,

Phosphoglycerate Mutase 1 Coordinates Glycolysis and Biosynthesis to Promote Tumor Growth, *Cancer Cell* **22**, 585–600 (2012).

82. J. Blagih, F. Coulombe, E. E. Vincent, F. Dupuy, G. Galicia-Vázquez, E. Yurchenko, T. C. Raissi, G. J. W. van der Windt, B. Viollet, E. L. Pearce, J. Pelletier, C. A. Piccirillo, C. M. Krawczyk, M. Divangahi, R. G. Jones, The Energy Sensor AMPK Regulates T Cell Metabolic Adaptation and Effector Responses In Vivo, *Immunity* **42**, 41–54 (2015).

83. A. L. Doedens, A. T. Phan, M. H. Stradner, J. K. Fujimoto, J. V. Nguyen, E. Yang, R. S. Johnson, A. W. Goldrath, Hypoxia-inducible factors enhance the effector responses of CD8+ T cells to persistent antigen, *Nat. Immunol.* **14**, 1173–1182 (2013).

84. C.-H. Chang, J. D. Curtis, L. B. Maggi, B. Faubert, A. V. Villarino, D. O’Sullivan, S. C.-C. Huang, G. J. W. van der Windt, J. Blagih, J. Qiu, J. D. Weber, E. J. Pearce, R. G. Jones, E. L. Pearce, Posttranscriptional Control of T Cell Effector Function by Aerobic Glycolysis, *Cell* **153**, 1239–1251 (2013).

85. R. F. C. W. Nagy Eszter, Cell Biology and Metabolism : Dehydrogenase Selectively Binds AU-rich RNA in the NAD + -binding Region ( Rossmann Fold ) Eszter Nagy and William F . C . Rigby, (1995).

86. E. Nagy, T. Henics, M. Eckert, a Miseta, R. N. Lightowlers, M. Kellermayer, Identification of the NAD(+)-binding fold of glyceraldehyde-3-phosphate dehydrogenase as a novel RNA-binding domain., *Biochem. Biophys. Res. Commun.* **275**, 253–60 (2000).

87. A. T. Phan, A. L. Doedens, A. Palazon, P. A. Tyrakis, K. P. Cheung, R. S. Johnson, A. W.

Goldrath, Constitutive Glycolytic Metabolism Supports CD8(+) T Cell Effector Memory Differentiation during Viral Infection., *Immunity* **45**, 1024–1037 (2016).

88. Y. Cao, J. C. Rathmell, A. N. Macintyre, M. Platten, Ed. Metabolic Reprogramming towards Aerobic Glycolysis Correlates with Greater Proliferative Ability and Resistance to Metabolic Inhibition in CD8 versus CD4 T Cells, *PLoS One* **9**, e104104 (2014).

89. R. M. Loftus, D. K. Finlay, Immunometabolism: Cellular metabolism turns immune regulator, *J. Biol. Chem.* **291**, 1–10 (2016).

90. M. Sukumar, J. Liu, Y. Ji, M. Subramanian, J. G. Crompton, Z. Yu, R. Roychoudhuri, D. C. Palmer, P. Muranski, E. D. Karoly, R. P. Mohney, C. A. Klebanoff, A. Lal, T. Finkel, N. P. Restifo, L. Gattinoni, Inhibiting glycolytic metabolism enhances CD8+ T cell memory and antitumor function, *J. Clin. Invest.* **123**, 4479–4488 (2013).

91. B. Bengsch, A. L. Johnson, M. Kurachi, P. M. Odorizzi, K. E. Pauken, J. Attanasio, E. Stelekati, L. M. McLane, M. A. Paley, G. M. Delgoffe, E. J. Wherry, Bioenergetic Insufficiencies Due to Metabolic Alterations Regulated by the Inhibitory Receptor PD-1 Are an Early Driver of CD8 + T Cell Exhaustion, *Immunity* **45**, 358–373 (2016).

92. E. Gatza, D. R. Wahl, A. W. Pipari, T. B. Sundberg, P. Reddy, C. Liu, G. D. Glick, J. L. Ferrara, Manipulating the bioenergetics of alloreactive T cells causes their selective apoptosis and arrests graft-versus-host disease., *Sci. Transl. Med.* **3**, 67ra8 (2011).

93. Y. Zheng, G. M. Delgoffe, C. F. Meyer, W. Chan, J. D. Powell, Anergic T cells are metabolically anergic., *J. Immunol.* **183**, 6095–101 (2009).

94. M. L. Hwang, J. R. Lukens, T. N. J. Bullock, Cognate Memory CD4+ T Cells Generated with Dendritic Cell Priming Influence the Expansion, Trafficking, and Differentiation of Secondary CD8+ T Cells and Enhance Tumor Control, *J. Immunol.* **179**, 5829–5838 (2007).
95. E. P. Salerno, W. C. Olson, C. McSkimming, S. Shea, C. L. Slingluff, T cells in the human metastatic melanoma microenvironment express site-specific homing receptors and retention integrins, *Int. J. Cancer* **134**, 563–574 (2014).
96. P.-C. Ho, J. D. Bihuniak, A. N. Macintyre, M. Staron, X. Liu, R. Amezcua, Y.-C. Tsui, G. Cui, G. Micevic, J. C. Perales, S. H. Kleinstein, E. D. Abel, K. L. Insogna, S. Feske, J. W. Locasale, M. W. Bosenberg, J. C. Rathmell, S. M. Kaech, Phosphoenolpyruvate Is a Metabolic Checkpoint of Anti-tumor T Cell Responses, *Cell* **162**, 1217–1228 (2015).
97. S. Sengupta, R. J. Vitale, P. M. Chilton, T. C. Mitchell, Adjuvant induced glucose uptake by activated T cells is not correlated with increased survival., *Adv. Exp. Med. Biol.* **614**, 65–72 (2008).
98. F. L. Byrne, I. K. H. Poon, S. C. Modesitt, J. L. Tomsig, J. D. Y. Chow, M. E. Healy, W. D. Baker, K. A. Atkins, J. M. Lancaster, D. C. Marchion, K. H. Moley, K. S. Ravichandran, J. K. Slack-Davis, K. L. Hoehn, Metabolic vulnerabilities in endometrial cancer, *Cancer Res.* (2014), doi:10.1158/0008-5472.CAN-14-0254.
99. X. Liu, Z. Ser, J. W. Locasale, Development and quantitative evaluation of a high-resolution metabolomics technology, *Anal. Chem.* **86**, 2175–2184 (2014).

100. J. R. Wiśniewski, A. Zougman, N. Nagaraj, M. Mann, Universal sample preparation method for proteome analysis, *Nat. Methods* **6**, 359–362 (2009).
101. C. E. Franks, S. T. Campbell, B. W. Purow, T. E. Harris, K.-L. Hsu, The Ligand Binding Landscape of Diacylglycerol Kinases, *Cell Chem. Biol.* **24**, 870–880.e5 (2017).
102. M. Bern, Y. J. Kil, C. Becker, in *Current Protocols in Bioinformatics*, (John Wiley & Sons, Inc., Hoboken, NJ, USA, 2012).
103. E. L. L. Sonnhammer, S. R. Eddy, R. Durbin, Pfam: A comprehensive database of protein domain families based on seed alignments, *Proteins Struct. Funct. Genet.* **28**, 405–420 (1997).
104. C. Clemente, Prognostic value of tumor infiltrating lymphocytes in the vertical growth phase of primary cutaneous melanoma *Cancer* **77**, 1303–1310 (1996).
105. J. Galon, A. Costes, F. Sanchez-Cabo, A. Kirilovsky, B. Mlecnik, C. Lagorce-Pagès, M. Tosolini, M. Camus, A. Berger, P. Wind, F. Zinzindohoué, P. Bruneval, P.-H. Cugnenc, Z. Trajanoski, W.-H. Fridman, F. Pagès, Type, density, and location of immune cells within human colorectal tumors predict clinical outcome., *Science* **313**, 1960–4 (2006).
106. D. M. Pardoll, The blockade of immune checkpoints in cancer immunotherapy, *Nat. Rev. Cancer* **12**, 252–264 (2012).
107. J. Duraiswamy, G. Freeman, G. Coukos, Replenish the source within: Rescuing tumor-infiltrating lymphocytes by double checkpoint blockade., *Oncoimmunology* **2**,

e25912 (2013).

108. M. Singer, C. Wang, L. Cong, N. D. Marjanovic, M. S. Kowalczyk, H. Zhang, J. Nyman, K. Sakuishi, S. Kurtulus, D. Gennert, J. Xia, J. Y. H. Kwon, J. Nevin, R. H. Herbst, I. Yanai, O. Rozenblatt-Rosen, V. K. Kuchroo, A. Regev, A. C. Anderson, A Distinct Gene Module for Dysfunction Uncoupled from Activation in Tumor-Infiltrating T Cells, *Cell* .

109. N. Chihara, A. Madi, T. Kondo, H. Zhang, N. Acharya, M. Singer, J. Nyman, N. D. Marjanovic, M. S. Kowalczyk, C. Wang, S. Kurtulus, T. Law, Y. Etminan, J. Nevin, C. D. Buckley, P. R. Burkett, J. D. Buenrostro, O. Rozenblatt-Rosen, A. C. Anderson, A. Regev, V. K. Kuchroo, Induction and transcriptional regulation of the co-inhibitory gene module in T cells, *Nature* **558**, 454–459 (2018).

110. K. E. Pauken, E. J. Wherry, Overcoming T cell exhaustion in infection and cancer, *Trends Immunol.* **36**, 1–12 (2015).

111. N. E. Scharping, A. V Menk, R. S. Moreci, R. D. Whetstone, R. E. Dadey, S. C. Watkins, R. L. Ferris, G. M. Delgoffe, The Tumor Microenvironment Represses T Cell Mitochondrial Biogenesis to Drive Intratumoral T Cell Metabolic Insufficiency and Dysfunction., *Immunity* **45**, 374–88 (2016).

112. R. Wang, C. P. Dillon, L. Z. Shi, S. Milasta, R. Carter, D. Finkelstein, L. L. McCormick, P. Fitzgerald, H. Chi, J. Munger, D. R. Green, The Transcription Factor Myc Controls Metabolic Reprogramming upon T Lymphocyte Activation, *Immunity* **35**, 871–882 (2011).

113. C. E. Widjaja, J. G. Olvera, P. J. Metz, A. T. Phan, J. N. Savas, G. de Bruin, Y. Leestemaker, C. R. Berkers, A. de Jong, B. I. Florea, K. Fisch, J. Lopez, S. H. Kim, D. A. Garcia, S. Searles, J. D. Bui, A. N. Chang, J. R. Yates, A. W. Goldrath, H. S. Overkleeft, H. Ovaa, J. T. Chang, Proteasome activity regulates CD8+ T lymphocyte metabolism and fate specification, *J. Clin. Invest.* **127**, 3609–3623 (2017).
114. D. K. Finlay, E. Rosenzweig, L. V Sinclair, C. Feijoo-Carnero, J. L. Hukelmann, J. Rolf, A. A. Panteleyev, K. Okkenhaug, D. A. Cantrell, PDK1 regulation of mTOR and hypoxia-inducible factor 1 integrate metabolism and migration of CD8+ T cells., *J. Exp. Med.* **209**, 2441–53 (2012).
115. C. M. Cham, T. F. Gajewski, Glucose Availability Regulates IFN- Production and p70S6 Kinase Activation in CD8+ Effector T Cells, *J. Immunol.* **174**, 4670–4677 (2005).
116. B. Bengsch, A. L. Johnson, M. Kurachi, P. M. Odorizzi, K. E. Pauken, J. Attanasio, E. Stelekati, L. M. McLane, M. A. Paley, G. M. Delgoffe, E. J. Wherry, Bioenergetic Insufficiencies Due to Metabolic Alterations Regulated by the Inhibitory Receptor PD-1 Are an Early Driver of CD8+T Cell Exhaustion, *Immunity* **45**, 358–373 (2016).
117. D. J. Roberts, N. a Franklin, L. M. Kingeter, H. Yagita, A. L. Tutt, M. J. Glennie, T. N. J. Bullock, Control of established melanoma by CD27 stimulation is associated with enhanced effector function and persistence, and reduced PD-1 expression of tumor infiltrating CD8(+) T cells., *J. Immunother.* **33**, 769–79 (2010).
118. R. D. Michalek, J. C. Rathmell, The metabolic life and times of a T-cell., *Immunol.*

*Rev.* **236**, 190–202 (2010).

119. A. N. Macintyre, V. A. Gerriets, A. G. Nichols, R. D. Michalek, M. C. Rudolph, D. Deoliveira, S. M. Anderson, E. D. Abel, B. J. Chen, L. P. Hale, J. C. Rathmell, The glucose transporter Glut1 is selectively essential for CD4 T cell activation and effector function., *Cell Metab.* **20**, 61–72 (2014).

120. D. K. Finlay, mTORC1 regulates CD8+ T-cell glucose metabolism and function independently of PI3K and PKB., *Biochem. Soc. Trans.* **41**, 681–6 (2013).

121. H. Cho, J. Um, J.-H. Lee, W.-H. Kim, W. S. Kang, S. H. Kim, H.-H. Ha, Y.-C. Kim, Y.-K. Ahn, D.-W. Jung, D. R. Williams, ENOblock, a unique small molecule inhibitor of the non-glycolytic functions of enolase, alleviates the symptoms of type 2 diabetes, *Sci. Rep.* **7**, 44186 (2017).

122. D.-W. Jung, W.-H. Kim, S.-H. Park, J. Lee, J. Kim, D. Su, H.-H. Ha, Y.-T. Chang, D. R. Williams, A Unique Small Molecule Inhibitor of Enolase Clarifies Its Role in Fundamental Biological Processes, *ACS Chem. Biol.* **8**, 1271–1282 (2013).

123. Y. Zhu, L. Chen, CD137 as a biomarker for tumor-reactive T cells: Finding gold in the desert, *Clin. Cancer Res.* **20**, 3–5 (2014).

124. H. D. Nguyen, S. Chatterjee, K. M. K. Haarberg, Y. Wu, D. Bastian, J. Heinrichs, J. Fu, A. Daenthanasanmak, S. Schutt, S. Shrestha, C. Liu, H. Wang, H. Chi, S. Mehrotra, X. Yu, Metabolic reprogramming of alloantigen-activated T cells after hematopoietic cell transplantation, *J. Clin. Invest.* **126**, 1337–1352 (2016).

125. W. C. Hallows, W. Yu, J. M. Denu, Regulation of glycolytic enzyme phosphoglycerate mutase-1 by Sirt1 protein-mediated deacetylation, *J. Biol. Chem.* **287**, 3850–3858 (2012).
126. W. Zhou, M. Capello, C. Fredolini, L. Piemonti, L. A. Liotta, F. Novelli, E. F. Petricoin, Mass Spectrometry Analysis of the Post-Translational Modifications of  $\alpha$ -Enolase from Pancreatic Ductal Adenocarcinoma Cells, *J. Proteome Res.* **9**, 2929–2936 (2010).
127. H. Ji, J. Wang, J. Guo, Y. Li, S. Lian, W. Guo, H. Yang, F. Kong, L. Zhen, L. Guo, Y. Liu, Progress in the biological function of alpha-enolase, *Anim. Nutr.* **2**, 12–17 (2016).
128. S. Gao, H. Li, Y. Cai, J. Ye, Z. Liu, J. Lu, X. Huang, X. Feng, H. Gao, S. Chen, M. Li, P. Liu, Mitochondrial binding of  $\alpha$ -enolase stabilizes mitochondrial membrane: Its role in doxorubicin-induced cardiomyocyte apoptosis, *Arch. Biochem. Biophys.* **542**, 46–55 (2014).
129. M. Capello, S. Ferri-Borgogno, P. Cappello, F. Novelli,  $\alpha$ -enolase: a promising therapeutic and diagnostic tumor target, *FEBS J.* **278**, 1064–1074 (2011).
130. A. Subramanian, D. M. Miller, Structural analysis of alpha-enolase. Mapping the functional domains involved in down-regulation of the c-myc protooncogene., *J. Biol. Chem.* **275**, 5958–65 (2000).
131. W. Zhou, M. Capello, C. Fredolini, L. Piemonti, L. a Liotta, F. Novelli, E. F. Petricoin, Mass spectrometry analysis of the post-translational modifications of alpha-enolase from pancreatic ductal adenocarcinoma cells., *J. Proteome Res.* **9**, 2929–2936 (2010).

132. D. O'Sullivan, G. J. W. van der Windt, S. C.-C. Huang, J. D. Curtis, C.-H. Chang, M. D. Buck, J. Qiu, A. M. Smith, W. Y. Lam, L. M. DiPlato, F.-F. Hsu, M. J. Birnbaum, E. J. Pearce, E. L. Pearce, Memory CD8(+) T Cells Use Cell-Intrinsic Lipolysis to Support the Metabolic Programming Necessary for Development., *Immunity* , 1–14 (2014).
133. B. Chaigne-Delalande, F.-Y. Li, G. M. O'Connor, M. J. Lukacs, P. Jiang, L. Zheng, A. Shatzer, M. Biancalana, S. Pittaluga, H. F. Matthews, T. J. Jancel, J. J. Bleesing, R. A. Marsh, T. W. Kuijpers, K. E. Nichols, C. L. Lucas, S. Nagpal, H. Mehmet, H. C. Su, J. I. Cohen, G. Uzel, M. J. Lenardo, Mg<sup>2+</sup> Regulates Cytotoxic Functions of NK and CD8 T Cells in Chronic EBV Infection Through NKG2D, *Science (80-. )*. **341**, 186–191 (2013).
134. S. Zhao, W. Xu, W. Jiang, W. Yu, Y. Lin, T. Zhang, J. Yao, L. Zhou, Y. Zeng, H. Li, Y. Li, J. Shi, W. An, S. M. Hancock, F. He, L. Qin, J. Chin, P. Yang, X. Chen, Q. Lei, Y. Xiong, K.-L. Guan, Regulation of Cellular Metabolism by Protein Lysine Acetylation, *Science (80-. )*. **327**, 1000–1004 (2010).
135. B. Schwer, J. Bunkenborg, R. O. Verdin, J. S. Andersen, E. Verdin, Reversible lysine acetylation controls the activity of the mitochondrial enzyme acetyl-CoA synthetase 2, *Proc. Natl. Acad. Sci.* **103**, 10224–10229 (2006).
136. N. Satani, Y. H. Lin, N. Hammoudi, S. Raghavan, D. K. Georgiou, F. L. Muller, ENOblock does not inhibit the activity of the glycolytic enzyme enolase, *PLoS One* **11**, 1–10 (2016).
137. M. Principe, P. Ceruti, N. Shih, M. S. Chattaragada, S. Rolla, L. Conti, M. Bestagno, L.

Zentilin, S.-H. Yang, P. Migliorini, P. Cappello, O. Burrone, F. Novelli, Targeting of surface alpha-enolase inhibits the invasiveness of pancreatic cancer cells, *Oncotarget* **6**, 11098–113 (2015).

138. S. Gao, H. Li, Y. Cai, J. Ye, Z. Liu, J. Lu, X. Huang, X. Feng, H. Gao, S. Chen, M. Li, P. Liu, Mitochondrial binding of  $\alpha$ -enolase stabilizes mitochondrial membrane: Its role in doxorubicin-induced cardiomyocyte apoptosis, *Arch. Biochem. Biophys.* **542**, 46–55 (2014).

139. A. D. D'Souza, N. Parikh, S. M. Kaech, G. S. Shadel, Convergence of multiple signaling pathways is required to coordinately up-regulate mtDNA and mitochondrial biogenesis during T cell activation, *Mitochondrion* **7**, 374–385 (2007).

140. G. J. W. Van Der Windt, D. O. Sullivan, B. Everts, S. C. Huang, M. D. Buck, J. D. Curtis, C. Chang, A. M. Smith, T. Ai, B. Faubert, R. G. Jones, E. J. Pearce, E. L. Pearce, CD8 memory T cells have a bioenergetic advantage that underlies their rapid recall ability, (2013), doi:10.1073/pnas.1221740110/-  
[/DCSupplemental.www.pnas.org/cgi/doi/10.1073/pnas.1221740110](http://DCSupplemental.www.pnas.org/cgi/doi/10.1073/pnas.1221740110).

141. C. A. Byersdorfer, V. Tkachev, A. W. Opipari, S. Goodell, J. Swanson, S. Sandquist, G. D. Glick, J. L. M. Ferrara, Effector T cells require fatty acid metabolism during murine graft-versus-host disease, *Blood* **122**, 3230–3237 (2013).

142. D. Wahl, B. Petersen, R. Warner, B. Richardson, G. Glick, A. Opipari, Characterization of the metabolic phenotype of chronically activated lymphocytes,

*Lupus* **19**, 1492–1501 (2010).

143. R. M. Loftus, D. K. Finlay, Immunometabolism: Cellular Metabolism Turns Immune Regulator, *J. Biol. Chem.* **291**, 1–10 (2016).

144. D. L. Herber, W. Cao, Y. Nefedova, S. V. Novitskiy, S. Nagaraj, V. A. Tyurin, A. Corzo, H. I. Cho, E. Celis, B. Lennox, S. C. Knight, T. Padhya, T. V. McCaffrey, J. C. McCaffrey, S. Antonia, M. Fishman, R. L. Ferris, V. E. Kagan, D. I. Gabrilovich, Lipid accumulation and dendritic cell dysfunction in cancer, *Nat. Med.* **16**, 880–886 (2010).

145. D. O’Sullivan, G. J. W. van der Windt, S. C.-C. Huang, J. D. Curtis, C.-H. Chang, M. D. Buck, J. Qiu, A. M. Smith, W. Y. Lam, L. M. DiPlato, F.-F. Hsu, M. J. Birnbaum, E. J. Pearce, E. L. Pearce, Memory CD8(+) T Cells Use Cell-Intrinsic Lipolysis to Support the Metabolic Programming Necessary for Development., *Immunity* **41**, 75–88 (2014).

146. L. A. J. O’Neill, R. J. Kishton, J. Rathmell, A guide to immunometabolism for immunologists, *Nat. Rev. Immunol.* **16**, 553–565 (2016).

147. J. Lee, M. C. Walsh, K. L. Hoehn, D. E. James, E. J. Wherry, Y. Choi, Regulator of Fatty Acid Metabolism, Acetyl Coenzyme A Carboxylase 1, Controls T Cell Immunity, *J. Immunol.* **192**, 3190–3199 (2014).

148. G. J. W. van der Windt, B. Everts, C.-H. Chang, J. D. Curtis, T. C. Freitas, E. Amiel, E. J. Pearce, E. L. Pearce, Mitochondrial Respiratory Capacity Is a Critical Regulator of CD8+ T Cell Memory Development, *Immunity* **36**, 68–78 (2012).

149. L. Almeida, M. Lochner, L. Berod, T. Sparwasser, Metabolic pathways in T cell activation and lineage differentiation, *Semin. Immunol.* **28**, 514–524 (2016).
150. K. Ryans, Y. Omosun, D. N. McKeithen, T. Simoneaux, C. C. Mills, N. Bowen, F. O. Eko, C. M. Black, J. U. Igietseme, Q. He, The immunoregulatory role of alpha enolase in dendritic cell function during Chlamydia infection, *BMC Immunol.* **18**, 27 (2017).
151. O. Warburg, On the Origin of Cancer Cells, *Science (80- )*. **123**, 309–314 (1956).
152. G. Andrejeva, J. C. Rathmell, Similarities and Distinctions of Cancer and Immune Metabolism in Inflammation and Tumors, *Cell Metab.* **26**, 49–70 (2017).
153. B. Bengsch, A. L. Johnson, M. Kurachi, P. M. Odorizzi, K. E. Pauken, J. Attanasio, E. Stelekati, L. M. McLane, M. A. Paley, G. M. Delgoffe, E. J. Wherry, Bioenergetic Insufficiencies Due to Metabolic Alterations Regulated by the Inhibitory Receptor PD-1 Are an Early Driver of CD8 + T Cell Exhaustion, *Immunity* **45**, 358–373 (2016).
154. K. S. Kim, N. Jacob, W. Stohl, In vitro and in vivo T cell oligoclonality following chronic stimulation with staphylococcal superantigens, *Clin. Immunol.* **108**, 182–189 (2003).
155. D. Rotili, S. Tomassi, M. Conte, R. Benedetti, M. Tortorici, G. Ciossani, S. Valente, B. Marrocco, D. Labella, E. Novellino, A. Mattevi, L. Altucci, A. Tumber, C. Yapp, O. N. F. King, R. J. Hopkinson, A. Kawamura, C. J. Schofield, A. Mai, Pan-Histone Demethylase Inhibitors Simultaneously Targeting Jumonji C and Lysine-Specific Demethylases Display High Anticancer Activities, *J. Med. Chem.* **57**, 42–55 (2014).

156. H.-L. Cheng, R. Mostoslavsky, S. Saito, J. P. Manis, Y. Gu, P. Patel, R. Bronson, E. Appella, F. W. Alt, K. F. Chua, Developmental defects and p53 hyperacetylation in Sir2 homolog (SIRT1)-deficient mice, *Proc. Natl. Acad. Sci.* **100**, 10794–10799 (2003).
157. D. S. Chen, I. Mellman, Oncology Meets Immunology: The Cancer-Immunity Cycle, *Immunity* **39**, 1–10 (2013).
158. E. I. Buchbinder, A. Desai, CTLA-4 and PD-1 Pathways, *Am. J. Clin. Oncol.* **39**, 98–106 (2016).
159. C. A. Sabatos, S. Chakravarti, E. Cha, A. Schubart, A. Sánchez-Fueyo, X. X. Zheng, A. J. Coyle, T. B. Strom, G. J. Freeman, V. K. Kuchroo, Interaction of Tim-3 and Tim-3 ligand regulates T helper type 1 responses and induction of peripheral tolerance, *Nat. Immunol.* **4**, 1102–1110 (2003).
160. J. Fourcade, Z. Sun, O. Pagliano, J.-M. Chauvin, C. Sander, B. Janjic, A. a Tarhini, H. a Tawbi, J. M. Kirkwood, S. Moschos, H. Wang, P. Guillaume, I. F. Luescher, A. Krieg, A. C. Anderson, V. K. Kuchroo, H. M. Zarour, PD-1 and Tim-3 Regulate the Expansion of Tumor Antigen-Specific CD8+ T Cells Induced by Melanoma Vaccines., *Cancer Res.* **74**, 1045–55 (2014).
161. V. Pancholi, Multifunctional  $\alpha$ -enolase: its role in diseases, *Cell. Mol. Life Sci.* **58**, 902–920 (2001).
162. J. M. Brewer, R. L. Robson, C. V. C. Glover, M. J. Holland, L. Lebioda, Preparation and characterization of the E168Q site-directed mutant of yeast enolase 1, *Proteins*

*Struct. Funct. Genet.* **17**, 426–434 (1993).

163. S. Gao, H. Li, X. Feng, M. Li, Z. Liu, Y. Cai, J. Lu, X. Huang, J. Wang, Q. Li, S. Chen, J. Ye, P. Liu,  $\alpha$ -Enolase plays a catalytically independent role in doxorubicin-induced cardiomyocyte apoptosis and mitochondrial dysfunction, *J. Mol. Cell. Cardiol.* **79**, 92–103 (2015).

164. J. Qin, G. Chai, J. M. Brewer, L. L. Lovelace, L. Lebioda, Fluoride Inhibition of Enolase: Crystal Structure and Thermodynamics † , ‡, *Biochemistry* **45**, 793–800 (2006).

165. W. Zhou, M. Capello, C. Fredolini, L. Piemonti, L. A. Liotta, F. Novelli, E. F. Petricoin, Mass spectrometry analysis of the post-translational modifications of r-enolase from pancreatic ductal adenocarcinoma cells, *J. Proteome Res.* **9**, 2929–2936 (2010).

166. L. Zhang, H. Wang, X. Dong, Diagnostic value of  $\alpha$ -enolase expression and serum  $\alpha$ -enolase autoantibody levels in lung cancer, *J. Bras. Pneumol.* **44**, 18–23 (2018).

167. S. J. Bennett, E. M. Augustyniak, C. R. Dunston, R. A. Brown, E. Shantsila, G. Y. H. Lip, R. D. C. Torrao, C. Pararasa, A. H. Remtulla, R. Ladouce, B. Friguet, H. R. Griffiths, CD4+ T cell surface alpha enolase is lower in older adults, *Mech. Ageing Dev.* **152**, 56–62 (2015).

168. M. Principe, P. Ceruti, N. Shih, M. S. Chattaragada, S. Rolla, L. Conti, M. Bestagno, L. Zentilin, S.-H. Yang, P. Migliorini, P. Cappello, O. Burrone, F. Novelli, Targeting of surface alpha-enolase inhibits the invasiveness of pancreatic cancer cells, *Oncotarget* **6**, 11098–113 (2015).

169. M. G. Vander Heiden, J. W. Locasale, K. D. Swanson, H. Sharfi, G. J. Heffron, D. Amador-Noguez, H. R. Christofk, G. Wagner, J. D. Rabinowitz, J. M. Asara, L. C. Cantley, Evidence for an Alternative Glycolytic Pathway in Rapidly Proliferating Cells, *Science* (80- . ). **329**, 1492–1499 (2010).
170. E. H. Ma, G. Bantug, T. Griss, S. Condotta, R. M. Johnson, B. Samborska, N. Mainolfi, V. Suri, H. Guak, M. L. Balmer, M. J. Verway, T. C. Raissi, H. Tsui, G. Boukhaled, S. Henriques da Costa, C. Frezza, C. M. Krawczyk, A. Friedman, M. Manfredi, M. J. Richer, C. Hess, R. G. Jones, Serine Is an Essential Metabolite for Effector T Cell Expansion, *Cell Metab.* **25**, 345–357 (2017).
171. T. Hitosugi, L. Zhou, S. Elf, J. Fan, H.-B. Kang, J. H. Seo, C. Shan, Q. Dai, L. Zhang, J. Xie, T.-L. Gu, P. Jin, M. Alečković, G. LeRoy, Y. Kang, J. A. Sudderth, R. J. DeBerardinis, C.-H. Luan, G. Z. Chen, S. Muller, D. M. Shin, T. K. Owonikoko, S. Lonial, M. L. Arellano, H. J. Khoury, F. R. Khuri, B. H. Lee, K. Ye, T. J. Boggon, S. Kang, C. He, J. Chen, Phosphoglycerate Mutase 1 Coordinates Glycolysis and Biosynthesis to Promote Tumor Growth, *Cancer Cell* **22**, 585–600 (2012).
172. E. Mullarky, N. C. Lucki, R. Beheshti Zavareh, J. L. Anglin, A. P. Gomes, B. N. Nicolay, J. C. Y. Wong, S. Christen, H. Takahashi, P. K. Singh, J. Blenis, J. D. Warren, S.-M. Fendt, J. M. Asara, G. M. DeNicola, C. A. Lyssiotis, L. L. Lairson, L. C. Cantley, Identification of a small molecule inhibitor of 3-phosphoglycerate dehydrogenase to target serine biosynthesis in cancers, *Proc. Natl. Acad. Sci.* **113**, 1778–1783 (2016).

173. T. Hitosugi, L. Zhou, S. Elf, J. Fan, H.-B. Kang, J. H. Seo, C. Shan, Q. Dai, L. Zhang, J. Xie, T.-L. Gu, P. Jin, M. Alečković, G. LeRoy, Y. Kang, J. A. Sudderth, R. J. DeBerardinis, C.-H. Luan, G. Z. Chen, S. Muller, D. M. Shin, T. K. Owonikoko, S. Lonial, M. L. Arellano, H. J. Khoury, F. R. Khuri, B. H. Lee, K. Ye, T. J. Boggon, S. Kang, C. He, J. Chen, Phosphoglycerate Mutase 1 Coordinates Glycolysis and Biosynthesis to Promote Tumor Growth, *Cancer Cell* **22**, 585–600 (2012).
174. G. Andrejeva, J. C. Rathmell, Similarities and Distinctions of Cancer and Immune Metabolism in Inflammation and Tumors, *Cell Metab* **26**, 49–70 (2017).
175. T. Fiaschi, P. Chiarugi, Oxidative stress, tumor microenvironment, and metabolic reprogramming: a diabolic liaison., *Int. J. Cell Biol.* **2012**, 762825 (2012).
176. N. Ron-Harel, D. Santos, J. M. Ghergurovich, P. T. Sage, A. Reddy, S. B. Lovitch, N. Dephoure, F. K. Satterstrom, M. Sheffer, J. B. Spinelli, S. Gygi, J. D. Rabinowitz, A. H. Sharpe, M. C. Haigis, Mitochondrial Biogenesis and Proteome Remodeling Promote One-Carbon Metabolism for T Cell Activation, *Cell Metab.* **24**, 104–117 (2016).
177. M. D. Buck, D. O’Sullivan, R. I. Klein Geltink, J. D. Curtis, C. Chang, D. E. Sanin, J. Qiu, O. Kretz, D. Braas, G. J. W. van der Windt, Q. Chen, S. C.-C. Huang, C. M. O’Neill, B. T. Edelson, E. J. Pearce, H. Sesaki, T. B. Huber, A. S. Rambold, E. L. Pearce, Mitochondrial Dynamics Controls T Cell Fate through Metabolic Programming, *Cell* **166**, 63–76 (2016).
178. R. I. Klein Geltink, D. O’Sullivan, M. Corrado, A. Bremser, M. D. Buck, J. M. Buescher, E. Firat, X. Zhu, G. Niedermann, G. Caputa, B. Kelly, U. Warthorst, A. Rensing-

Ehl, R. L. Kyle, L. Vandersarren, J. D. Curtis, A. E. Patterson, S. Lawless, K. Grzes, J. Qiu, D. E. Sanin, O. Kretz, T. B. Huber, S. Janssens, B. N. Lambrecht, A. S. Rambold, E. J. Pearce, E. L. Pearce, Mitochondrial Priming by CD28, *Cell* **171**, 385–397.e11 (2017).